MAJOR PROJECT-II

CORRELATION BETWEEN $PM_{2.5}$ AND TROPOSPHERIC O_3 IN DELHI: TEMPORAL VARIATIONS AND METEOROLOGICAL IMPACTS

Thesis Submitted
in Partial Fulfillment of the Requirements for the Degree of

MASTER OF TECHNOLOGY
in
ENVIRONMENTAL ENGINEERING
by

SHASHANK S KHARE
(2K18/ENE/09)

Under the Supervision of

Dr. LOVLEEN GUPTA
ASSISTANT PROFESSOR
DEPARTMENT OF ENVIRONMENTAL ENGINEERING
DELHI TECHNOLOGICAL UNIVERSITY

To the
DEPARTMENT OF ENVIRONMENTAL ENGINEERING
DELHI TECHNOLOGICAL UNIVERSITY
(Formerly Delhi College of Engineering)
Shahbad Daulatpur, Main Bawana Road, Delhi-110042, India

MAY, 2024

DELHI TECHNOLOGICAL UNIVERSITY
(Formerly Delhi College of Engineering)
Shahbad Daulatpur, Main Bawana Road, Delhi-42

CANDIDATE'S DECLARATION

I SHASHANK S KHARE hereby certify that work which is being presented in the thesis entitled "CORRELATION BETWEEN $PM_{2.5}$ AND TROPOSPHERIC O_3 IN DELHI: TEMPORAL VARIATIONS AND METEOROLOGICAL IMPACTS" in partial fulfillment of the requirements for the award of the Degree of Master of Technology in Environmental Engineering submitted in the Department of Environmental Engineering, Delhi Technological University is an authentic record of my own work carried out during the period from January 2023 to May 2024 under the supervision of Dr. Lovleen Gupta.

The matter presented in the thesis has not been submitted by me for the award of any degree of this or any other Institute.

Shashank S Khare

This is to certify that the student has incorporated all the corrections suggested by the examiners in the thesis and the statement made by the candidate is correct to the best of our knowledge.

Signature of Supervisor **Signature of External Examiner**

DELHI TECHNOLOGICAL UNIVERSITY
(Formerly Delhi College of Engineering)
Shahbad Daulatpur, Main Bawana Road, Delhi-42

CERTIFICATE BY THE SUPERVISOR

Certified that **Shashank S Khare** (2K18/ENE/09) has carried out their research work presented in this thesis entitled "**CORRELATION BETWEEN $PM_{2.5}$ AND TROPOSPHERIC O_3 IN DELHI: TEMPORAL VARIATIONS AND METEOROLOGICAL IMPACTS**" for the award of **Master of Technology** from Department of Environmental Engineering, Delhi Technological University, Delhi, under my supervision. The thesis embodies results of original work, and studies are carried out by the student himself and the contents of the thesis do not form the basis for the award of any other degree to the candidate or to anybody else from this or any other University/Institution.

(Dr. Lovleen Gupta)
Assistant Professor
Department of Environmental Engineering
Delhi Technological University

Date:

ACKNOWLEDGEMENTS

I sincerely thank the Department of Environmental Engineering, Delhi Technological University for providing me with this opportunity to learn more about tropospheric ozone and about correlations and covariations between O_3 and its precursors, especially $PM_{2.5}$.

I am highly indebted to and wish to sincerely thank my project supervisor,Dr. Lovleen Gupta, for her constant guidance and motivation, without which developing this report would not have been possible. Her invaluable support has allowed me to expand the horizons of our knowledge.

I would like to express my gratitude towards Dr. Anil Kumar Haritash, HOD (Environmental Engineering) for his continual encouragement and support.

Mr. Sachin Dhawan (Research Scholar, IIT Delhi) is greatly appreciated for his help in coding aspects of the study.

Lastly, I also express my gratitude towards my family.

Date:

Place:

Shashank S Khare

(2K18/ENE/09)

ABSTRACT

Ambient air pollution in India, especially in Delhi, poses severe health risks. The capital experiences alarming levels of pollutants due to vehicular emissions, industrial activities, and crop burning. This pollution leads to cardiovascular issues, respiratory problems and shorter life expectancy.

The pollutant of interest in the present study is ground-level ozone or tropospheric ozone – a secondary air pollutant. Ozone (O_3) is a highly oxidizing triatomic molecule that is desirable in the stratosphere but can be a lethal pollutant in the troposphere. Ecosystems and human health are both harmed by it. Research on tropospheric O_3 is essential to understand its formation, impacts, and to develop effective mitigation strategies, ensuring healthier air quality and environmental protection. While extensive research has taken place on chemistry of O_3 formation, there has been little work done on exploring the relationship between $PM_{2.5}$ and ozone.

This work explores the relationship of O_3 with other gaseous pollutants, particulate matter (PM) and meteorological parameters in Delhi over a six-year period (January 2018-December 2023). Comprehensive statistical analysis for exploring factors influencing ozone formation in Delhi was done on diurnal-basis and seasonal-basis using data from six CAAQMS. Data was taken at hourly intervals throughout the study period.

The maximum concentration of O_3 observed was 53.44 ± 28.7 μg/m³ which was experienced in Summer of 2020 (April -June 2020). A negative correlation existed between O_3 and $PM_{2.5}$, except during monsoon season (July-September), with maximum negative correlation observed in Summer of 2020 as -0.55. This may be attributed to: higher concentrations of $PM_{2.5}$ observed throughout Delhi during postmonsoon (maximum of 200.77±140.03 μg/m³ observed in postmonsoon of 2020) and winter (maximum of 210.77 ± 125.87 μg/m³ observed in winter of 2018-19) seasons that reduces solar radiation available for O_3 formation (low scattering albedo) (Concentration during winter was <30 μg/m³ for all the years); along with smog, haze, low mixing heights

and temperature inversion which exacerbates the situation. In spring and summer season, though O_3 concentrations increase due to increasing solar radiation and temperature, the relative concentration of $PM_{2.5}$ reduces (maximum concentration: 94.89 ± 54.77 µg/m³ observed in summer of 2022). Biogenic VOCs also contribute more to $PM_{2.5}$ concentration proportion, thereby increasing O_3 concentrations. However, during monsoon, a mildly positive, but statistically insignificant, correlation was generally observed. This may be attributed to cleansing effect of rainfall that diminishes $PM_{2.5}$ concentration (maximum concentration of 38.41 ± 20.02 µg/m³ observed in monsoon of 2022). Also, wind, that carries relatively less dust, blows in monsoon and overcast weather reduces O_3 formation.

This study will aid policy makers in formulating policies to curb co-pollution of O_3 and $PM_{2.5}$ in Delhi. Also, studies at micro-level are deemed necessary to conclusively establish a theory explaining relationship between O_3 and $PM_{2.5}$ in Delhi; as similar studies in other regions show significant spatial variation in the same.

TABLE OF CONTENTS

LIST OF TABLES

LIST OF FIGURES

LIST OF ABBREVIATIONS

CPCB: Central Pollution Control Board

GLO: Ground level ozone

TPO: Tropospheric Column Ozone

WHO: World Health Organisation

VOC: Volatile Organic Compounds

MAH: Monocyclic Aromatic Hydrocarbons

OECD: Organisation for Economic Cooperation and Development

STE: Stratosphere Troposphere Exchange

NMHC: Non-Methane Hydrocarbons

PBLH: Planetary Boundary Layer Height

Chapter 1: Introduction

Ambient air is the natural state of air in the outdoor environment. The tropospheric ambient air is majorly composed of N_2 (78%), O_2 (20.94%), Ar (0.934%) and CO_2 (0.0315%) (Khare and Nagendra, 2007). In addition to this, its composition varies with the presence of local air pollution sources, meteorological conditions and geographical features. Ambient air quality is influenced by complex interactions between natural and anthropogenic environmental conditions (Mayer, 1999). Its quantification depends upon flow and dispersion of ambient air pollutants – gaseous or particulate.

Ambient air quality has become an area of great concern due to rapid industrialization and urbanization, especially in developing countries. Since the last two decades, air quality is deteriorating alarmingly due to increasing population which leads to unplanned development of industrial and transport sectors. These anthropogenic sources release huge amounts of air pollutants in the ambient air which ultimately affects the public health. Using air quality monitoring texhniques to evaluate the current state of ambient air quality is crucial.

As per the Organisation for Economic Cooperation and Development (OECD), air pollution is the result of contaminant or polluting elements present in the atmosphere that do not adequately disperse, endanger human health or welfare, or have other negative consequences on the environment.

Air pollution can be described as the presence of one or more contaminants or their combinations in the outdoor atmosphere in quantities and for durations that may harm human, plant, or animal life, damage property, or significantly interfere with the enjoyment of life or the environment. Any substance occurring in the atmosphere that may have adverse effects on humans, animals, plant life, or inanimate materials is an air pollutant(Wark et al., 1998).

Since the industrial revolution, rapid expansion of industries has taken place. This has been accompanied and characterized by and increase in concentrated human activities, which has led to a rise in air pollution levels in most major cities and has become a serious problem for most developing countries. Vehicular (mobile sources), industrial and domestic sources (stationary sources) are the major anthropogenic sources of air pollution. Urbanization is expected to increase further, and hence the emissions from vehicles and industries. This has the potential to negatively impact people's health by exposing a large number of individuals to high levels of ambient air pollution over extended periods of time.

To alleviate the problem of ambient air pollution, it is necessary to study the system being polluted, assess the air quality, and study the transport regime of pollutants. The preceding discussion shows that air pollution, particularly in urban areas, is a serious threat (Hall, 1996; Khare and Nagendra, 2007; Mage et al., 1996).

Air pollution is becoming a major concern globally, especially in developing countries like India, where air quality standards are contravened in 78% of the cities(CPCB, 2020). While there have been significant attempts in India to lower the amount of particulate matter in the atmosphere, emissions of gaseous pollutants, volatile organic compounds (VOCs) and NO_x have been steadily rising. NO_x and VOCs are regarded as the main gaseous precursors of ground level ozone (GLO), a major secondary air pollutant.

Stratospheric ozone shields us from the ultra-violet radiations of the Sun, but O_3

formed at ground level is detrimental to human health and crop productivities and is regarded a pollutant.

The pollutant of interest in the present study is GLO or tropospheric ozone. Ozone is a highly oxidizing triatomic molecule that is desirable in the stratosphere (as it blocks harmful ultraviolet radiation from the sun), but can be a lethal pollutant in the troposphere. The Indian subcontinent exhibits high levels of ozone, which can adversely impact human health, crop productivity, and regional climatic patterns. As a secondary pollutant, ozone forms through reactions involving pollutants such as NOx, CO, and VOCs in the presence of sunlight.

1.1 Effects of tropospheric ozone

Ozone (O_3) causes a wide range of adverse effects on human health, including throat irritation, reduced lung function, respiratory problems like chronic obstructive pulmonary disease (COPD), emphysema, increased mortality, eye irritation, aggravated allergies, and skin damage. Its impact extends to the environment, where it damages the stomata in plants, reducing crop yield and the life expectancy of plants and trees, and causes cracking of rubber, leading to significant material loss. O_3 also contributes to haze and reduced visibility and is recognized as a potent greenhouse gas (GHG). Despite comprising only about one-tenth of the total atmospheric ozone and being primarily located in the troposphere, ground-level ozone (GLO) has a critical role in photochemical reactions, causing the recycling of gases emitted by both anthropogenic and natural sources (Masters, 1998; Rao, 1988). Ozone at this level is significant for two primary reasons: it acts as a secondary pollutant and possesses substantial greenhouse potential, ranking it as the third most potent greenhouse gas following carbon dioxide (CO_2) and methane (CH_4)(Shukla, 2019).

GLO's health impacts are well-documented, with epidemiological studies indicating that exposure to high O_3 concentrations can lead to rise in mortality and morbidity. Clinical studies have provided regional estimates of O_3's impact on residential populations, with WHO estimating that 21,000 premature deaths occur every year in 25 European Union countries on and post high O_3 levels days(WHO, 2008). Beyond human health, O_3 significantly affects agriculture by damaging plant growth on its stems, roots, leaves, etc. It also adversely affects partitioning of biomass, flowers, seeds, etc. Yields of crops like maize, wheat, etc. are reduced. For example, loss of 36% yield has been observed for wheat in India (Burney and Ramanathan, 2014).

O_3 impacts not just agriculture and health but also materials such as rubber goods and surface coatings, textiles, fabrics, polymeric materials, etc. and causes colour fading (Lee et al., 1996). O_3 is a strong greenhouse gas that contributes to long-term climate change in addition to its local effects. Tropospheric ozone significantly contributes to radiative forcing with estimates of about 0.3 W/m^2, making it a notable greenhouse gas. The IPCC Fourth Assessment Report highlighted that tropospheric ozone is the third most important greenhouse gas after CO_2 and CH_4 (Chalita et al., 1996; Worden et al., 2008).

Chapter 2: Literature Review

The Indian sub-continent has shown relatively high ozone concentrations, even in regions with low populations and precursor emission intensities, due to atmospheric transport or meteorological processes (Sharma, 2017). O_3 is a secondary pollutant and the primary element of photo-chemical smog, which involves reactions of different precursor species. The principal species known to contribute to the formation of O_3 are NO_x, VOCs, and CO. The relationship between O_3 and its precursors is primarily regulated by complex non-linear photochemical reactions (Sharma, 2017), and it varies significantly with the environmental conditions, including land use, types of weather, emission source intensity, and type of emissions.

2.1 Precursors of Ozone and Formation of ozone

Main cause of occurrence of tropospheric ozone is anthropogenic. However, Stratosphere Troposphere Exchange (STE) and long-range transport also causes occurrence of tropospheric ozone in a region. Ozone is a secondary pollutant that is formed when photochemical reactions take place between Volatile Organic Carbon (VOCs) and NO_x. NO_x includes NO, NO_2, N_2O, N_2O_2, N_2O_3, N_2O_4, N_2O_5. However, only NO and NO_2 are known to cause ground-level ozone formation. These are most prevalent and well-established precursors to ozone formation (Shukla, 2019). Other precursors may include complex hydrocarbons, CO, hydroxyl (OH) ions and NMHC (Non-Methane Hydrocarbons). Besides, photocopy machines are point sources of ozone emissions.

Anthropogenic sources of NO_x include vehicular exhaust emissions, DG sets, power plants, and some industries (such as cement manufacturing, chemical industries that emit NO_x as by-product, etc.). Lightening is a natural source of NO_x. VOCs are compounds characterized with high reactivity and comprising of eight or less carbon atoms in a molecule (Batterman et al., 2014). Main sources of VOCs include plants/trees (biogenic), evaporative emissions from petrol stations and chemical solvents used in various industrial processes, paints and solvents, evaporating gasolines, vehicular exhausts, consumer products such as sprays and perfumes, etc. Several Monocyclic Aromatic Hydrocarbons (MAH) such as benzene, toluene, xylene, etc. are also VOCs. Incomplete combustion processes, vehicular emissions, biomass burning, agricultural residue burning, etc. are sources of CO.

Apart from the aforementioned precursors, the present study also explores the relationship between ozone and other pollutants such as NH_3, Monocyclic Aromatic Hydrocarbons (MAH) and $PM_{2.5}$ in Delhi. $PM_{2.5}$ represents particulate matter that is less than 2.5 micrometers in diameter; while for the purpose of the present study Monocyclic Aromatic Hydrocarbons (MAH) represents summation of benzene, toluene, xylene, ethyl benzene, ortho xylene, meta para xylene, etc.

The following table summarises the sources and adverse effects of pollutants explored in the present study (Rao, 1988).

Table 2. 1: Pollutants of concern: Sources and Effects

Pollutant	Sources	Effects
NO_2	Lightening, microbial activity in soils, vehicles, power plants, diesel generator sets	Decrease lung function; Acid rain; irritation to eyes, lungs.
NO	Lightening, microbial activity in soils, vehicles, power plants,	Forms NO_2, O_3; acid rain

	diesel generator sets at higher temperatures.	
CO	Incomplete combustion of fossil fuels (vehicular emissions; biomass or kerosene burning for cooking or heating)	Asphyxiation; anoxemia
VOCs	Combustion sources (biomass burning, automobiles, industries, etc.); painting, printing, leather coating, use of personal products, exploration and handling of oil products etc.; Biogenic sources (Plants)	CH_4 – Grennhouse gas; Monocyclic Aromatic Hydrocarbons (MAH) – carcinogenic; pulmonary problems; allergies; CNS problems; damages liver, kidney, etc.
$PM_{2.5}$	Vehicles, power plants, industrial processes; wildfires; sea spray; chemical reactions in atmosphere	Penetrates deep into the lungs and enter the bloodstream, causing respiratory and cardiovascular diseases; Reduces visibility (haze)
Ozone	Secondary pollutant formed by chemical/photochemical reactions in the atmosphere	Damage crops, forests, and other vegetation; Throat irritation, coughing, and difficulty breathing; cardiovascular and pulmonary diseases; Respiratory problems, asthma, bronchitis etc.;

		Assists in formation of Peroxy acetyl nitrate (PAN); cracking of rubber
NH_3	Fertilizers and animal husbandry operations; ammonia synthesis; Emitted from soils, wildlife, and decomposition of organic matter	Irritation to eyes, lungs.

Importance of GLO has been duly recognised by the regulatory authorities in India and Worldwide. WHO prescribes air quality guideline for O_3 as 100 µg/m³ (8-hour average) as per its latest revision in 2021(WHO, 2021). In India, the Central Pollution Control Board (CPCB) notified the National Ambient Air Quality Standards (NAAQS) which is as follows:

Table 2. 2 National Ambient Air Quality Standards (NAAQS), CPCB (CPCB, 2009)

Pollutant	**Time Weighted Average**	**Standard Concentration (µg/m³)**	**Eco-Sensitive Zone Standard (µg/m³)**
Particulate Matter (PM_{10})	24 hours	100	60
	Annual	60	40

Particulate Matter ($PM_{2.5}$)	24 hours	60	40
	Annual	40	20
Nitrogen Dioxide (NO_2)	Annual	40	20
	24 hours	80	40
Sulphur Dioxide (SO_2)	24 hours	80	50
	Annual	50	20
Carbon Monoxide (CO)	8 hours	2000	1000
	1 hour	4000	2000
Ozone (O_3)	8 hours	100	50
	1 hour	180	90
Lead (Pb)	Annual	0.5	0.2
Ammonia (NH_3)	Annual	100	50
Benzene (C_6H_6)	Annual	5	2

2.2 Chemistry of Ozone Formation

In the 1970s, P.J. Crutzen pioneered research into the photochemistry of tropospheric ozone generation(Crutzen, 1979, 1974). Subsequently, research into its production, chemistry, precursors, destruction, and transport have all improved our understanding regarding GLO. An understanding of the non-linear chemistry between O_3 and its predecessors has become crucial for policy formulation. Numerous studies have provided explanations of this non-linear connection and the photochemical behavior of O_3 (Zhang et al., 2008).

At the stratosphere and tropospheric levels, O_3 is created by a variety of chemical processes. Ozone is created naturally in the stratosphere when sunlight's UV radiation (λ < 240 nm) is absorbed by oxygen, leading to the formation of nascent oxygen atoms. Following its reaction with the O_2 molecule, this atom subsequently produces ozone. This naturally occurring stratospheric ozone descends to the troposphere in part. Sunlight radiation breaks down ozone in the troposphere into O_2 molecules and atoms.

Oxygen converts to O_3 in stratosphere, some of which transports to troposphere and forms OH radicals.

$O_3 \rightarrow O_2 + O$

$O + H_2O \rightarrow 2OH$

Primary pollutants like VOCs and CO react with OH and forms RO_2 and OH_2. RO_2 is an organic chain with an attached O_2 (replacing H).

$VOC + OH \rightarrow RO_2 + H_2O$

$CO + OH \rightarrow OH_2 + CO_2$

RO_2 and OH_2 oxidise NO to NO_2.

$RO_2 + NO \rightarrow HO_2 + VOC + NO_2$

$OH_2 + NO \rightarrow OH + NO_2$

NO_2 undergoes photolysis to form atomic oxygen, that combines with oxygen to form O_3 in the troposphere.

The chemical reactions below illustrate the same:

Chemical reactions showing ozone formation are as follows:

NO_2 + hv (sunlight) $\rightarrow$ NO + O

O + O_2 + Stable Molecule that absorbs excess energy (O_2/N_2) $\rightarrow$ O_3 + Stable Molecule (O_2/N_2)

O_3 is generated in the presence of sunlight. At night, the primary NO emitted from sources such as vehicles and power plants reacts with O_3, converting it back to O_2. This process is known as NO_x titration.

O_3 + NO $\rightarrow$ NO_2 + O_2

The above reactions are cyclic in nature.

It can be concluded that solar radiation intensity, NO_x concentration and VOC levels, and their ratios significantly influence the formation of ground-level ozone (GLO). These reactions and photochemistry of ozone are further explained in this section in detail.

The formation of ozone depends on local geography, meteorology, and land-use patterns. For example, “trapping regions” and where temperature inversion occurs tend to have higher O_3 concentrations (For example, the infamous Los Angeles smog episode.). Similarly, urban and industrial regions have higher O_3 concentrations due to higher concentrations of precursors present. It is well-established in literature that high temperature and solar radiation favours ozone formation.

There are two primary regimes under which GLO is produced: the NO_x-sensitive regime and the VOC-sensitive regime. In the NO_x-sensitive regime, the NO_x/VOC ratio is low, making ozone concentrations more dependent on NO_x levels. Conversely, in the VOC-sensitive regime, where NO_x/VOC ratios are high, ozone levels decrease with an increase in NO_x and increase with a rise in VOCs.

The reactions involving CO are explained below, wherein O_3 acts as a source of OH (hydroxyl radical) and CO represents VOCs.

$CO + OH (+O_2) \rightarrow CO_2 + HO_2$

The destruction and generation of O_3 along with limited regimes can be seen in Figures 2.1 and 2.2. O_3 production takes place, both in *VOC-limited* and *NO_x limited* regimes. However, in most cases O_3 generation is in NO_x limited regimes, except during peak summers when O_3 production is mostly governed in VOC-limited regimes (Shukla, 2019).

With presence of VOCs the following reactions occur:

a. $RH + OH^* \rightarrow R^* + H_2O$

b. $R^* + O_2 \rightarrow RO_2^*$ (Initiation stage)

c. $RO_2^* + NO \rightarrow RO^* + NO_2$

d. $RO^* + O_2 \rightarrow HO_2^* + R'CHO$ (aldehyde)

e. $HO_2^* + NO \rightarrow NO_2 + OH^*$ (Propagation stage)

Reaction e. shows that removal of NO, formation of NO2 and OH* takes place which all contribute to O_3 formation. These reactions together go through initiation, propagation and termination stages. Reaction terminates when RO_2^* and HO_2^* react together. Therefore, these complex cyclic reactions are very tough to stop.

An example of VOC reacting to produce ozone is as follows:

$CH_3CH_3 + 2O_2 + h\vartheta \rightarrow CH_3CHO + H_2O + 2O_3$

The general mechanism of OH-initiated ozone generation can be extended to more complex VOCs i.e., alkanes (Sharma, 2017).

Atkinson (2000) and Kleinman et al. (2002) outlined a fundamental scheme (general reaction scheme) of reactions based on photochemical equations(Shukla, 2019). These equations are categorized into three groups, representing the initiation, cycling, and termination phases, as described below:

Initiation:

$O_3 + h\upsilon \rightarrow O + O_2$

$O + H_2O \rightarrow 2OH$

$HCHO + h\upsilon \rightarrow 2HO_2$

Alkene + $O_3 \rightarrow$ Radicals

Cycling (chain propagation):

$OH + VOCi \rightarrow aHO_2 + b\ RO_2 + cRCO_3$

$NO + HO_2 \rightarrow OH + NO_2$

$NO + RO_2 \rightarrow$ d ($NO \rightarrow NO_2$ conversion) + HC oxidation products

$NO + RCO_3 \rightarrow$ e ($NO \rightarrow NO_2$ conversion) + HC oxidation products

$NO_2 + h\upsilon \rightarrow O + NO$

$O_2 + O \rightarrow O_3$

Termination

$NO_2 + OH \rightarrow HNO_3$

$NO + RO_2 \rightarrow$ Organic nitrate

$NO_2 + CH_3CO_3 \rightarrow PAN$

$PAN \rightarrow NO_2 + CH_3CO_3$

Radical + *Radical*

$HO_2 + HO_2 \rightarrow H_2O_2$

$RO_2 + HO_2 \rightarrow RCOOH$

$OH + HO_2 \rightarrow H_2O + O_2$

$RO_2 + R'O_2 \rightarrow Products$

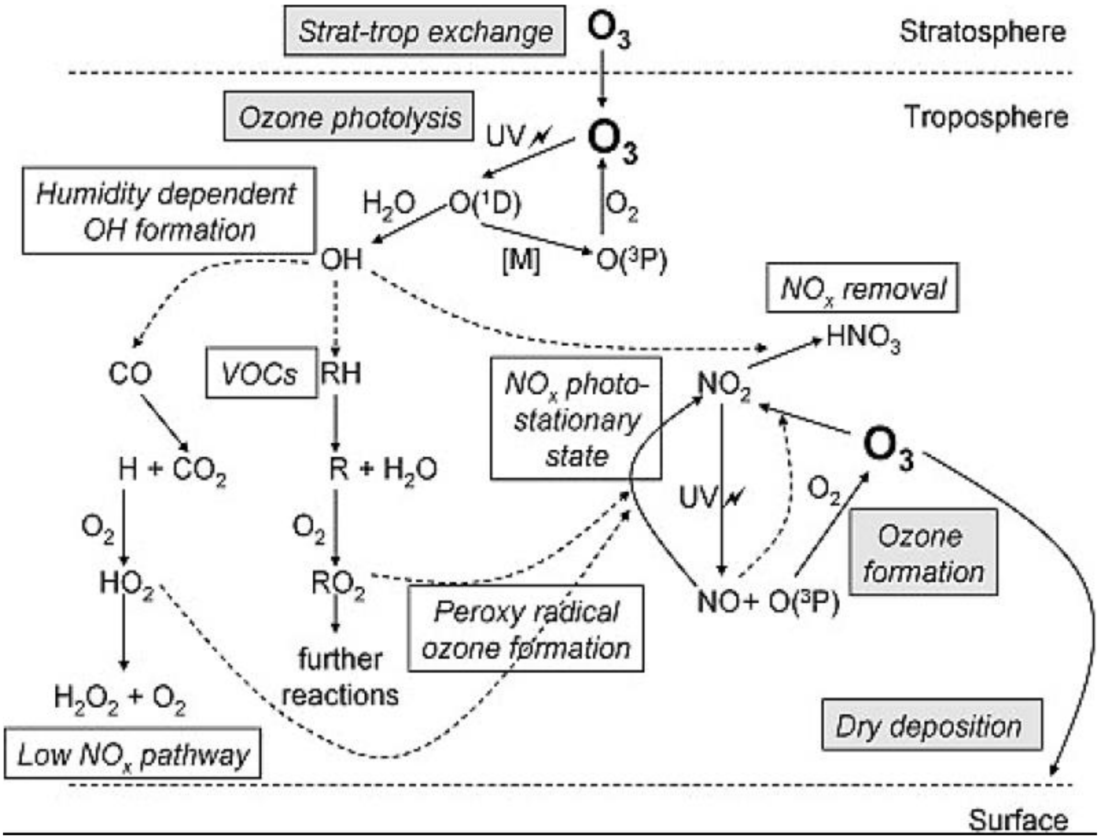

Figure 2.1 Formation of O_3 in Troposphere(Atkinson, 2000)

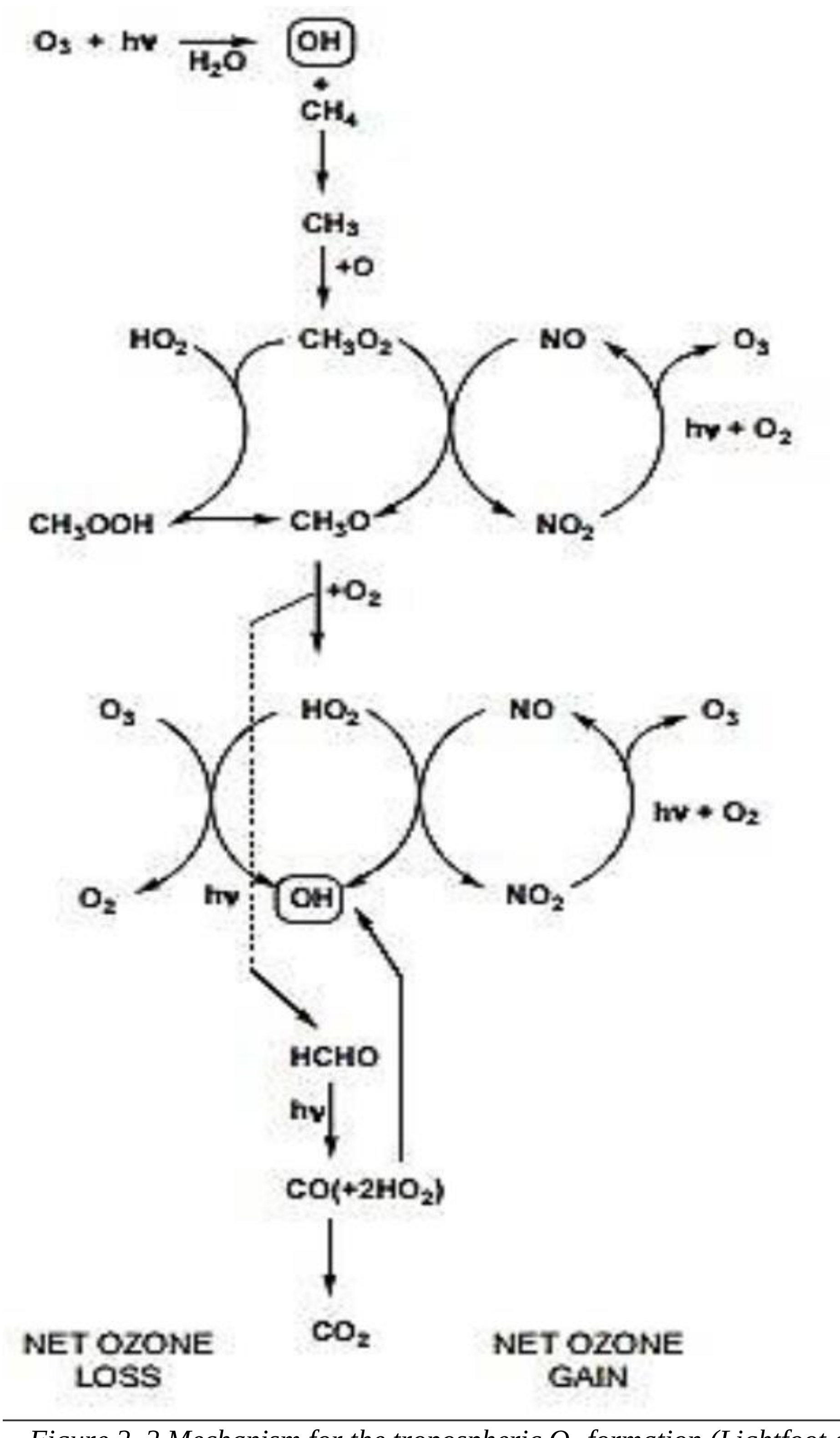

Figure 2. 2 Mechanism for the tropospheric O_3 formation (Lightfoot et al., 1992)

Ground-level ozone (GLO) production can be either limited by nitrogen oxides (NO_x)

or volatile organic compounds (VOCs). In NO_x-limited conditions, reactions between RO_2 and NO don't significantly reduce peroxy radicals. In VOC-limited conditions, often found in urban areas, high NO_x levels lead to the production of NO_2 and subsequently ozone (O_3). The concentration of NO_x in the air determines whether the process is NO_x or VOC-limited. Non-methane hydrocarbons (NMHCs) add complexity as they can act as sinks for GLO. Understanding the origins and regional movement of VOCs, HO_x species, OH reactivity, and GLO levels remains inconsistent, emphasizing the need for more targeted research.

In India, NO_x-limited conditions are generally more common, but this varies between rural and urban areas. The NO_x/VOC ratio is lower in India compared to developed countries due to high VOC emissions from both natural and human activities, such as the use of biofuels for cooking in rural areas. Urban areas see higher NO_x emissions from vehicles, while rural areas have significant VOC emissions from biomass burning. This suggests that Indian cities are more sensitive to VOCs, whereas rural areas are more sensitive to NO_x in terms of GLO production. VOCs from biomass burning, like alkanes, alkenes, acetylenes, oxygenated compounds, and aromatics, mostly fall within the C2–C4 range and have a high potential to form ozone. Studies in Dehradun and Delhi identified toluene and xylene as having the highest potential to form ozone during winter (Sharma, 2017; Shukla, 2019).

NO_x is crucial in both forming and breaking down ground-level ozone (GLO). Reducing VOCs affects O_3 generation, but in rural areas where O_3 is NO_x-limited, reducing VOCs is less effective in lowering O_3 levels.

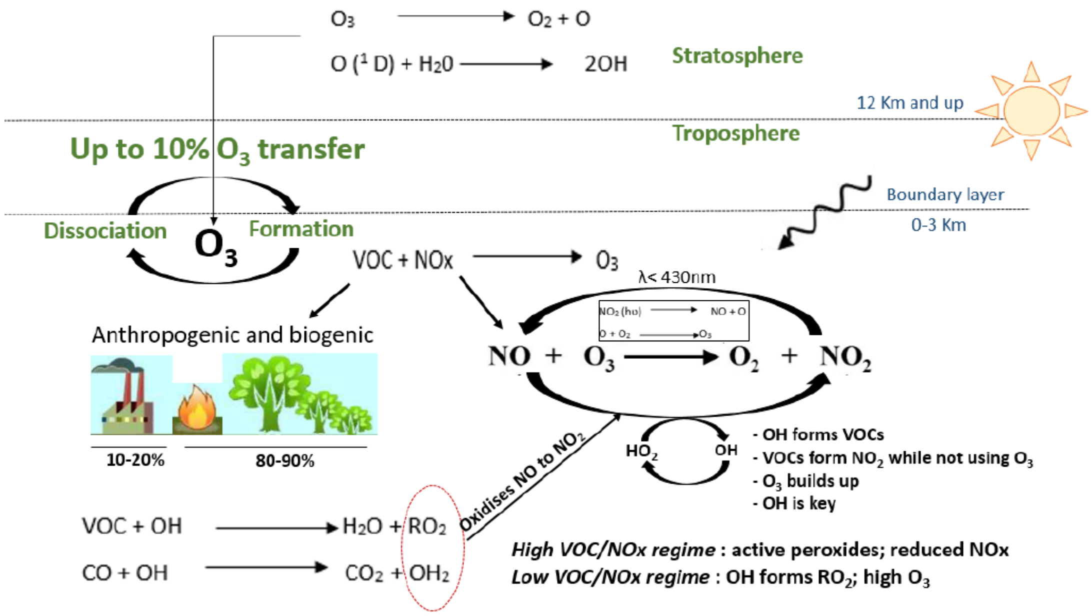

Figure 2. 3 Ozone formation in NO_x limiting and VOC limiting regimes (Shukla, 2019)

Literature on influencing meteorological parameters reveals GLO's relationship with mainly Ambient temperature, relative humidity and solar radiation. Ozone's dependence on other precursors – NO_2, NO, CO, NMHC, etc. have already been discussed.

High ambient temperatures typically enhance ground-level ozone (GLO) formation, as observed in various studies (Dhawan et al., 2023; Lacour et al., 2006).

GLO mixing ratios are adversely affected by relative humidity (RH). Excess moisture generates hydroxyl radicals, which are efficient sinks for GLO. Moisture also impacts heterogeneous processes including N_2O_5 hydrolysis and the absorption of NO_3 and NO_2 on wet aerosol surfaces, which in turn consumes HO_2. It also encourages the hygroscopic development of aerosols. GLO concentrations are lowered by these mechanisms, which include HO_2 consumption and N_2O_5 hydrolysis (Shukla, 2019).

Thus, relative humidity is generally negatively correlated with ozone concentrations.

On the other hand, GLO concentrations may rise as a result of the irreversible absorption of NO_x molecules, which increases the amounts of OH radicals (Shukla, 2019).

Rainfall is directly related to water vapor dynamics and has a major effect on ground-level ozone (GLO) concentrations. GLO levels frequently alter noticeably in response to rain patterns. Additionally, via affecting the ambient atmosphere's dispersion coefficients, wind speed and the atmospheric boundary layer are critical in controlling GLO dynamics (Shukla, 2019).

Dhawan et al. (2023) observed positive correlation between ozone and windspeed, temperature, solar radiation and a negative one between ozone and relative humidity. They also observed high ozone concentration around green areas, possibly indicating biogenic VOCs contributing to ozone formation (Dhawan et al., 2023).

As previously discussed, ozone is known to vary with its precursors following complex chemical reactions. Zhang et al. (2008) used an observation-based model (OBM) to study the connection between ozone and its precursors. Their research showed that high O_3 concentrations in the upwind direction are mostly caused by on-site photochemical production, which has a non-linear relationship with NO_x (Zhang et al., 2008). Ozone Production Efficiency (OPE) is the number of oxidant molecules (O_3 + NO_2) created photochemically when one molecule of NO_x (NO + NO_2) is oxidized. Seinfeld and Pandis studied OPE(Seinfeld et al., 1998). This indicates a negative correlation between ozone and NO_x. The immediate chemistry of ambient air was studied by Kleinman et al. (2002) using a Constrained Steady State box modeling approach, with a focus on how NO_x/NO_y rises. Their results imply that regional features, rather than only NO_x levels, determine the effectiveness of O_3 synthesis, mainly because of proportionate variations in the reactivity ratio of VOCs to NO_2. Many factors resulting from emission patterns affect this reactivity ratio (Kleinman et al., 2002). This indicates the unpredictability of O_3 synthesis which varies spatiotemporally. Another example of temporal variance has been studied by Han et al. Their study explored the "weekend effect," where differences in pollutant levels between weekdays and weekends were noted. During weekends, there are typically reductions in NO and NO_x levels compared to weekdays. This reduction is attributed to lower traffic volumes as fewer people commute. Interestingly, despite lower levels of NO_x (which are precursors to ozone), ozone levels do not proportionally decrease during weekends. This counterintuitive result is partly due to the complex chemistry of ozone formation and the reduced titration of ozone by NO (Han et al., 2011). Stratosphere Troposphere Exchange (STE) can also influence O_3 concentrations as shown by Rathore et al. Rathore et al. (2023) have observed that Stratosphere Troposphere Exchange (STE) is maximum during spring season in India and have observed long-range transport of O_3. The study also underscores the substantial contribution of tropospheric ozone to radiative forcing.

Sinha et al. (2021) investigated the levels of surface ozone (O_3) and its interactions with other air pollutants such as nitrogen oxides (NO_x) and carbon monoxide (CO) in various locations throughout Delhi from 2013 to 2019. It found that ozone levels are highest during the summer months. This increase is due to the strong sunlight in summer, which accelerates the chemical reactions that produce ozone from its precursor pollutants like NO_x and CO. However, the study also highlights a complex relationship between ozone and nitrogen oxides. During daylight hours, as the concentration of nitrogen oxides increases, the level of ozone actually decreases, contrary to what might be expected. This occurs because in urban areas like Delhi, which are sensitive to volatile organic compounds (VOCs), the presence of NO_x can lead to the breakdown of ozone through various chemical reactions. This implies a negative correlation exists between ozone and NO_x (Sinha et al., 2021). During the literature review, studies typically indicated high O_3 concentration during summer and postmonsoon.

2.3 Studies on Interrelationship between ozone and $PM_{2.5}$

Literature, until very recently, had not explored the interrelationship between GLO and $PM_{2.5}$; and the influence of other meteorological parameters on this relationship. Findings from some papers that did explore this relationship have been summarized as follows:

Munir et al (2011)

Munir et al.’s (2011) findings include a positive correlation between previous day ozone levels and current ozone levels, indicating that ozone tends to persist over time affecting subsequent concentrations. The study also notes negative correlations between ozone and nitrogen oxides (NO and NO_2) as well as carbon monoxide (CO), which are primarily emitted from traffic sources. This means that higher levels of these pollutants are associated with lower levels of ozone. The relationship with particulate matter ($PM_{2.5}$) varies; it is negatively correlated with ozone at lower quantiles and turns positive at higher quantiles, suggesting complex dynamics influenced by the concentration levels of ozone. The quantile regression approach used in the study offers a more detailed understanding of how these pollutants influence ozone compared to traditional regression methods, demonstrating that the impact of air pollutants on ozone varies across different environmental conditions and pollution levels (Munir et al., 2011).

Zhang et al., 2015

Zhang et al. examined the long-term trends and daily variations of $PM_{2.5}$ and ozone (O_3) concentrations and their relationship with meteorological conditions in Beijing over the past decade. It shows that $PM_{2.5}$ levels have decreased whilst ozone concentrations have increased. It also says that light rainfall can reduce ozone concentrations (Zhang et al., 2015).

Coates et al. (2016)

Coates et al. (2016) have discussed in the current section as it focusses on biogenic VOCs – an important precursor to both $PM_{2.5}$ and O_3. The 2016 study by Coates et al. explores how temperature affects ozone production when nitrogen oxides (NO_x) levels vary, using simulations from a box model incorporating multiple chemical mechanisms. Their research demonstrates that higher temperatures expedite chemical reactions and increase emissions of biogenic volatile organic compounds (BVOCs) like isoprene, both of which elevate ozone concentrations. It was also observed that rate in increase of ozone-mixing ratio was half that of increase in ozone due to rise in temperature. It was recommended that NO_x emissions need to be curbed to control O_3

pollution (Coates et al., 2016).

Jia et al. (2017)

Jia et al. (2017) investigate the seasonal relationships between $PM_{2.5}$ (fine particulate matter) and O_3 (ozone) in Nanjing, China, using environmental data from 2013 to 2015. During the hot seasons (June to August), Jia et al. found a positive correlation between $PM_{2.5}$ and ozone, with a correlation coefficient of 0.40. This positive relationship can be attributed to increased solar radiation and higher temperatures, which enhance photochemical reactions. These reactions are crucial for the formation of ozone. Sunlight drives the photolysis of nitrogen dioxide (NO_2), which leads to the production of ozone. Simultaneously, the increased temperatures and sunlight accelerate the emission of volatile organic compounds (VOCs) from both natural and anthropogenic sources, further fueling the formation of both ozone and secondary particulate matter, which contributes to higher $PM_{2.5}$ levels. Conversely, in the cold seasons (December to February), the correlation between $PM_{2.5}$ and ozone is negative, with a correlation coefficient of -0.16. During this period, the reduced intensity of sunlight and lower temperatures decrease the rate of photochemical reactions necessary for ozone formation. Furthermore, higher concentrations of $PM_{2.5}$ during the cold months can exacerbate this effect by absorbing and scattering solar radiation, which reduces the energy available for these reactions. The study notes that under high $PM_{2.5}$ conditions, surface ozone concentrations can significantly drop, which demonstrates the inhibitory effect of particulate matter on ozone production during colder times (Jia et al., 2017).

Shao et al., 2021

Shao et al. (2021) conducted their study in Beijing and Los Angeles. They state that the importance of $PM_{2.5}$-induced ozone amplification is contingent upon the optical characteristics of the particles as well as the amounts of $PM_{2.5}$. The author hypothesizes that as $PM_{2.5}$ concentration decreases, the absorption of solar radiation decreases enabling more ozone formation through photochemical reactions. However, this effect becomes less significant once $PM_{2.5}$ concentration falls below 40 μg/m^3 (Shao et al., 2021).

Liu et al., 2019

The study by Liu et al. provides a detailed analysis of how aerosols, including particulate matter ($PM_{2.5}$), influence the generation of surface ozone through complex atmospheric interactions, particularly during summer in Shanghai. Aerosol Optical Depth (AOD) is a measure of aerosols' ability to block sunlight. A higher AOD means more particles are present in the atmosphere. The presence of $PM_{2.5}$ can directly reduce the amount of UV light available for ozone formation due to absorption and scattering. Indirectly, the changes in UV radiation affect the photolysis rates of nitrogen dioxide (NO_2), which is a precursor to ozone. This can either suppress or modify the efficiency of ozone production depending on the concentration and type of particulate matter. While high levels of $PM_{2.5}$ generally decrease UV radiation reaching the surface (thus potentially reducing ozone formation), the scattering effect from high SSA can increase diffuse UV radiation, which might still promote ozone formation under certain conditions (Liu et al., 2019).

Chen et al., 2019

Chen et al. (2019) conducted a study using data from 1458 air quality monitoring stations in mainland China from 2013 to 2017 exploring the correlation between $PM_{2.5}$ and ozone on seasonal and diurnal temporal scales. According to the study, precursors to $PM_{2.5}$ include oxides of Sulphur, Nitrogen and VOCs. VOCs are a common precursor to both $PM_{2.5}$ and ozone. The study generally observed a positive correlation between $PM_{2.5}$ and ozone during summer season and a negative correlation during winter and other seasons. It is also to be noted that the study classifies correlation coefficients more than 0.4 in magnitude to be "strong relationships." During summers, high ozone concentrations, low $PM_{2.5}$ concentrations and high Pearson's correlation coefficient (r) were observed. In winter, ozone concentrations were low, $PM_{2.5}$ concentrations were high and Pearson's correlation coefficient was low. It was observed that Pearson's correlation coefficient tended to be positive when O_3 concentration was high, and $PM_{2.5}$ concentration was low; and vice-versa. On a diurnal scale, r tended to be minimum at approx. 10:00 hrs. and maximum at approx. 15:00 hrs. Values of r have been plotted seasonally, which exhibits a trend of having negative Pearson's correlation coefficient at high concentration of $PM_{2.5}$. However, relationship between Pearson's correlation coefficient and O_3 was not apparent.

The reason for having positive correlation between O_3 and $PM_{2.5}$ in summer season is because of complex chemical reactions occurring. Gaesous pollutants (SO_2, NO_x, NH_3) and VOCs undergo condensation to form secondary organic aerosols (SOA) and particulate matter ($PM_{2.5}$). These reactions are promoted at higher temperatures, under solar radiation, low windspeed and under ozone that provides an oxidizing environment, thereby causing a positive correlation between ozone and $PM_{2.5}$. It is to be noted, however, that in China, summers have been said to be warm, but having high precipitation, as per the study.

During winters, the authors reason that as $PM_{2.5}$ levels increase, the extinction effect and absorption of radiation during intermixing of particulate matter becomes dominant, thereby causing a negative correlation between O_3 and $PM_{2.5}$. $PM_{2.5}$ also acts as a sink of HO_2 (Hydroperoxy) radicals, thereby bolstering O_3 production. Additionally, during winters vehicular exhausts increase as the vehicles start slowly and may experience knocking problems. Low mixing heights, low wind speeds and temperature inversions exacerbate the situation.

Further, the study has also explored spatial variability in trends observed. Where temperatures and rainfall are low (Inland and Northern China), correlation coefficient is observed to be more negative. In Southern, Eastern and Coastal China, where temperatures and rainfall are higher, correlation coefficient tends to be positive. Authors further explain that monsoons tend to have a cleansing effect that reduce both O_3 and $PM_{2.5}$, with overcast weather decreasing ozone formation. It is also possible that stable conditions brought by monsoon air mass facilitates $PM_{2.5}$ formation, while ozone is being formed simultaneously due to photochemical reactions (Chen et al., 2019).

Chen et al. (2020)

Chen et al. (2020) discovered that Stratosphere Troposphere Exchange (STE) increases $PM_{2.5}$ concentration. This happens because additional ozone increases atmospheric oxidation capacity forming Secondary Organic Aerosols (SOA). STE’s impact is more pronounced during winter and spring when inherent ozone and oxidation capacity is low. Diurnally, the highest enhancements in $PM_{2.5}$ are observed in the morning due to the accumulation of pollutants overnight and reduced mixing in the atmosphere (Chen et al., 2020).

Dai et al., 2021

Dai et al. (2021) investigated relationship between ozone and $PM_{2.5}$ in the Yangtze River Delta (YRD) from 2013 to 2019. For overall for annual concentrations, the two seem to be negatively correlated. But they exhibited a weak positive correlation during warm months (Dai et al., 2021).

Sharma et al., 2021

Sharma et al. (2021) have measured parameters at only one location at CSIR-National Physical Laboratory in Delhi. Based on this they have observed positive correlation between ozone and NO_x and a negative one with NMHC. The study observed that ozone concentration was more sensitive to NO_x than NMHC (Sharma et al., 2021).

Wang et al., 2023

Wang et al. (2023) conducted a detailed study was conducted from 2015 to 2019, focusing on Eastern China, utilizing data from 883 monitoring locations to analyze the relationship between $PM_{2.5}$ and O_3 across three different regions. Despite stringent air quality measures initiated in 2013, $PM_{2.5}$ levels still exceed standards while O_3 levels are on the rise, indicating a shifting air pollution pattern in China. Both $PM_{2.5}$ and O_3 share common precursors, and their concentrations are influenced by various meteorological conditions; for instance, high temperatures and low wind speeds promote O_3 formation, whereas low temperatures and stagnant conditions favor

$PM_{2.5}$ accumulation.

The study found that at high $PM_{2.5}$ concentrations, typically, a negative correlation exists with O_3, notably with an annual average of about 80 μg/m^3 in Nanjing in 2008. However, this correlation turns positive in summer and has recently shown a tendency to be weakly positive or remain negative in winters, due to substantial emissions from heating fuels which boost $PM_{2.5}$ levels and poor meteorological dispersal conditions. Interestingly, the correlation between $PM_{2.5}$ and O_3 becomes more positive as $PM_{2.5}$ levels decrease, influenced strongly by temperature, which not only enhances the generation of secondary particulate matter under high conditions but also reduces the inhibitory effects of $PM_{2.5}$ on ozone production when low.

Spatially, the correlation exhibits notable north-south and seasonal variations; it is generally more positive in southern regions and during summer, turning negative or weakly positive during colder months. This shift suggests a dynamic interplay between air pollution and climatic factors across different parts of Eastern China. Furthermore, the study observed that while $PM_{2.5}$ pollution days decreased annually by 8.6%, O_3 pollution days increased by 19.2%, underscoring the evolving nature of air quality issues in the region. High temperatures and low relative humidity greatly enhance O_3 production, whereas low temperatures, low wind speeds, and low planetary boundary layer heights promote the accumulation of surface $PM_{2.5}$. Relative humidity was negatively correlated with the O_3 concentration and positively correlated with the $PM_{2.5}$ concentration in the NCP, but was negatively correlated with it in the YRD and PRD.

PBLH was positively correlated with the O_3 concentrations and negatively correlated with the $PM_{2.5}$ concentrations. Intense solar radiation is a key factor in the formation of O_3, often associated with a high planetary boundary layer height (PBLH). While an increased PBLH aids in the dissipation of O_3, the photochemical reactions driving ozone generation may outweigh the dispersion effects, especially as temperatures rise. RH was positively correlated with $PM_{2.5}$ (till a threshold precipitation) and negatively correlated otherwise, and it was negatively correlated with the O_3 concentration. High humidity enhances the formation of secondary aerosols through aqueous-phase aerosol chemistry. Generally, high wind speeds help disperse $PM_{2.5}$ and O_3. It is noteworthy that the O_3 concentrations exhibited a weak positive correlation in one region. This may be because the high WS reduced the $PM_{2.5}$ and thus reduced the inhibitory effect of the $PM_{2.5}$ on O_3 generation.

This nuanced study highlights the complexities of air pollution control, particularly in a region with diverse meteorological and geographical influences, and underscores the critical need for region-specific strategies in managing air quality (Wang et al., 2023).

Yadav et al., 2023

The study conducted by Yadav et al. delves into the intricate relationships between particulate matter ($PM_{2.5}$) and ozone (O_3) across different urban settings in India, examining how these relationships change with the seasons—specifically comparing summer and winter scenarios. In cities like Delhi and Bengaluru, the study observed a negative correlation between $PM_{2.5}$ and O_3 during winter. This means that when $PM_{2.5}$ concentrations are high, ozone levels tend to be lower. This phenomenon occurs because particulate matter can block or absorb sunlight, which is essential for the photochemical reactions that produce ozone. Therefore, high levels of particulates can inhibit the formation of ozone, which relies heavily on solar radiation. In contrast, during the summer months in Bengaluru, there is a positive correlation between these two pollutants. In this case, higher temperatures and more intense sunlight not only increase the rate of ozone formation through enhanced photochemical reactions but also contribute to the secondary formation of particulate matter. This suggests that both pollutants are being driven by similar conditions—mainly temperature and solar radiation. Further, higher humidity can facilitate the formation of secondary organic aerosols, a component of $PM_{2.5}$. Wind speed affects the dispersion and dilution of pollutants; calmer conditions might lead to higher concentrations of pollutants due to less dispersion, while higher wind speeds can disperse pollutants more widely, potentially lowering local concentrations but spreading pollution over a broader area.

During winter, Delhi experiences a negative correlation between $PM_{2.5}$ and O_3. Several factors contribute to this pattern (Yadav et al., 2023):

- Reduced Solar Radiation: Winter months see lower levels of sunlight due to shorter days and more frequent foggy and overcast conditions. Since sunlight drives the photochemical reactions necessary for ozone formation, less sunlight means less ozone production.
- High Levels of Particulates: Increased particulate matter during winter can absorb and scatter solar radiation, further reducing the sunlight available for ozone formation. Additionally, particulate matter can also provide surfaces for heterogeneous reactions where ozone can be destroyed.
- Stable Atmospheric Conditions: The colder temperatures bring about more stable atmospheric conditions with less vertical mixing. This stability often results in a shallower boundary layer (the part of the troposphere directly influenced by the

surface and where we experience weather and pollution). With pollutants trapped closer to the ground, higher concentrations of particulates are common, and the dispersal of pollutants is limited.

- Temperature Inversions: Common during winter, temperature inversions occur when a layer of warm air overlays cooler air near the surface, further trapping pollutants like $PM_{2.5}$ and reducing the vertical dispersion that might otherwise disperse ozone.

Conversely, during summer, the study found instances of both non-significant and positive correlations between $PM_{2.5}$ and ozone.

- Increased Solar Radiation: With longer days and more intense sunlight, there's an increase in photochemical activity, leading to higher ozone formation. The sunlight not only drives the formation of ozone from its precursors (NO_x and volatile organic compounds) but also contributes to the secondary formation of particulate matter.
- Higher Temperatures: Elevated temperatures can increase the rate of photochemical reactions, boosting ozone production. Higher temperatures also lead to a deeper boundary layer, which can dilute pollutants but also allows for the vertical accumulation of ozone formed aloft to mix down to the surface.
- Variable Particulate Matter Effects: While particulate matter in summer can still absorb sunlight, the overall higher levels of radiation and heat often offset this effect by enhancing ozone production. Additionally, certain types of particulate matter can act as surfaces for photochemical reactions that generate more secondary organic aerosols, contributing to both $PM_{2.5}$ and ozone levels.

2.4 Research Gap

Understanding the dynamics of ozone (O_3) and its variations in Delhi is crucial for multiple reasons. Ozone, a secondary pollutant, forms through complex chemical reactions involving precursor pollutants such as nitrogen oxides (NO_x) and non-methane volatile organic compounds (NMVOCs) in the presence of sunlight. Given that Delhi is characterized by high population density, congested roads, and significant industrial activities, the study of ozone variations and its influencing factors is indispensable for effective air quality management and public health protection.

Variations in concentrations of ozone are observed to be dependent on complex chemical reactions and meteorological parameters. As highlighted in the literature review, these variations can change spatially and temporally, exhibiting diurnal as well as seasonal fluctuations. Despite extensive global research on ozone, studies focusing on its interaction with other parameters, particularly in the Indian context, remain limited. Specifically, there is only one notable studies exploring the relationship between $PM_{2.5}$ (particulate matter with a diameter of less than 2.5 micrometers) and ozone in Delhi: Yadav et al. (2023). Yadav et al. (2023) studied the relationship using parameters such as ozone, NO_x, temperature, relative humidity, wind speed, and $PM_{2.5}$. This gap in research is significant because understanding the interplay between $PM_{2.5}$ and ozone can inform targeted pollution control strategies. A thorough understanding of this relationship is essential for regulatory bodies to formulate policies that prevent the co-pollution of $PM_{2.5}$ and ozone. A theory regarding variations in ozone and $PM_{2.5}$ in context of Delhi may help regulatory bodies formulate policies to prevent co-pollution of $PM_{2.5}$ and ozone. Efforts by regulatory authorities to reduce pollution in

Delhi include measures included in Graded Response Action Plan (GRAP) and National Clean Air Programme (NCAP). Learning from China's experience, where successful pollution-reduction measures managed to reduce particulate matter pollution but inadvertently caused an increase in ozone concentration, it is prudent to further explore the relationship between ozone and $PM_{2.5}$ in Delhi. This knowledge will aid in developing effective strategies to manage both pollutants simultaneously.

2.5 Scope and Objectives

The current study is an exploratory analysis of variations in ozone in Delhi on diurnal and seasonal timescales. The study also seeks to explore the factors on which it depends, with particular attention to exploring the correlation between ozone and $PM_{2.5}$. In the current exploratory analysis, data from six stations in Delhi were used to analyse temporal variations in ozone on diurnal and seasonal timescales. All parameters that could influence ozone formation monitored by CAAQMS ($PM_{2.5}$, NO_2, NO, CO, NH_3, MAH, windspeed, relative humidity, temperature, solar radiation) were considered. Following this, the key parameters found to be influencing ozone were considered more closely.

The specific objectives of the study were as follows:

1. To analyse the trends in O_3 formation in Delhi over a six-year period.
2. To determine influencing factors for O_3 formation.
3. To explore nature of correlation between O_3 and $PM_{2.5}$.

Chapter 3: Study Area and Site Selection

3.1 Study Area: Delhi

Indian capital, Delhi is bordered by Uttar Pradesh to its east and the state of Haryana borders it from all other directions. It spans an area of about 1483 km^2. The latitudes binding are 28◦24′17″ and 28◦53′ N. The binding longitudes are 76◦50′24″ and 77◦20′37″ E. As per the Census, 2011 Delhi has a population of over 1.6 crores. Delhi continues to grow owing to urbanization, rising population and rising living standards in general. In 2022, Delhi received a total rainfall of approx. 811.7 mm, receiving an average annual rainfall of 774.4 mm (Delhi Statistical Handbook, 2023). Due to its geographical location, Delhi experiences a semi-arid climate, with hot summers and cold winters. The temperature can vary from as high as about 45^{o}C during summer season to as low as 4^{o}C during the winter season. Summer is characterised by hot dry winds (loo), winds from Thar desert, dry and hot days. After the southwest monsoon, winds are known to blow from northwest direction in the post-monsoon and winter season (NCERT, 2022). The month-wise seasonal classification for the present study has been done separately and has been described subsequently. The ambient air quality in Delhi shares characteristics with the Indo-Gangetic Plains due to similar climatic conditions (Sharma et al., 2021). In winter, reduced mixing heights limit pollutant dispersion, as the region experiences low wind speeds and high relative humidity. Delhi is infamous for being one of the most polluted cities of the world as anthropogenic pollution combined with unfavourable meteorological conditions adversely affect

Delhi's air quality.

3.2 Site Selection

In the present study six Continuous Ambient Air Quality Monitoring Stations (CAAQMS) were selected. UV Photometric / Chemiluminiscence being used to monitor ozone using analysers at CAAQMS according to "Technical Specifications For Continuous Ambient Air Quality Monitoring (CAAQM) Station (Real Time)" by CPCB. The criteria for selecting these stations, in order of importance for the present study, is as follows:

- Availability of hourly-data for important parameters, especially for ozone and $PM_{2.5}$, during the study period (2018-2023).
- Diversity in types of surroundings of each station.
- Geographical representativeness for Delhi on a macro-scale.

A screenshot showing locations of all stations selected for the study has been placed as Fig. 3.1.

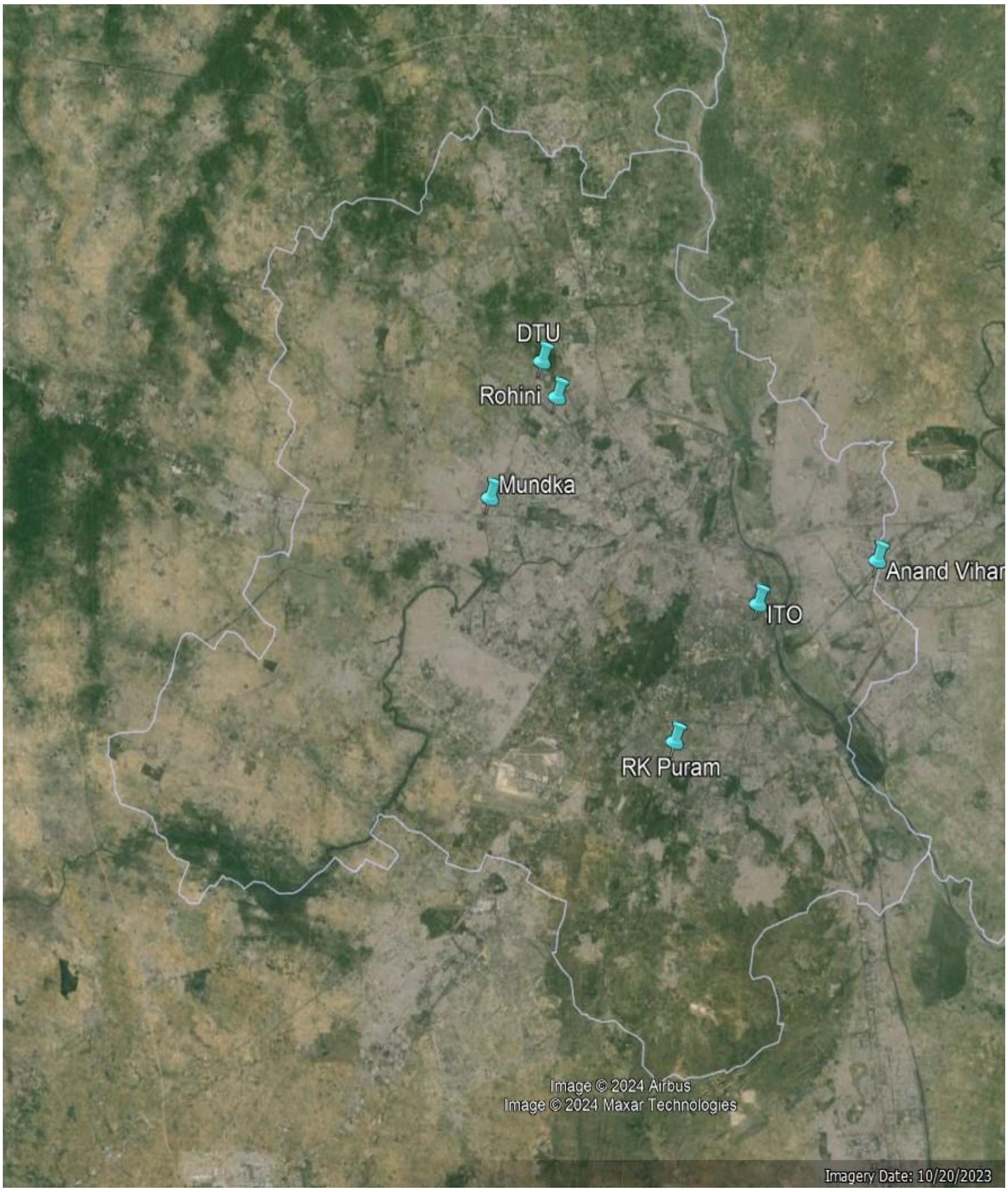

Figure 3. 1 Monitoring site selection in Delhi

Table 3.1 provides approximate geographical coordinates of the CAAQM Stations considered for the study. The type of area has also been mentioned based on past literature (Dhawan et al., 2023) and visual observation.

Table 3. 1 CAAQMS Locations and Area types

S.No.	CAAQM Station	Latitude (degrees East)	Longitude (degrees North)	Type of area around station
1	Anand Vihar	28.65	77.32	Traffic-dominant
2	DTU	28.75	77.11	Institutional
3	ITO	28.63	77.24	Traffic-dominant
4	Mundka	28.68	77.08	Commercial
5	RK Puram	28.56	77.19	Residential
6	Rohini	28.73	77.12	Residential

DTU and Rohini represented north Delhi. RK Puram represented South Delhi. Anand Vihar represented East Delhi, while ITO was assumed to represent Central Delhi. Mundka was assumed to represent western part of Delhi. DTU represents an institutional area with relatively high green cover. Rohini and RK Puram represented residential areas. ITO and Anand Vihar represented traffic-dominant areas.

Therefore, the stations selected for the present study was expected to provide a good representation of Delhi's air quality.

Chapter 4: Methodology

An important aspect that needs to be considered while studying air pollution problems is the meteorology of the region. Meteorology literally means science of atmospheric phenomena. It involves the study of dynamics of the atmosphere. Meteorology mainly depends on factors like sunlight, precipitation, humidity, temperature profile, wind direction and wind speed. Therefore, the present study not only considered pollutants, but also meteorological parameters. Data cleaning, validation and appropriate bifurcation was done for all parameters monitored by CPCB's CAAQMS. In this study, the following parameters were considered:

Table 4. 1 Parameters considered - Units and Abbreviations used

S.No.	Parameter	Unit	Abbreviation used
1	Particulate Matter < 2.5 µm	µg/m³	$PM_{2.5}$
2	Nitrogen Monoxide	µg/m³	NO
3	Nitrogen Dioxide	µg/m³	NO_2
4	Ammonia	µg/m³	NH_3
5	Carbon monoxide	mg/m³	CO
6	Ozone	µg/m³	Ozone/O_3
7	Benzene	µg/m³	Benzene
8	Toluene	µg/m³	Toluene
9	Xylene	µg/m³	Xylene

10	Ortho Xylene	µg/m³	O Xylene
11	Ethylbenzene	µg/m³	Eth-Benzene
12	Meta-xylene and Para-xylene	µg/m³	MP-Xylene
13	Atmospheric Temperature	°C	AT
14	Relative Humidity	%	RH
15	Wind speed	m/s	WS
16	Wind direction	deg	WD
17	Solar radiation	W/m²	SR
18	Monocyclic Aromatic Hydrocarbon (MAH) (=Benzene+Toluene+Xylene + O Xylene + Eth-Benzene + MP-Xylene)	µg/m³	MAH

Subsequently, the parameters may be referred to by their abbreviations and the units for them would be the same as stated in the aforementioned table.

4.1 Data Validation

In the present study, data at hourly intervals was downloaded from 1st January 2018 to 31st December 2023 from the Central Pollution Control Board (CPCB) website (URL: airquality.cpcb.gov.in). After downloading the data, the data for each station was validated using the following data validation protocol, which is listed step-wise as follows:

- Negative values, if obtained for parameters that could not have negative values, have been replaced by "NA".
- If value for any parameter repeats consecutively for more than four times consecutively, all such values have been replaced by "NA".
- Values below lower detection limit (LDL) have been replaced by the numeric LDL value for that parameter (thus giving a conservative estimate).
- Absurd values for parameters (such as where PM_{10} is observed to be greater than $PM_{2.5}$) have been replaced by "NA".

4.2 Preparation of Data for Analysis

After validation of data, data for each station was combined together to represent the air quality of Delhi. Averaging out such voluminous amount of data over a period of six years was expected to better represent seasonal trends of air quality in Delhi.

The data was then been bifurcated month-wise and season-wise for analysis of air quality data on different temporal scales.

A flowchart depicting the methodology has been placed as Fig. 4.1.

Figure 4. 1 Overview of Data Analysis Procedure

Data analysis was conducted using Microsoft Excel and "Jeffreys's Amazing Statistics Program" (JASP). JASP is an open-source statistical software based on R.

4.3 Classification of Seasons

Classification of seasons of Delhi for the purpose of this study was done based on mean temperature of each month. Months having broadly similar characteristics were clubbed together. Such classification is in line with the mean monthly climate data available online for Palam, Ayanangar and Delhi Ridge ("Climate of Delhi," 2024). Such a classification was deemed necessary to better streamline the subsequent statistical analysis, compile the results efficiently and make the same readilyunderstandable for regulatory bodies. The classification of seasons is as follows:

Table 4. 2 Classification of Seasons

S.No.	Season	Months	Remarks in context of the present study
1	Winter	December, January, February	These months have similar temperature ranges (Mean daily temperature less than 25^oC). Solar insolation is low from winter solstice to spring equinox. Temperature inversion is observed in Delhi with elevated pollution levels. Western disturbances may cause some rainfall.
2	Spring	March	Moderate temperatures (Mean daily temperatures between 25 and 30^oC). After western disturbances and NE monsoon have ceded, RH is more than that of summer but less than that of winter in our study. Increased pollination is expected.
3	Summer	April, May, June	Dry weather (typically RH observed <50% in our study) till mid-June. High temperatures (Mean temperature > 30 ^{o}C).

4	Monsoon	July, August, September	High relative humidity (typically RH observed >50% in our study).
5	Post-monsoon	October, November	With withdrawing monsoon, RH is less than preceding monsoon and succeeding winter in our study. “October Heat” phenomenon observed during this period. Period of stubble burning, festivities, etc. that may cause elevated pollution levels.

The above classification seems to be optimally conducive to the objective of the present study and the said classification was observed to ensure that trends observed are not diluted or averaged-out in any way, allowing one to better infer results obtained.

Chapter 5: Results and Discussion

5.1 Diurnal variations

Data for the years 2023 (latest available year) and 2020 (during COVID-19 lockdown) were used for observing diurnal variations in ozone and other related pollutants in every month of the year. This comparison was drawn to see if trends in variations of pollutants depend on their absolute concentrations. In 2020, lockdown was announced across the nation from late-March to June. Following this, the lockdown was relaxed in a phase-wise manner. It is assumed that commercial and vehicular activities throughout 2020 was much lower than in 2023. Therefore, it is presumed (and which was corroborated by data being used) that the year 2020 exhibited lower levels of pollution for all pollutants considered except for ozone.

Values at each hour of the day were averaged for the entire month and the same were plotted on a graph. Sample graphs for month of March 2023 and March 2020 have been placed as Fig. 5.1 and 5.2. All graphs for diurnal variations are annexed as Appendix-II. However, for analysing descriptive statistics for data, months were classified into seasons to analyse seasonal trends in subsequent sections.

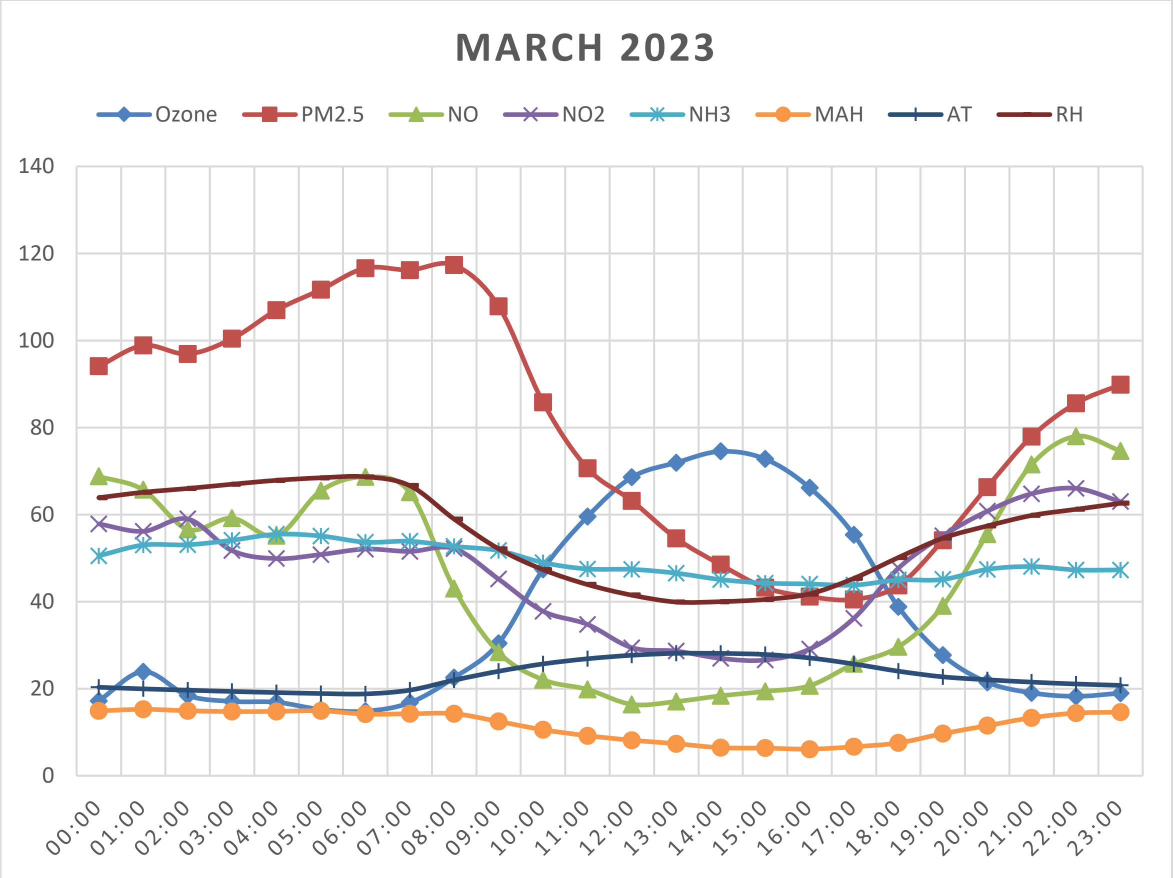

Figure 5. 1 Diurnal variations in parameters considered (March 2023)

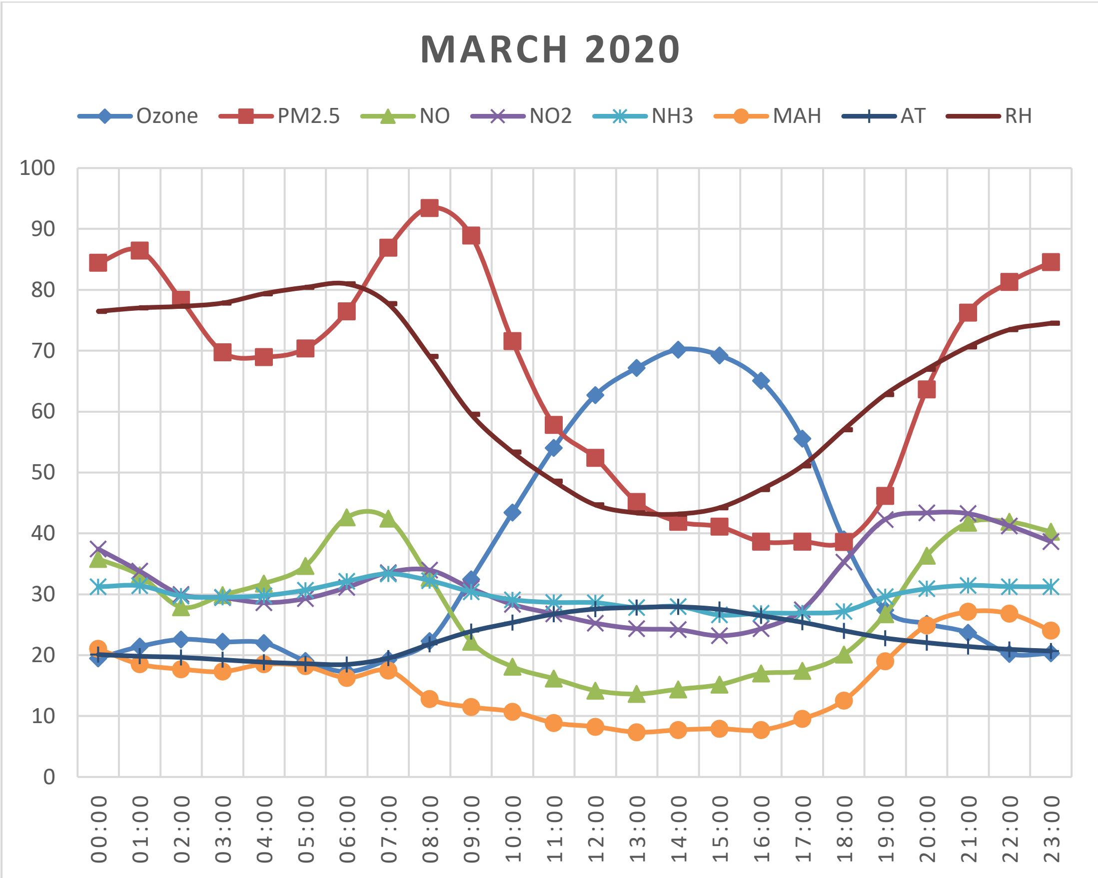

Figure 5. 2 Diurnal variations in parameters considered (March 2020)

Parameters considered were as follows: Ozone, $PM_{2.5}$, NO, NO_2, NH_3, MAH, AT, RH. SR was also compared, but is not been shown on the graph; while CO was not considered for visual comparison graphically due to large difference in scales of concentration in which they were found to occur. The graphs for diurnal variations suggested that the time-lag between ozone and parameters such as $PM_{2.5}$, CO, NO, NO_2, RH, WS, SR was not significant on an hourly time-scale throughout the year.

This concurred with literature citing high reactivity with such parameters and short lifespan in troposphere of ozone. In general, concentration of ozone peaked between 13:00 and 15:00 during both – 2020 and 2023. However, during lockdown in Delhi during April-June 2020, the ozone concentration curve was slightly negatively skewed and the peak concentration of ozone occurred at around 16:00. Graphs showing diurnal variations in May, 2020 and June, 2020 (when there was little human activity outdoors due to lockdown) is attached as Figures 5.3 and 5.4.

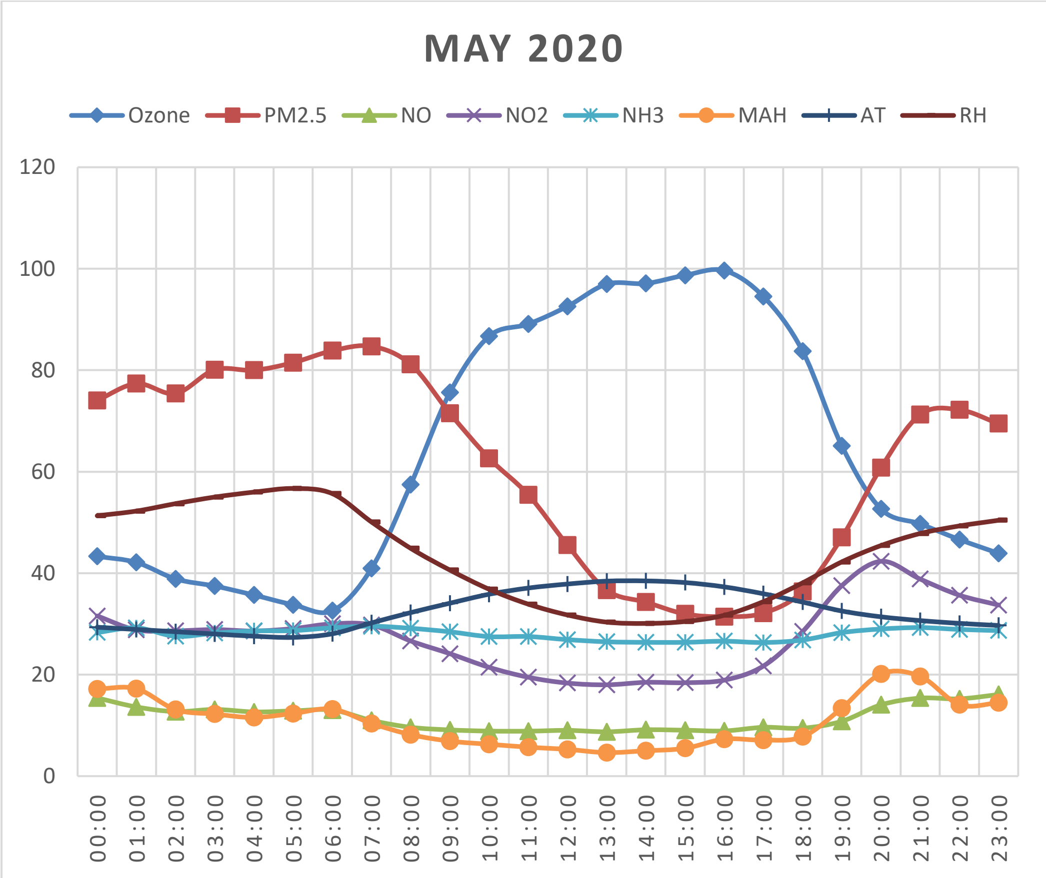

Figure 5. 3 Diurnal variations in parameters considered (May 2020)

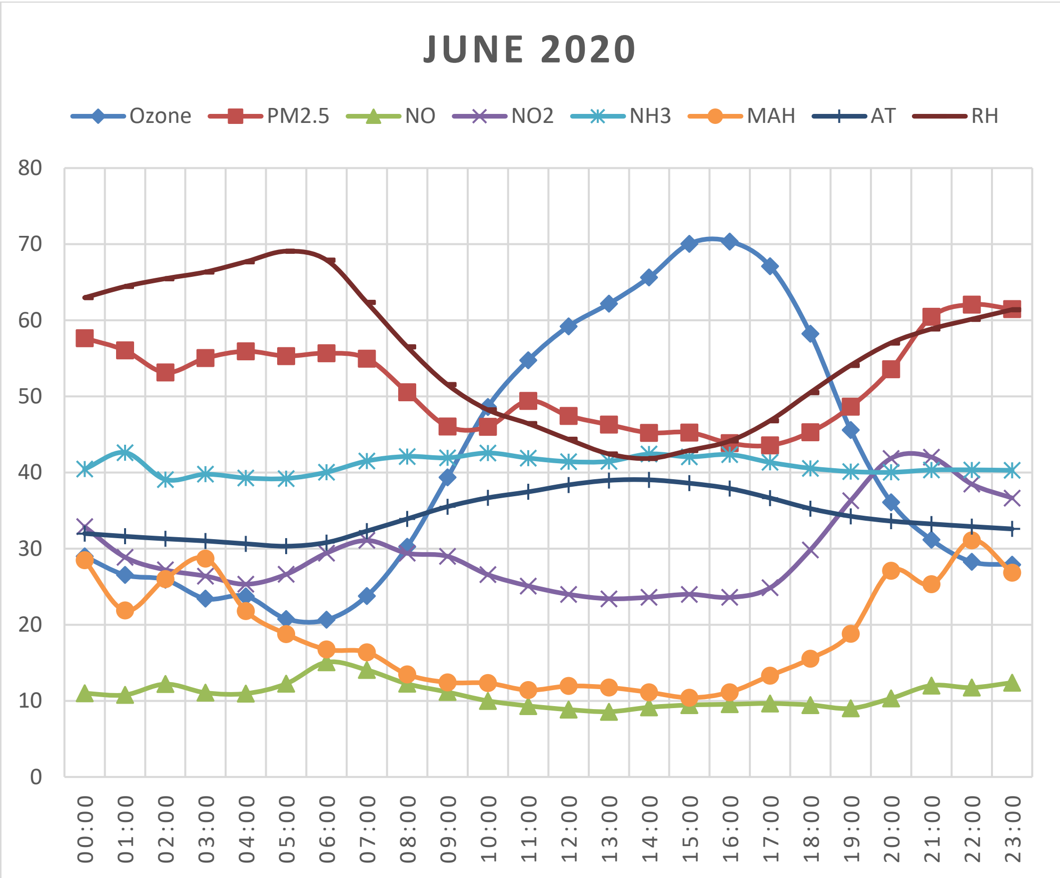

Figure 5. 4 Diurnal variations in parameters considered (June 2020)

Both months- May, 2020 and June, 2020 showed lower concentrations of precursors of O_3, but trends similar to the usual scenario exhibited during the same months of different years. Such diurnal trends indicated that correlations between ozone and other parameters considered followed a similar trend every year on diurnal basis regardless of quantum of concentrations in which they occurred on a daily-average basis. The reason for O_3 concentration being skewed negatively during lockdown period may have been due to unavailability of residual anthropogenic precursors from the previous day and little new emissions of these precursors during the morning hours. Biogenic VOCs were expected to peak during the afternoon hours. Therefore, the peak in O_3 concentration was delayed by about two hours.

Examining the graphs visually, a negative correlation seemed to exist between ozone and RH, $PM_{2.5}$, NO, NO_2, MAH and RH. A positive correlation seemed to exist between ozone and AT and SR. However, no clear trend could be inferred from the graphs visually in respect of NH_3. These diurnal trends were broken during months of July and August. This may have been due to the cleansing effect of rain, changes in emission of biogenic VOCs, etc.

Diurnal variations followed trends that did not seem out of the ordinary, which isexplained as follows: Ozone formation begins as the day temperature begins to rise in the morning; and O_3 concentration peaks during afternoons. MAH, NO and NO_2 are precursors to O_3 formation and are consumed in formation of O_3 and thus exhibit a negative correlation. RH impedes ozone formation. The reason for variation for $PM_{2.5}$ may be more complex. If single scattering albedo (SSA) of $PM_{2.5}$ is less and its absorption potential is more, then it can impede ozone formation. For a city like Delhi, black carbon, haze, etc. often occurs and thus this reason may be a likely explanation. Moreover, during day-time, the mixing height typically increases allowing for more dispersion of $PM_{2.5}$ and thus reducing its concentration. The reasons for the exhibited trends have been well-explained in the literature review section.

5.2 Seasonal Analysis

Data from calendar years 2018 to 2023 were considered for the present study. Seasonal variations in tropospheric ozone, and its relationship with other relevant parameters were studied statistically. Table 6.1 shows the seasonal means of all relevant parameters chronologically. The values are colour coded on red-green scale, with red indicating higher values and green lower.

Table 5. 1 Mean seasonal concentrations of parameters considered

Period	O_3	$PM_{2.5}$	NO	NO_2	CO	NH3	AT	RH	WS	SR
Spring 18	45.53 ± 38.451	100.58 ± 54.512	47.72 ± 42.196	61.25 ± 24.857	1.38 ± 1.043	43.32 ± 11.472	24.28 ± 5.442	48.22 ± 19.461	1.12 ± 0.662	149.06 ± 173.249
Summer 18	37.61 ± 26.609	94.43 ± 55.669	40.21 ± 38.673	64.62 ± 38.145	2.17 ± 1.979	52.48 ± 22.395	32.09 ± 5.258	40.03 ± 15.326	1.87 ± 1.614	205.08 ± 185.45
Monsoon 18	19.57 ± 14.435	45.05 ± 21.676	19.82 ± 26.044	29.44 ± 12.818	0.93 ± 0.445	38.68 ± 14.656	29.47 ± 3.54	73.61 ± 15.509	1.22 ± 0.584	142.85 ± 166.013
Postmonsoon 18	35.29 ± 27.91	192.54 ± 107.146	96.41 ± 83.173	79.96 ± 28.524	2.15 ± 1.261	50.83 ± 14.316	23.14 ± 5.686	54.95 ± 18.619	0.86 ± 0.457	117.24 ± 144.413
Winter 18-19	28.91 ± 19.742	210.77 ± 125.866	83.24 ± 82.936	66.22 ± 25.428	2.12 ± 1.479	46.14 ± 15.83	14.39 ± 4.737	58.7 ± 16.038	1.01 ± 0.598	101.48 ± 131.105
Spring 19	30.18 ± 23.323	95.87 ± 50.645	38.72 ± 35.991	52.25 ± 15.636	1.26 ± 0.583	31.39 ± 7.916	21.52 ± 6.053	46.67 ± 16.409	1.24 ± 0.671	151.95 ± 182.383
Summer 19	44.91 ± 33.91	87.7 ± 56.404	39.37 ± 43.473	53.42 ± 21.838	1.57 ± 0.749	38.12 ± 12.053	32.72 ± 5.88	34.96 ± 15.21	1.38 ± 0.784	172.84 ± 191.084
Monsoon 19	25.37 ± 14.031	44.53 ± 22.26	18.92 ± 16.612	33.27 ± 10.816	1.26 ± 0.425	32.75 ± 8.008	30.62 ± 3.392	65.32 ± 12.762	1.2 ± 0.566	131.49 ± 150.512
Postmonsoon 19	31.28 ± 24.113	178.31 ± 137.924	50.08 ± 43.729	45.19 ± 15.072	1.59 ± 0.927	34.78 ± 9.641	24.67 ± 4.559	65.07 ± 14.069	0.9 ± 0.416	100.91 ± 132.779
Winter 19-20	27.75 ± 18.168	176.74 ± 98.486	53.36 ± 48.134	47.51 ± 19.14	1.66 ± 1.117	43.21 ± 15.456	14.59 ± 3.92	72.97 ± 15.276	1.08 ± 0.591	96.11 ± 128.828
Spring 20	35.89 ± 22.709	65.91 ± 39.883	27.76 ± 24.766	31.92 ± 15.715	0.91 ± 0.572	29.78 ± 7.305	22.79 ± 4.183	64.03 ± 16.048	1.29 ± 0.72	145.04 ± 177.746
Summer 20	53.44 ± 28.7	56.21 ± 34.833	10.75 ± 5.6	25.13 ± 13.256	1.06 ± 0.399	31.41 ± 9.529	31.98 ± 5.142	48.2 ± 14.253	1.24 ± 0.648	152.06 ± 182.499
Monsoon 20	28.19 ± 13.033	38.41 ± 20.016	17.71 ± 13.67	29.74 ± 10.587	1.05 ± 0.376	28.94 ± 6.005	32.6 ± 3.057	66.94 ± 11.76	1.16 ± 0.572	136.04 ± 152.761
Postmonsoon 20	32.99 ± 30.538	200.77 ± 140.025	62.89 ± 57.976	55.22 ± 21.109	2.21 ± 1.283	40.83 ± 11.289	25.42 ± 5.733	56.02 ± 15.469	0.83 ± 0.371	100.61 ± 127.638
Winter 20-21	27.75 ± 18.168	176.74 ± 98.486	53.36 ± 48.134	47.51 ± 19.14	1.66 ± 1.117	43.21 ± 15.456	14.59 ± 3.92	72.97 ± 15.276	1.08 ± 0.591	96.11 ± 128.828
Spring 21	33.84 ± 25.287	114.92 ± 62.354	44.08 ± 46.688	45.27 ± 15.778	1.44 ± 0.878	78.61 ± 24.636	24.16 ± 4.764	49.2 ± 14.89	1.32 ± 0.695	125.82 ± 155.532
Summer 21	37.74 ± 26.774	72.53 ± 55.184	19.28 ± 21.846	35.01 ± 18.373	1.42 ± 0.51	59.54 ± 12.328	30.67 ± 5.065	45.22 ± 15.94	1.34 ± 0.746	148.45 ± 169.317
Monsoon 21	27.44 ± 10.381	43.42 ± 19.043	15.92 ± 11.504	25.19 ± 8.187	1.01 ± 0.399	38.04 ± 11.343	32.08 ± 3.226	68.93 ± 13.498	1.17 ± 0.521	118.82 ± 148.513
Postmonsoon 21	30.83 ± 23.827	164.93 ± 120.553	66.48 ± 60.204	54.72 ± 22.838	1.96 ± 1.289	42.03 ± 10.384	24.69 ± 5.59	63.71 ± 15.748	0.88 ± 0.334	109.27 ± 141.04
Winter 21-22	28.47 ± 19.292	182.65 ± 110.686	69.63 ± 72.814	44.21 ± 18.512	1.78 ± 1.161	41.11 ± 11.255	14.88 ± 4.3	71.9 ± 16.728	0.96 ± 0.496	97.67 ± 135.77
Spring 22	34.29 ± 26.583	114.03 ± 54.716	42.45 ± 51.91	42.3 ± 17.977	1.23 ± 0.782	36.58 ± 10.183	25.44 ± 5.847	55.05 ± 17.955	0.99 ± 0.456	156.62 ± 191.69

Summer 22	46.37 ± 35.165	94.89 ± 54.767	35.83 ± 39.93	45.7 ± 19.108	1.23 ± 0.679	41.03 ± 8.293	33.27 ± 4.949	43.92 ± 14.679	1.1 ± 0.528	165.63 ± 187.733
Monsoon 22	37 ± 14.576	39.02 ± 20.146	17.61 ± 14.322	27 ± 9.094	1.01 ± 0.382	35.96 ± 5.917	29.02 ± 2.924	68.03 ± 12.71	1.06 ± 0.511	138.84 ± 164.315
Postmonsoon 22	29.54 ± 23.962	146.12 ± 91.917	70.75 ± 70.412	67.88 ± 34.193	1.74 ± 1.227	50.24 ± 20.823	22.81 ± 4.766	56.33 ± 14.51	0.82 ± 0.336	100.31 ± 134.158
Winter 22-23	23.41 ± 20.181	171.28 ± 90.87	75.57 ± 65.658	58.9 ± 28.335	1.51 ± 0.882	57.85 ± 18.35	16.74 ± 4.737	63.34 ± 14.444	1.05 ± 0.537	76.48 ± 103.309
Spring 23	35.58 ± 25.22	80.5 ± 43.233	45.16 ± 40.542	47.23 ± 22.784	1.24 ± 0.538	49.22 ± 9.636	22.97 ± 3.8	55.46 ± 13.515	1.03 ± 0.458	109.61 ± 137.16
Summer 23	37.19 ± 27.126	66.91 ± 44.33	38.54 ± 39.869	50.57 ± 25.096	1.17 ± 0.588	38.31 ± 8.999	31.51 ± 5.219	51.95 ± 16.569	1.13 ± 0.498	129.8 ± 153.165
Monsoon 23	29.57 ± 13.242	41.97 ± 16.401	19.16 ± 13.452	32.76 ± 12.784	0.88 ± 0.317	43.32 ± 17.999	31.63 ± 2.726	69.15 ± 12.641	1.03 ± 0.442	237.97 ± 170.323
Postmonsoon 23	27.26 ± 21.575	180.62 ± 110.411	64.95 ± 63.624	68.03 ± 38.844	1.92 ± 1.23	50.45 ± 21.101	24.25 ± 5.419	60.17 ± 13.148	0.65 ± 0.308	298.66 ± 129.909

The data in Table 5.1 is shown graphically below:

The following graph illustrates the variations in ozone concentrations and meteorological parameters – AT, RH, WS and SR.

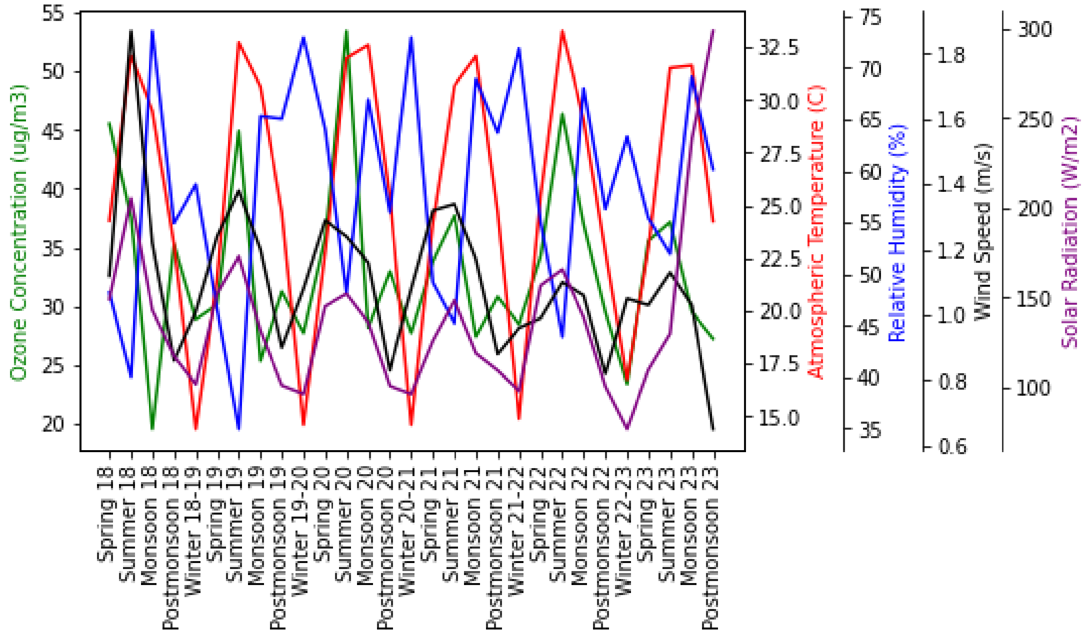

Figure 5. 5 Seasonal variations in concentration of O_3 and meteorological parameters

The following graph shows variations in ozone concentration and other gaseous pollutants: NO, NO_2, CO and NH_3.

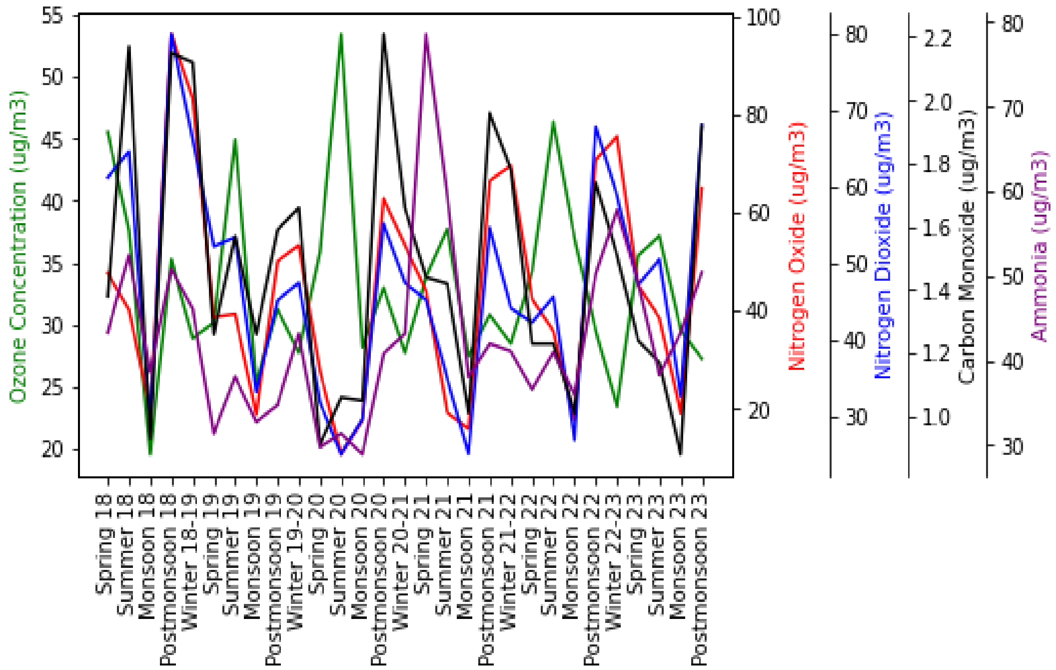

Figure 5. 6 Seasonal variations in concentration of O_3 and gaseous pollutants

However, since the present study was specifically focused on relationship between ozone and $PM_{2.5}$, the following graph illustrates the variation of ozone concentration against $PM_{2.5}$ and meteorological parameters, followed by a graph showing only ozone and $PM_{2.5}$ variations:

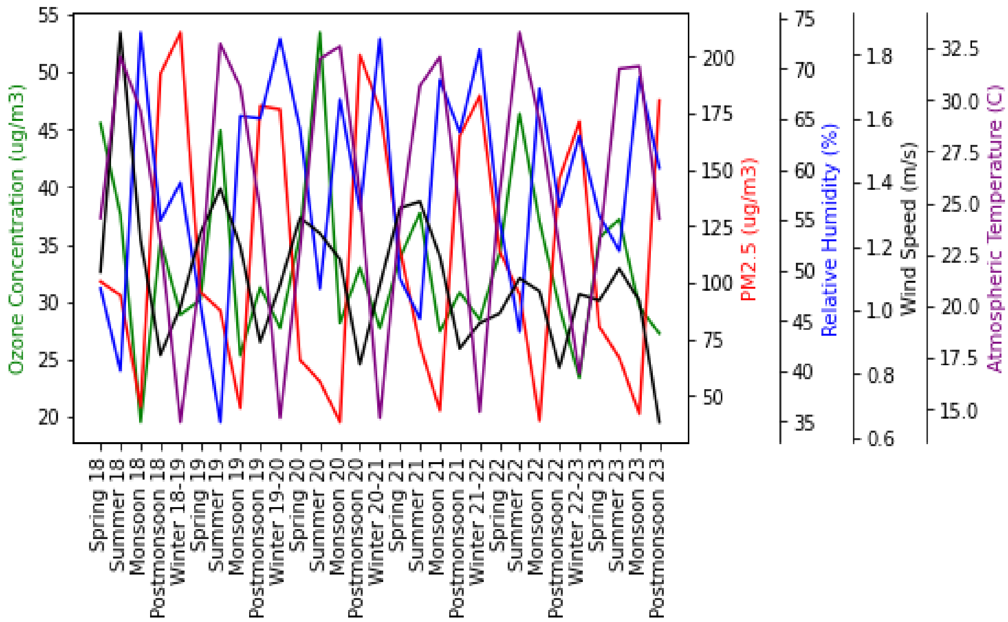

Figure 5. 7 Seasonal variations in concentrations of O_3, $PM_{2.5}$, RH, WS, AT

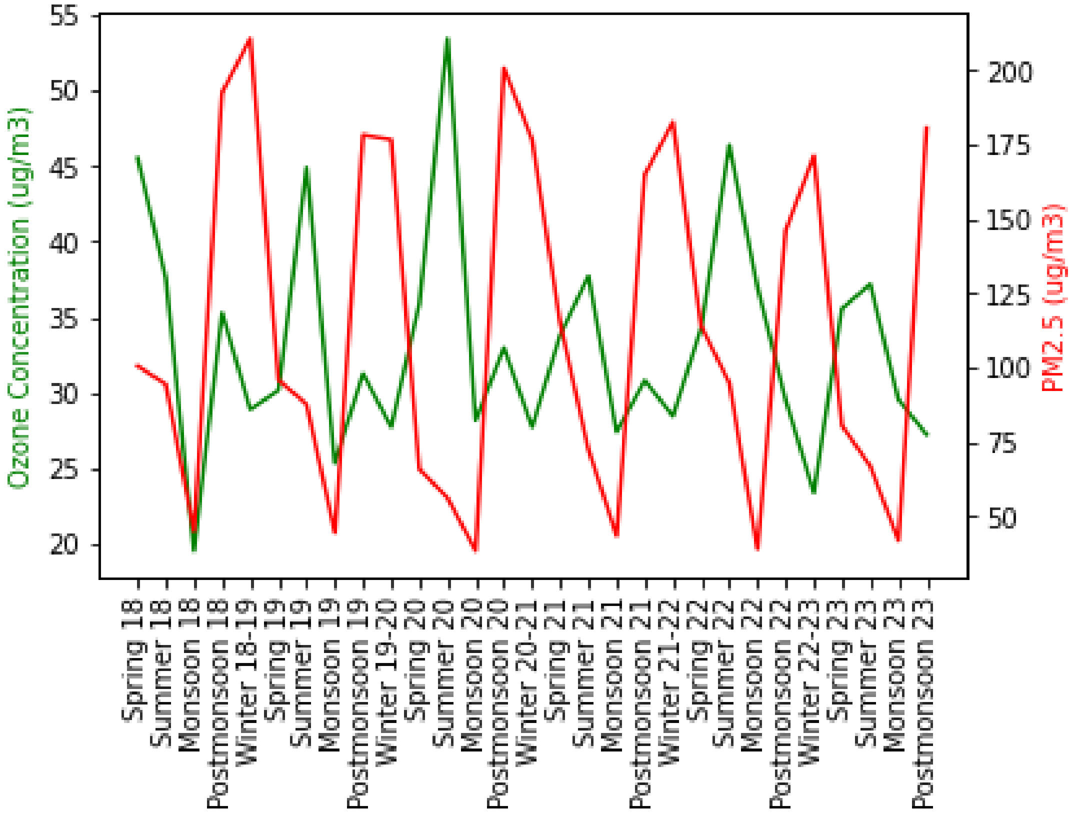

Figure 5. 8 Seasonal variations in concentrations of O_3 and $PM_{2.5}$

The following table shows how the Pearson's Correlation coefficient between ozone and all other parameters considered varied seasonally throughout the years. Colour coding has been done on a red-green scale for each parameter with red indicating lower values and green indicating higher values.

Table 5. 2 Ozone's Correlation Coefficient against other parameters considered

Period	$PM_{2.5}$	NO	NO_2	CO	NH_3	MAH	AT	RH	WS	SR
Spring 18	-0.46	-0.51	-0.51	-0.48	-0.52	-0.34	0.80	-0.77	0.67	0.70
Summer 18	-0.17	-0.35	-0.22	-0.14	-0.18	-0.22	0.53	-0.49	0.17	0.55
Monsoon 18	0.05*	-0.15	-0.04*	-0.13	-0.12	0.01*	0.61	-0.61	0.31	0.54
Postmonsoon 18	-0.31	-0.50	-0.36	-0.44	-0.34	-0.35	0.65	-0.71	0.39	0.67
Winter 18-19	-0.12	-0.28	-0.17	-0.18	-0.08*	-0.08*	0.62	-0.65	0.30	0.60

Spring 19	-0.55	-0.52	-0.60	-0.44	-0.42	-0.50	0.79	-0.82	0.64	0.71
Summer 19	-0.29	-0.44	-0.38	-0.41	-0.01*	-0.38	0.71	-0.64	0.39	0.70
Monsoon 19	0.06*	-0.21	-0.07	-0.10	0.04*	-0.03*	0.50	-0.43	0.06*	0.45
Postmonsoon 19	-0.27	-0.47	-0.26	-0.39	-0.13	-0.40	0.74	-0.81	0.34	0.67
Winter 19-20	-0.30	-0.37	-0.20	-0.34	0.41	-0.20*	0.64	-0.77	0.49	0.62
Spring 20	-0.34	-0.45	-0.32	-0.43	-0.29	-0.33	0.77	-0.83	0.43	0.62
Summer 20	-0.34	-0.33	-0.40	-0.40	0.03*	-0.36	0.50	-0.70	0.39	0.55
Monsoon 20	0.03*	-0.28	-0.21	-0.11	0.09*	0.07*	0.58	-0.57	0.21	0.40
Postmonsoon 20	-0.27	-0.51	-0.44	-0.47	-0.33	-0.32	0.75	-0.79	0.46	0.70
Winter 20-21	-0.30	-0.37	-0.20	-0.34	-0.08	-0.20	0.64	-0.77	0.49	0.62
Spring 21	-0.53	-0.41	-0.43	-0.48	-0.25	-0.31	0.75	-0.77	0.50	0.63
Summer 21	-0.18	-0.30	-0.22	-0.32	-0.25	-0.03*	0.57	-0.60	0.26	0.57
Monsoon 21	0.15	-0.14	-0.03*	-0.03*	0.06*	-0.01*	0.29	-0.22	0.10	0.23
Postmonsoon 21	-0.10	-0.44	-0.34	-0.29	-0.25	-0.27	0.45	-0.75	0.30	0.61
Winter 21-22	-0.36	-0.41	-0.31	-0.39	-0.17	-0.26	0.69	-0.79	0.44	0.65
Spring 22	-0.48	-0.40	-0.40	-0.43	-0.07*	-0.31	0.65	-0.72	0.52	0.69
Summer 22	-0.31	-0.51	-0.50	-0.50	-0.06*	-0.35	0.76	-0.52	0.36	0.67
Monsoon 22	-0.10	-0.33	-0.16	-0.29	0.12	-0.24	0.67	-0.60	0.27	0.50
Postmonsoon 22	-0.32	-0.51	-0.49	-0.47	-0.05*	-0.40	0.81	-0.63	0.37	0.69
Winter 22-23	-0.34	-0.44	-0.31	-0.40	-0.17	-0.32	0.71	-0.78	0.36	0.63
Spring 23	-0.47	-0.50	-0.54	-0.57	-0.37	-0.47	0.85	-0.73	0.46	0.70
Summer 23	-0.30	-0.46	-0.41	-0.42	-0.08*	-0.39	0.57	-0.57	0.42	0.65
Monsoon 23	0.09*	-0.21	-0.14	-0.13	0.06*	-0.04*	0.59	-0.49	0.14	0.30
Postmonsoon 23	-0.30	-0.36	-0.33	-0.37	-0.22	-0.34	0.59	-0.70	0.32	0.47

*: Statistically insignificant due to higher p values ($p>0.01$)

The following table shows the count of number of positive and negative correlations observed over the course of six years.

Table 5. 3 Count of positive and negative correlations of parameters with O_3

	$PM_{2.5}$	NO	NO_2	CO	NH_3	MAH	AT	RH	WS	SR
No. of Positive Correlations	5	0	0	0	7	2	29	0	29	29
No. of Negative Correlations	24	29	29	29	22	27	0	29	0	0
Total	29	29	29	29	29	29	29	29	29	29

Average Correlation coefficients with ozone were calculated season-wise and then each parameter was ranked according to the correlation they had with ozone.

Table 5. 4 Seasonwise ranking of each parameter as per correlation with O3

Season	$PM_{2.5}$	NO	NO_2	CO	NH_3	MAH	AT	RH	WS	SR
Spring 18	9	7	6	8	5	10	1	2	4	3
Summer 18	8	4	6	10	7	5	2	3	9	1
Monsoon 18	8	5	9	6	7	10	2	1	4	3
Postmonsoon 18	10	4	7	5	9	8	3	1	6	2
Winter 18-19	8	5	7	6	10	9	2	1	4	3
Spring 19	6	7	5	9	10	8	2	1	4	3
Summer 19	9	4	8	5	10	7	1	3	6	2
Monsoon 19	7	4	6	5	9	10	1	3	7	2
Postmonsoon 19	8	4	9	6	10	5	2	1	7	3
Winter 19-20	8	6	9	7	5	10	2	1	4	3
Spring 20	7	4	9	6	10	8	2	1	5	3
Summer 20	8	9	4	5	10	7	3	1	6	2
Monsoon 20	10	4	5	7	8	9	1	2	6	3
Postmonsoon 20	10	4	7	5	8	9	2	1	6	3
Winter 20-21	7	5	8	6	10	9	2	1	4	3
Spring 21	4	8	7	6	10	9	2	1	5	3
Summer 21	9	5	8	4	7	10	2	1	6	3
Monsoon 21	4	5	8	8	7	10	1	3	6	2
Postmonsoon 21	10	4	5	7	9	8	3	1	6	2
Winter 21-22	7	5	8	6	10	9	2	1	4	3
Spring 22	5	7	8	6	10	9	3	1	4	2
Summer 22	9	4	5	5	10	8	1	3	7	2
Monsoon 22	10	4	8	5	9	7	1	2	6	3
Postmonsoon 22	9	4	5	6	10	7	1	3	8	2
Winter 22-23	7	4	9	5	10	8	2	1	6	3
Spring 23	8	6	5	4	10	7	1	2	9	3
Summer 23	9	4	7	6	10	8	3	2	5	1
Monsoon 23	8	4	5	7	9	10	1	2	6	3
Postmonsoon 23	9	5	7	4	10	6	2	1	8	3

The following table shows the order in which each parameter influences O_3 season-wise.

Table 5. 5 Overall ranking of each parameter in each season

Order of influence on O_3/Seasons	Spring	Summer	Monsoon	Postmonsoon	Winter	Overall
$PM_{2.5}$	5	9	7	10	5	7
NO	5	3	3	3	4	3
NO_2	7	6	6	6	7	6
CO	5	5	5	5	5	5
NH_3	10	10	8	10	9	10
MAH	9	8	10	8	10	9
AT	3	1	1	4	3	3
RH	1	2	2	1	1	1
WS	4	7	4	7	4	4
SR	2	2	2	2	2	2

It was observed that ozone had the strongest negative relationship with relative humidity; followed by solar radiation and atmospheric temperature. With reference to the parameters considered, $PM_{2.5}$ had a stronger correlation with O_3 than that of MAH and NH_3 only. The strength of correlation of $PM_{2.5}$ with ozone was significantly more during winter and spring season. The non-linear relation with all other parameters considered have been very well-researched in literature for the past four decades. However, research on relation between $PM_{2.5}$ and O_3 is still in its nascent stages. Further, it is to be noted that there was a statistically weak negative linear correlation between ozone and $PM_{2.5}$ that is statistically significant ($p<0.001$). However, literature cites parameters such as NO, NO_2 and CO having negative correlation with ozone as ozone reacts with these pollutants. However, their Pearson's coefficient was also observed in a similar range as that of $PM_{2.5}$. It is also observed that Pearson's coefficient for ozone and $PM_{2.5}$ was comparable to that between ozone and NO_2, and ozone and CO in many seasons. Moreover, Chen et al. (2019) have classified correlation more than 0.4 as "strong"(Chen et al., 2019). This indicates that $PM_{2.5}$ and ozone may have had a relatively strong, albeit not statistically strong, correlation. It is to be noted that ozone's chemical relationships with other gaseous pollutants is non-linear. Therefore, in the present study the terms used to determine strengths of relationships may not be accurate in terms of statistics, but in context of well-established theories in environmental studies, the same may be applicable. Therefore, in context of environmental studies, the relationship may not be assumed to be "weak".

The findings of the study suggested a correlation between ozone and $PM_{2.5}$. However, a theory for establishing a causal relationship between ozone and $PM_{2.5}$ may be established. An attempt at hypothesizing a theory for explaining the variations in correlation between $PM_{2.5}$ and ozone is made in the present study subsequently.

The cyclicity in the variations in correlation coefficients of Ozone and $PM_{2.5}$ was also observed. The same has been shown graphically below:

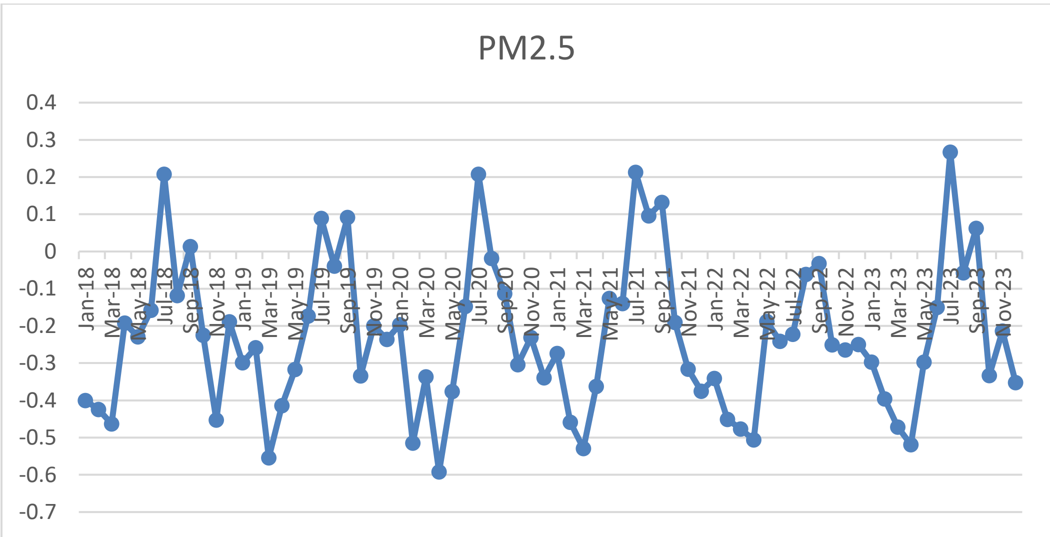

Figure 5. 9 Variations in O_3-$PM_{2.5}$ correlation coefficient (January, 2018-December, 2023)

As per Wang et al. correlation tends to be positive at low $PM_{2.5}$ concentration; and vice-versa (Wang et al., 2023).

The explanation for the trends observed are as follows: It is hypothesized that during winters, there is haze, smog and higher concentrations of $PM_{2.5}$ observed throughout Delhi. Moreover, the high concentration of black carbon and highly absorbing particulate matter reduces solar radiation available for ozone formation (low scattering albedo). Therefore, there exists a statistically weak negative correlation between $PM_{2.5}$ and ozone. $PM_{2.5}$ can be assumed to have a causal influence on ozone. Moreover, there is relatively more RH compared to summer. This is because of mist in air due to lower temperatures, and due to western disturbance.

During summers, the solar radiation and temperature increases. This causes a substantial increase in O_3 levels. The same is the case during spring season. However, there are two important differences. Firstly, during summers, there is incoming winds from the Thar deserts and dry hot winds (loo), which may cause an increase in particulate matter concentration. However, there is also an increase in mixing heights which causes $PM_{2.5}$ concentrations to reduce. The latter factor should dominate as dry winds usually cause an increase in larger sizes of particulate matter. Therefore, there is a negative correlation between ozone and $PM_{2.5}$, but a direct causal relationship between the two is not obvious.

In spring season, the correlation is observed to be highly negative. This seems to be the case because around spring the time the rates of change in $PM_{2.5}$ and ozone seem to be the maximum, wherein $PM_{2.5}$ concentrations are falling and ozone concentrations are increasing. Further, biogenic VOCs may be being released into the atmosphere which increase ozone formation. Rathore et al. and Chen et al. also state that stratosphere-troposphere exchange is maximum during this period (Chen et al., 2020; Rathore et al., 2023). The rates of variation may slow down in summer due to relative increase in $PM_{2.5}$ from dusty winds.

During monsoon, a mildly positive correlation is observed. This trend has been corroborated by similar findings for summer in China. This is because summer season described in China is characteristically similar to monsoon in India (Chen et al., 2019). During monsoon, cleansing effect of rainfall is observed. Wind, that carries relatively less dust, also blows at relatively higher speeds in monsoon. These factors inhibit $PM_{2.5}$. O_3 concentration is low due to overcast weather and lower availability of precursors. In absence of rain, with higher temperatures at play, both increase together. Therefore, both decrease or increase together. Wang et al. has explained reasons behind this positive correlation. Counter-intuitively, high relative humidity can enhance secondary aerosol formation, increasing $PM_{2.5}$ levels, while also promoting wet deposition, which reduces ozone levels. Low wind speeds can lead to the accumulation of pollutants, including $PM_{2.5}$, which can inhibit ozone production by similar mechanisms. Further, when $PM_{2.5}$ concentrations are low, there is less scattering of sunlight, which increases the intensity of solar radiation reaching the ground, thereby promoting ozone formation. Under these conditions, $PM_{2.5}$ and ozone concentrations are positively correlated because they share common precursors and favorable meteorological conditions. The positive correlation is evident when $PM_{2.5}$ concentrations are below a certain threshold, as both pollutants are generated from similar sources and conditions conducive to their formation. (Wang et al., 2023).

Post-monsoon season is when monsoon withdraws and the season starts to change, bringing back the negative correlation between O_3 and $PM_{2.5}$.

Chapter 6: Conclusion, Future Scope and Social Impact

In this concluding chapter, key findings of our research, highlighting the significant contributions to the field. Based on limitations encountered during the study, potential directions for future research to address research gaps are proposed. Broader social implications of this study, emphasizing how they can influence policy, practice, and future technological advancements are briefly discussed. This work not only advances academic understanding but also holds the potential to drive meaningful changes in society, promoting sustainability, inclusivity, and improved quality of life.

6.1 Conclusion and Future Scope

The study examined variations in ozone concentration seasonally and diurnally over the city of Delhi and has provided an outcome not previously documented in literature, i.e., in Delhi, there exists a negative correlation between ozone and $PM_{2.5}$ in all periods except during monsoon (July-September), with maximum negative correlation observed in Summer of 2020 as -0.55. In general, the negative correlation seems to be the maximum during spring season (month of March). During monsoon, a mildly positive, but statistically insignificant, correlation was generally observed.

Higher concentrations of $PM_{2.5}$ were observed throughout Delhi during the post-monsoon season (with a peak of 200.77 ± 140.03 µg/m³ in 2020) and the winter season (with a peak of 210.77 ± 125.87 µg/m³ in 2018-19). These elevated levels reduce the solar radiation available for ozone formation due to low scattering albedo. During winter, though ozone concentrations were below 30 µg/m³ across all years, factors like smog, haze, low mixing heights, and temperature inversion worsen the situation. In contrast, during spring and summer, although O_3 concentrations increased with rising solar radiation and temperature, the relative concentration of $PM_{2.5}$ decreased (with a maximum of 94.89 ± 54.77 µg/m³ in the summer of 2022). Biogenic VOCs may have also contributed more to the $PM_{2.5}$ proportion, further increasing O_3 concentrations. However, during the monsoon season, there was a mildly positive but statistically insignificant correlation, likely due to the cleansing effect of rainfall reducing $PM_{2.5}$ levels (maximum concentration of 38.41 ± 20.02 µg/m³ in the monsoon of 2022). Additionally, monsoon winds, which carry less dust, and overcast weather conditions also reduced O_3 formation.

Future works investigating relationship between ozone and its precursors, especially $PM_{2.5}$, should be considered for the city of Delhi. Reasons behind having a negative correlation in summer and positive correlation in monsoon season may be explored further. The hypothesis proposed in the present study need to be corroborated by more evidence through experiments or models. Aqueous phase aerosol chemistry involved needs further research. More number of stations should be considered to study the city of Delhi on different temporal scales – monthly, seasonal, etc. Further spatial variations in the correlation should also be investigated. The effect of nearby vegetation and water bodies may play an important role in influencing local concentrations of ozone and its precursors. If monitoring of VOCs such as isoprenes can be undertaken at monitoring sites, then the data may reveal other factors upon which the correlation between ozone and $PM_{2.5}$ depends. Since ozone is a secondary pollutant, it's difficult to comprehend its formation just by monitoring its concentration. Thus, we need models to simulate its creation under different weather and chemical conditions in the atmosphere. Models may also be used to simulate different scenarios and boundary conditions. The current study has considered only two variables at a time to calculate Pearson's relationship coefficient. A multivariate analysis of ozone and other parameters is required to conclusively derive a theory relating ozone and $PM_{2.5}$. Such analysis may reveal other factors upon which this relationship depends. Moreover, it is imperative to explore the boundary conditions and inflexion points of relevant parameters where observed behaviour between ozone and $PM_{2.5}$ changes drastically. For example, at what percentage RH does the aqueous chemistry become dominant leading to formation of more $PM_{2.5}$; or at what concentration of $PM_{2.5}$ does the correlation between ozone and $PM_{2.5}$ change its nature (positive to negative) in Delhi. Models that simulate the direct and indirect effect of other parameters on ozone and $PM_{2.5}$ would be vital to conclusively establish the strength of correlation between the two. For example, RH reducing the temperature required for photochemical reactions is an indirect negative impact on ozone. A model can simulate the strength of this effect in isolation. Such perspectives would offer new insights to regulatory policies being formed.

In conclusion, comprehensive research on the variations of ozone and its relationship with $PM_{2.5}$, precursor pollutants, and meteorological parameters in Delhi is vital. Such studies will not only enhance our understanding of ozone dynamics but also aid in developing effective action plans to mitigate its adverse effects on health and the environment. Addressing this research gap is essential for formulating targeted and efficient pollution control strategies tailored to the unique characteristics of Delhi and other Indian cities.

6.2 Social Impact

Research gap highlighted in 6.1 is important because targeted pollution reduction efforts can be informed by an understanding of the interaction between $PM_{2.5}$ and ozone. Regulatory agencies must have a complete understanding of this relationship in order to develop regulations that stop $PM_{2.5}$ and ozone from co-polluting. Regulatory agencies may find it useful to use a theory about changes in ozone and $PM_{2.5}$ in the Delhi setting when developing measures to avoid co-pollution of $PM_{2.5}$ and ozone. The National Clean Air Programme (NCAP) and the Graded Response Action Plan (GRAP) are two regulatory bodies' efforts to lessen pollution in Delhi. It is wise to investigate the relationship between ozone and $PM_{2.5}$ in more detail in light of China's experience, where effective pollution-reduction strategies managed to reduce particulate matter pollution but unintentionally generated an increase in ozone concentration.

REFERENCES

1. Atkinson, R., 2000. Atmospheric chemistry of VOCs and NOx. Atmospheric Environment 34, 2063–2101. https://doi.org/10.1016/S1352-2310(99)00460-4

2. Batterman, S., Su, F.-C., Li, S., Mukherjee, B., Jia, C., 2014. Personal Exposure to Mixtures of Volatile Organic Compounds: Modeling and Further Analysis of the RIOPA Data. Research report (Health Effects Institute) 3–63.

3. Burney, J., Ramanathan, V., 2014. Recent climate and air pollution impacts on Indian agriculture. Proceedings of the National Academy of Sciences 111, 16319–16324. https://doi.org/10.1073/pnas.1317275111

4. Chalita, S., Hauglustaine, D.A., Le Treut, H., Müller, J.-F., 1996. Radiative forcing due to increased tropospheric ozone concentrations. Atmospheric Environment 30, 1641–1646. https://doi.org/10.1016/1352-2310(95)00431-9

5. Chen, L., Xing, J., Mathur, R., Liu, S., Wang, S., Hao, J., 2020. Quantification of the enhancement of PM2.5 concentration by the downward transport of ozone from the stratosphere. Chemosphere 255, 126907. https://doi.org/10.1016/j.chemosphere.2020.126907

6. Chen, Shen, Li, Peng, Cheng, Ma, 2019. Temporal and Spatial Features of the Correlation between PM2.5 and O3 Concentrations in China. IJERPH 16, 4824. https://doi.org/10.3390/ijerph16234824

7. Climate of Delhi, 2024. . Wikipedia.

8. Coates, J., Mar, K.A., Ojha, N., Butler, T.M., 2016. The influence of temperature on ozone production under varying NO_{<i>x</i>} conditions – a modelling study. Atmos. Chem. Phys. 16, 11601–11615. https://doi.org/10.5194/acp-16-11601-2016

9. CPCB, C.P.C.B., 2009. National Ambient Air Quality Standards.

10. CPCB, M., 2020. National Ambient Air Quality Status & Trends 2019.

11. Crutzen, P.J., 1979. The Role of NO and NO $_2$ in the Chemistry of the Troposphere and Stratosphere. Annu. Rev. Earth Planet. Sci. 7, 443–472. https://doi.org/10.1146/annurev.ea.07.050179.002303

12. Crutzen, P.J., 1974. Photochemical reactions initiated by and influencing ozone in unpolluted tropospheric air. Tellus 26, 47–57. https://doi.org/10.1111/j.2153-3490.1974.tb01951.x

13. Dai, H., Zhu, J., Liao, H., Li, J., Liang, M., Yang, Y., Yue, X., 2021. Co-occurrence of ozone and PM2.5 pollution in the Yangtze River Delta over 2013–2019: Spatiotemporal distribution and meteorological conditions. Atmospheric Research 249, 105363. https://doi.org/10.1016/j.atmosres.2020.105363

14. Delhi Statistical Handbook, D.O.E.& S.G.O.N.C.T.O.D., 2023. Delhi Statistical

Handbook 2023. DIRECTORATE OF ECONOMICS & STATISTICS GOVERNMENT OF NATIONAL CAPITAL TERRITORY OF DELHI.

15. Dhawan, S., George, M.P., Jayachandran, K.S., Khare, M., 2023. Tropospheric ozone variability in Delhi during pre & post monsoon periods: Decoding influence of seasonal variation, diurnal variation, short-range and long-range transport. Urban Climate 47, 101374. https://doi.org/10.1016/j.uclim.2022.101374

16. Hall, J.V., 1996. Assessing health effects of air pollution. Atmospheric Environment, Supercities: Environment Quality and Sustainable Development 30, 743–746. https://doi.org/10.1016/1352-2310(95)00014-3

17. Han, S., Bian, H., Feng, Y., Liu, A., Li, X., Zeng, F., Zhang, X., 2011. Analysis of the Relationship between O3, NO and NO2 in Tianjin, China. Aerosol Air Qual. Res. 11, 128–139. https://doi.org/10.4209/aaqr.2010.07.0055

18. Jia, M., Zhao, T., Cheng, X., Gong, S., Zhang, X., Tang, L., Liu, D., Wu, X., Wang, L., Chen, Y., 2017. Inverse Relations of PM2.5 and O3 in Air Compound Pollution between Cold and Hot Seasons over an Urban Area of East China. Atmosphere 8, 59. https://doi.org/10.3390/atmos8030059

19. Khare, M., Nagendra, S.M.S. (Eds.), 2007. Introduction, in: Artificial Neural Networks in Vehicular Pollution Modelling. Springer, Berlin, Heidelberg, pp. 1–6. https://doi.org/10.1007/978-3-540-37418-3_1

20. Kleinman, L.I., Daum, P.H., Lee, Y.-N., Nunnermacker, L.J., Springston, S.R., Weinstein-Lloyd, J., Rudolph, J., 2002. Ozone production efficiency in an urban area. Journal of Geophysical Research: Atmospheres 107, ACH 23-1-ACH 23-12. https://doi.org/10.1029/2002JD002529

21. Lacour, S.A., De Monte, M., Diot, P., Brocca, J., Veron, N., Colin, P., Leblond, V., 2006. Relationship between ozone and temperature during the 2003 heat wave in France: consequences for health data analysis. BMC Public Health 6, 261. https://doi.org/10.1186/1471-2458-6-261

22. Lee, D.S., Holland, M.R., Falla, N., 1996. The potential impact of ozone on materials in the U.K. Atmospheric Environment 30, 1053–1065. https://doi.org/10.1016/1352-2310(95)00407-6

23. Lightfoot, P.D., Cox, R.A., Crowley, J.N., Destriau, M., Hayman, G.D., Jenkin, M.E., Moortgat, G.K., Zabel, F., 1992. Organic peroxy radicals: Kinetics, spectroscopy and tropospheric chemistry. Atmospheric Environment. Part A. General Topics, Organic Peroxy Radicals: Kinetics, Spectroscopy and Tropospheric Chemistry 26, 1805–1961. https://doi.org/10.1016/0960-1686(92)90423-I

24. Liu, Q., Liu, T., Chen, Y., Xu, J., Gao, W., Zhang, H., Yao, Y., 2019. Effects of aerosols on the surface ozone generation via a study of the interaction of ozone and its precursors during the summer in Shanghai, China. Science of The Total Environment 675, 235–246. https://doi.org/10.1016/j.scitotenv.2019.04.121

25. Mage, D., Ozolins, G., Peterson, P., Webster, A., Orthofer, R., Vandeweerd, V., Gwynne, M., 1996. Urban air pollution in megacities of the world. Atmospheric

Environment 30, 681–686. https://doi.org/10.1016/1352-2310(95)00219-7

26. Masters, G.M., 1998. Introduction to Environmental Engineering and Science. Prentice Hall.

27. Mayer, H., 1999. Air pollution in cities. Atmospheric Environment 33, 4029–4037. https://doi.org/10.1016/S1352-2310(99)00144-2

28. Munir, S., Chen, H., Ropkins, K., 2011. An investigation into the association of ozone with traffic-related air pollutants using a quantile regression approach. Presented at the ENVIRONMENTAL HEALTH AND BIOMEDICINE 2011, Riga, Latvia, pp. 21–32. https://doi.org/10.2495/EHR110031

29. NCERT, N.C. of E.R. and T., 2022. India: Physical Environment.

30. Rao, 1988. Air Pollution. Tata McGraw-Hill.

31. Rathore, A., Gopikrishnan, G.S., Kuttippurath, J., 2023. Changes in tropospheric ozone over India: Variability, long-term trends and climate forcing. Atmospheric Environment 309, 119959. https://doi.org/10.1016/j.atmosenv.2023.119959

32. Seinfeld, J.H., Pandis, S.N., Noone, K., 1998. *Atmospheric Chemistry and Physics: From Air Pollution to Climate Change*. Physics Today 51, 88–90. https://doi.org/10.1063/1.882420

33. Shao, M., Wang, W., Yuan, B., Parrish, D.D., Li, X., Lu, K., Wu, L., Wang, X., Mo, Z., Yang, S., Peng, Y., Kuang, Y., Chen, W., Hu, M., Zeng, L., Su, H., Cheng, Y., Zheng, J., Zhang, Y., 2021. Quantifying the role of PM2.5 dropping in variations of ground-level ozone: Inter-comparison between Beijing and Los Angeles. Science of The Total Environment 788, 147712. https://doi.org/10.1016/j.scitotenv.2021.147712

34. Sharma, A., Sharma, S.K., Mandal, T.K., 2021. Ozone sensitivity factor: NOX or NMHCs?: A case study over an urban site in Delhi, India. Urban Climate 39, 100980. https://doi.org/10.1016/j.uclim.2021.100980

35. Sharma, S., 2017. MODELLING OF TROPOSPHERIC OZONE AND SOURCE SPECIE APPORTIONMENT IN AN URBAN AREA. Indian Institute of Technology, Delhi.

36. Shukla, K., 2019. PHOTOCHEMICAL MODELLING OF GROUND LEVEL OZONE. Indian Institute of Technology, Delhi.

37. Sinha, P., Singh, S., Saroj, P., Beig, G., Murthy, B.S., 2021. Study of surface ozone (O3) and its relationship with NO, NO2, NOx, OX and CO at five different locations in New Delhi, India from 2013 to 2019. https://doi.org/10.21203/rs.3.rs-783427/v1

38. Wang, L., Zhao, B., Zhang, Y., Hu, H., 2023. Correlation between surface PM2.5 and O3 in eastern China during 2015–2019: Spatiotemporal variations and meteorological impacts. Atmospheric Environment 294, 119520. https://doi.org/10.1016/j.atmosenv.2022.119520

39. Wark, K., Warner, C.F., Davis, W.T., 1998. Air Pollution: Its Origin and Control.

Addison-Wesley.

40. WHO, W.H.O., 2021. WHO Global Air Quality Guidelines. World Health Organisation.

41. WHO, W.H.O.E., 2008. Health risks of ozone from long-range transboundary air pollution. World Health Organisation.

42. Worden, H.M., Bowman, K.W., Worden, J.R., Eldering, A., Beer, R., 2008. Satellite measurements of the clear-sky greenhouse effect from tropospheric ozone. Nature Geosci 1, 305–308. https://doi.org/10.1038/ngeo182

43. Yadav, R.K., Gadhavi, H., Arora, A., Mohbey, K.K., Kumar, S., Lal, S., Mallik, C., 2023. Relation between PM2.5 and O3 over Different Urban Environmental Regimes in India. Urban Science 7. https://doi.org/10.3390/urbansci7010009

44. Zhang, Y.H., Su, H., Zhong, L.J., Cheng, Y.F., Zeng, L.M., Wang, X.S., Xiang, Y.R., Wang, J.L., Gao, D.F., Shao, M., Fan, S.J., Liu, S.C., 2008. Regional ozone pollution and observation-based approach for analyzing ozone–precursor relationship during the PRIDE-PRD2004 campaign. Atmospheric Environment, PRIDE-PRD 2004 Campaign : Program of Regional Integrated Experiments on Air Quality over Pearl River Delta of China 42, 6203–6218. https://doi.org/10.1016/j.atmosenv.2008.05.002

45. Zhang, Z., Zhang, X., Gong, D., Quan, W., Zhao, X., Ma, Z., Kim, S.-J., 2015. Evolution of surface O3 and PM2.5 concentrations and their relationships with meteorological conditions over the last decade in Beijing. Atmospheric Environment 108, 67–75. https://doi.org/10.1016/j.atmosenv.2015.02.071

APPENDIX-I

The code for implementing the validation protocol has been written using R and is as follows:

```
# Load the dplyr package for data manipulation
library(dplyr)
# Define a function to clean air pollution data
data_cleaning <- function(file_path) {
  # Announce the start of the data cleaning process
  cat("Start data cleaning process...\n")


  # Announce the reading of data from a file
  cat("Reading data...\n")
  # Read the CSV file into a dataframe
  data <- read.csv(file_path, header = TRUE, sep = ",")
  # Confirm that the data has been read
  cat("Data read successfully.\n")
  # Start initial data cleaning
  cat("Performing initial data cleaning...\n")
  # Identify all columns except timestamp, date, and time
  numeric_cols <- names(data)[!(names(data) %in% c("Timestamp", "Date",
"Time"))]
  # Replace all negative, zero values, and blanks with NA
```

```
data[numeric_cols] <- lapply(data[numeric_cols], function(x) ifelse(x <= 0 | x ==
"", NA, x))
# Confirm initial cleaning is complete
cat("Initial data cleaning complete.\n")
# Ensure PM25 is less than PM10
cat("Ensuring PM2.5 is less than PM10...\n")
# Replace PM25 and PM10 values with NA where PM25 >= PM10
data <- data %>%
  mutate(across(c(PM25, PM10), ~ if_else(PM25 >= PM10, NA_real_, .)))
# Replace values that repeat more than 4 times consecutively with NA
cat("Replacing more than 4 consecutive repeats with NA...\n")
data[numeric_cols] <- lapply(data[numeric_cols], function(column) {
  # Use run-length encoding to find sequences
  r <- rle(column)
  # Extract the values and their lengths from the encoding
  values <- r$values
  lengths <- r$lengths
  # Replace values where sequences are 4 or longer with NA
  values[lengths >= 4] <- NA
  # Return data with replaced values
  inverse.rle(list(values = values, lengths = lengths))
})
```

```
 # Confirm replacement is complete
 cat("Consecutive repeats replacement complete.\n")
 # Applying additional criteria to set minimum allowable values for pollutants
 cat("Applying additional criteria for specific pollutants...\n")
 data <- data %>%
   mutate(
     PM25 = if_else(PM25 < 4, 4, PM25),   # Ensure PM25 is not below 4
     PM10 = if_else(PM10 < 4, 4, PM10),   # Ensure PM10 is not below 4
     SO2 = if_else(SO2 < 1.5, 1.5, SO2),  # Ensure SO2 is not below 1.5
     NH3 = if_else(NH3 < 3, 3, NH3),      # Ensure NH3 is not below 3
     NO2 = if_else(NO2 < 3, 3, NO2),      # Ensure NO2 is not below 3
     CO = if_else(CO < 0.1, 0.1, CO),     # Ensure CO is not below 0.1
     Ozone = if_else(Ozone < 3, 3, Ozone), # Ensure Ozone is not below 3
     Benzene = if_else(Benzene < 0.2, 0.2, Benzene) # Ensure Benzene is not below
0.2
   )
 # Validate that NO + NO2 is less than NOx
 #cat("Validating NO + NO2 < NOx...\n")
 #data <- data %>%
 # mutate(across(c(NO, NO2, NOx), ~ if_else((NO + NO2) > NOx, NA_real_, .)))
 # Confirm the criterion has been applied
 cat("Validation criteria applied.\n")
```

```
    # Save the cleaned and modified data to a new CSV file
    cat("Saving the final modified data...\n")
    write.csv(data, "validated_data.csv", row.names = FALSE)
    # Confirm that the data has been saved
    cat("Data saved to 'validated_data.csv'.\n")
    # Announce the completion of the data cleaning process
    cat("Data cleaning process complete.\n")
    # Return the modified data
    return(data)
}
```

APPENDIX-II

Diurnal variations in ozone and parameters that influence it in the year 2023:

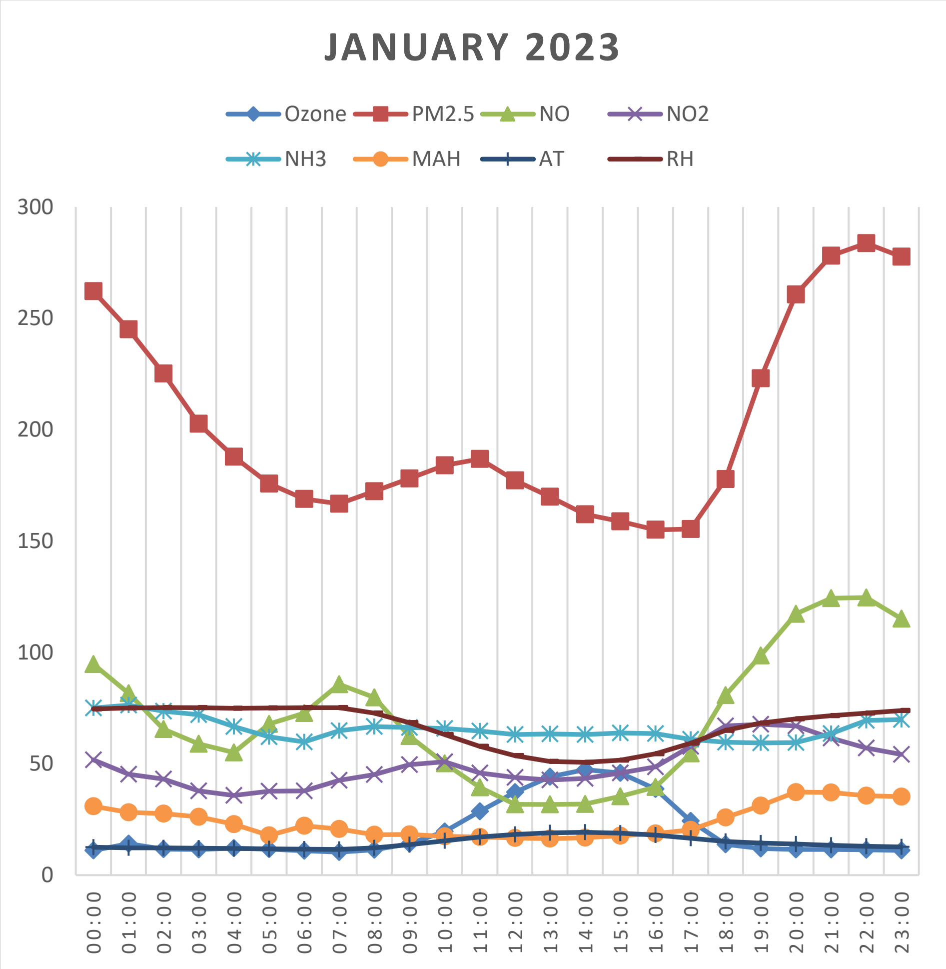

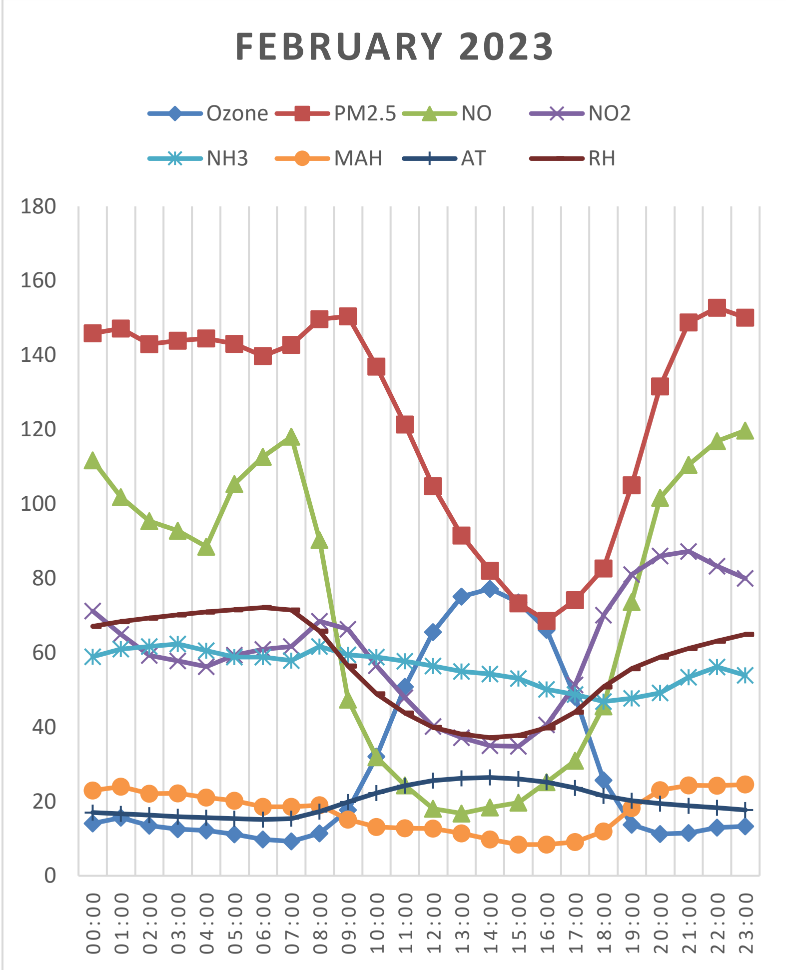

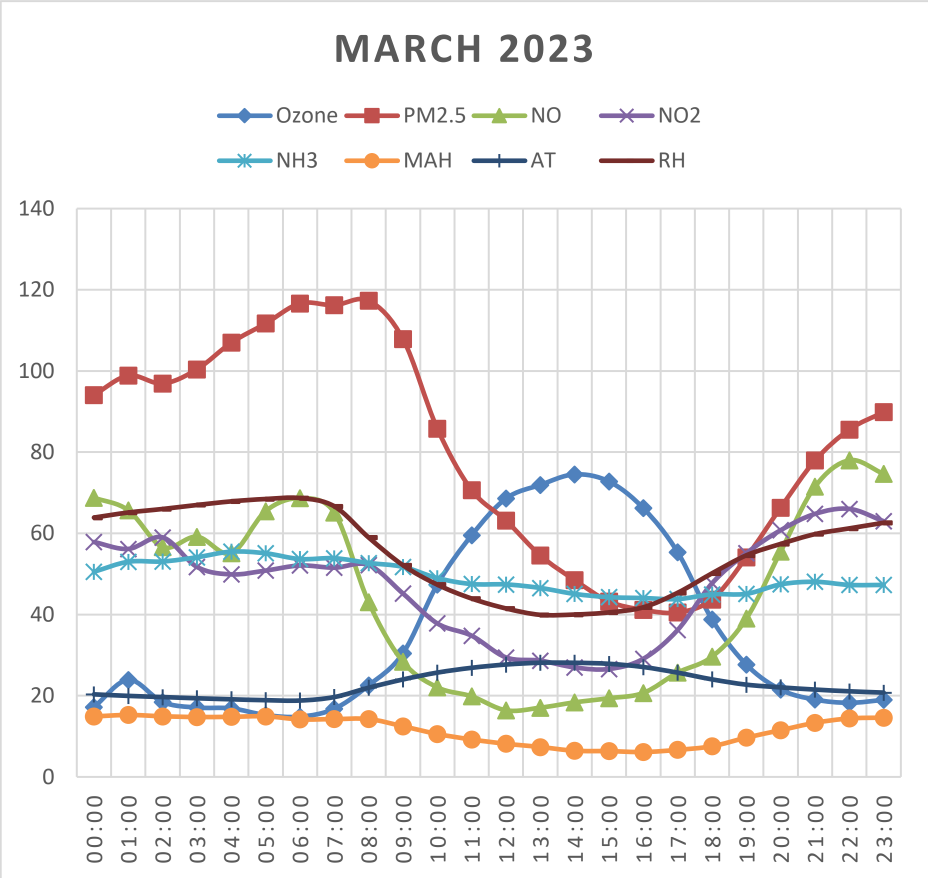
MARCH 2023
Ozone
PM2.5
NO
NO2
NH3
MAH
AT
RH
140
120
100
80
60
40
20
0
00:00
01:00
02:00
03:00
04:00
05:00
06:00
07:00
08:00
09:00
10:00
11:00
12:00
13:00
14:00
15:00
16:00
17:00
18:00
19:00
20:00
21:00
22:00
23:00

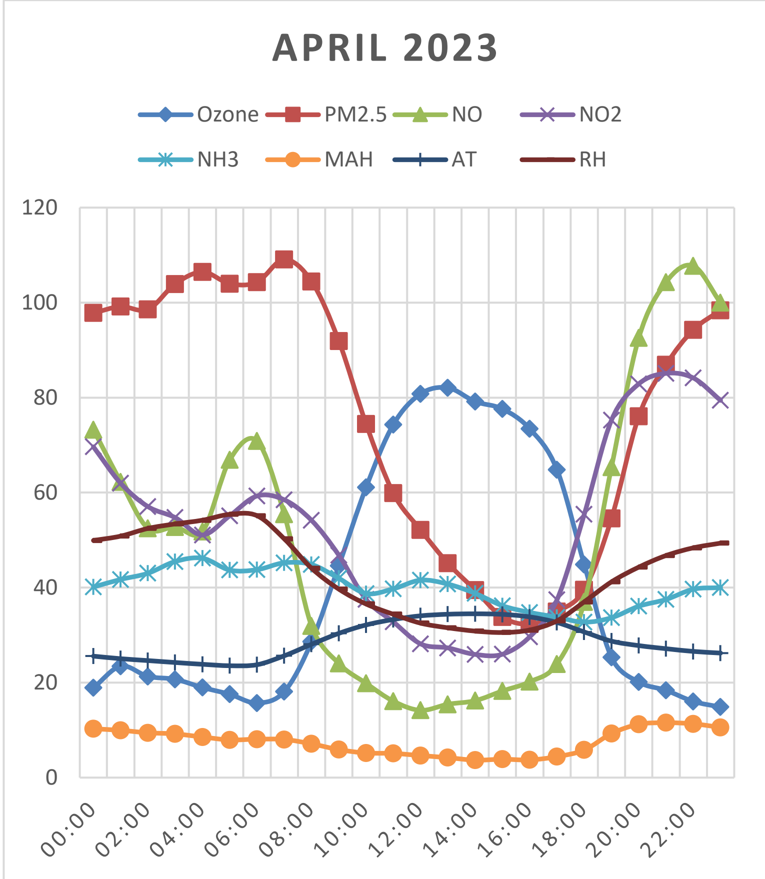
APRIL 2023
Ozone
PM2.5
NO
NO2
NH3
MAH
AT
RH
120
100
80
60
40
20
0
00:00
02:00
04:00
06:00
08:00
10:00
12:00
14:00
16:00
18:00
20:00
22:00

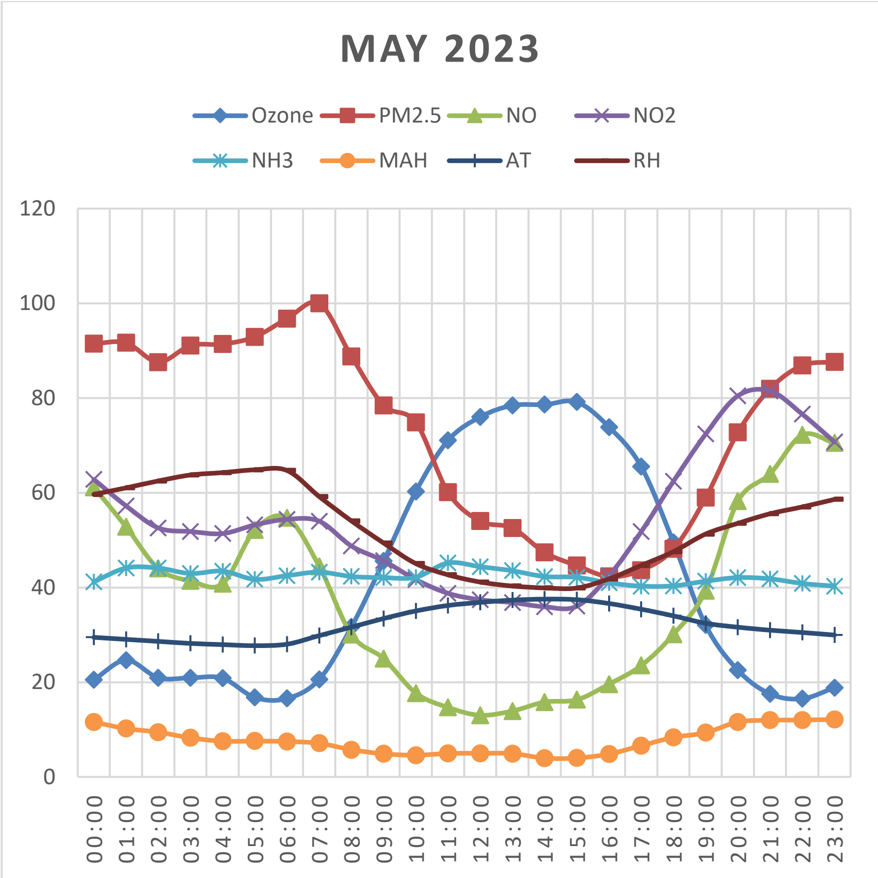
MAY 2023
Ozone
PM2.5
NO
NO2
NH3
MAH
AT
RH
120
100
80
60
40
20
0
00:00
01:00
02:00
03:00
04:00
05:00
06:00
07:00
08:00
09:00
10:00
11:00
12:00
13:00
14:00
15:00
16:00
17:00
18:00
19:00
20:00
21:00
22:00
23:00

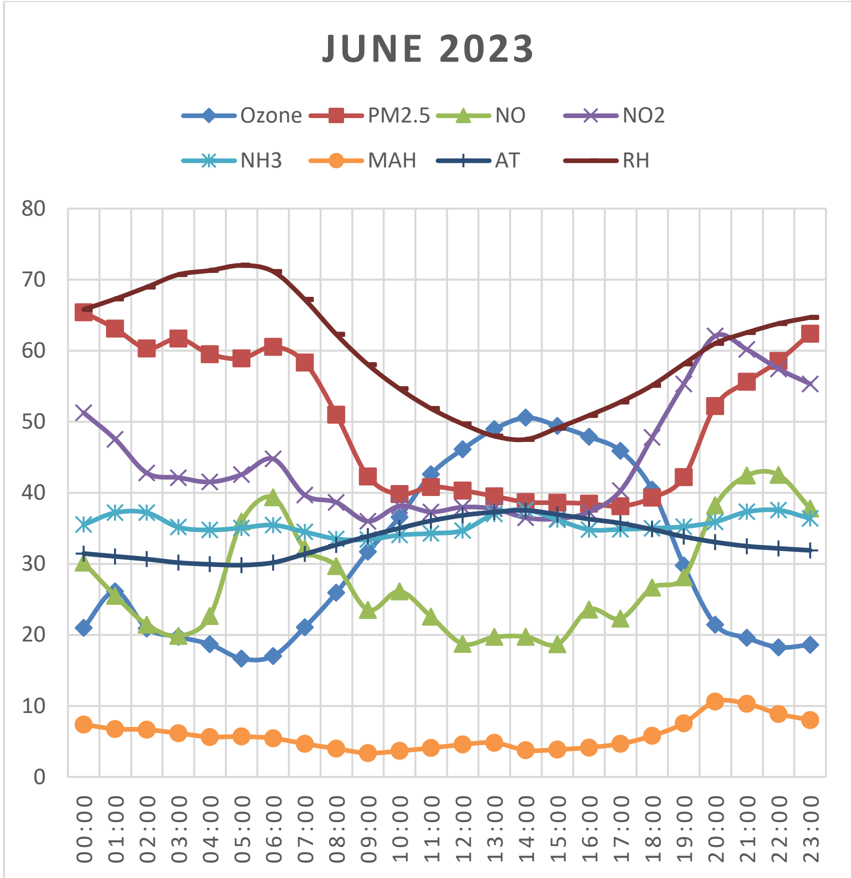
JUNE 2023
Ozone
PM2.5
NO
NO2
NH3
MAH
AT
RH
80
70
60
50
40
30
20
10
0
00:00
01:00
02:00
03:00
04:00
05:00
06:00
07:00
08:00
09:00
10:00
11:00
12:00
13:00
14:00
15:00
16:00
17:00
18:00
19:00
20:00
21:00
22:00
23:00

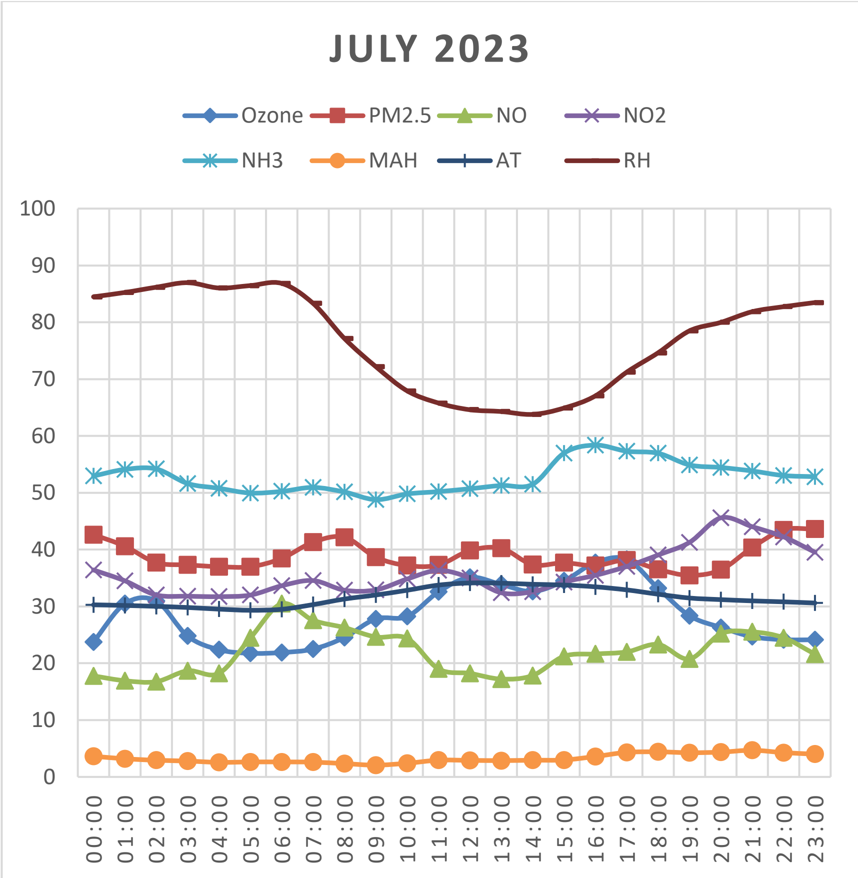
JULY 2023
Ozone
PM2.5
NO
NO2
NH3
MAH
AT
RH
100
90
80
70
60
50
40
30
20
10
0
00:00
01:00
02:00
03:00
04:00
05:00
06:00
07:00
08:00
09:00
10:00
11:00
12:00
13:00
14:00
15:00
16:00
17:00
18:00
19:00
20:00
21:00
22:00
23:00

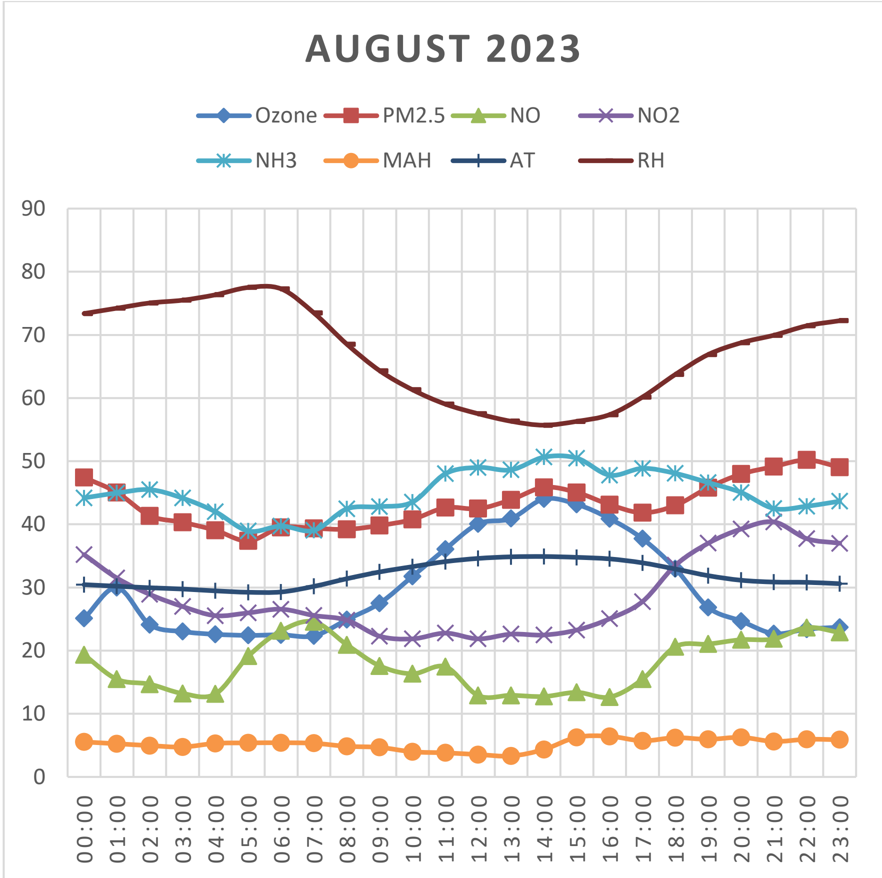
AUGUST 2023
Ozone
PM2.5
NO
NO2
NH3
MAH
AT
RH
90
80
70
60
50
40
30
20
10
0
00:00
01:00
02:00
03:00
04:00
05:00
06:00
07:00
08:00
09:00
10:00
11:00
12:00
13:00
14:00
15:00
16:00
17:00
18:00
19:00
20:00
21:00
22:00
23:00

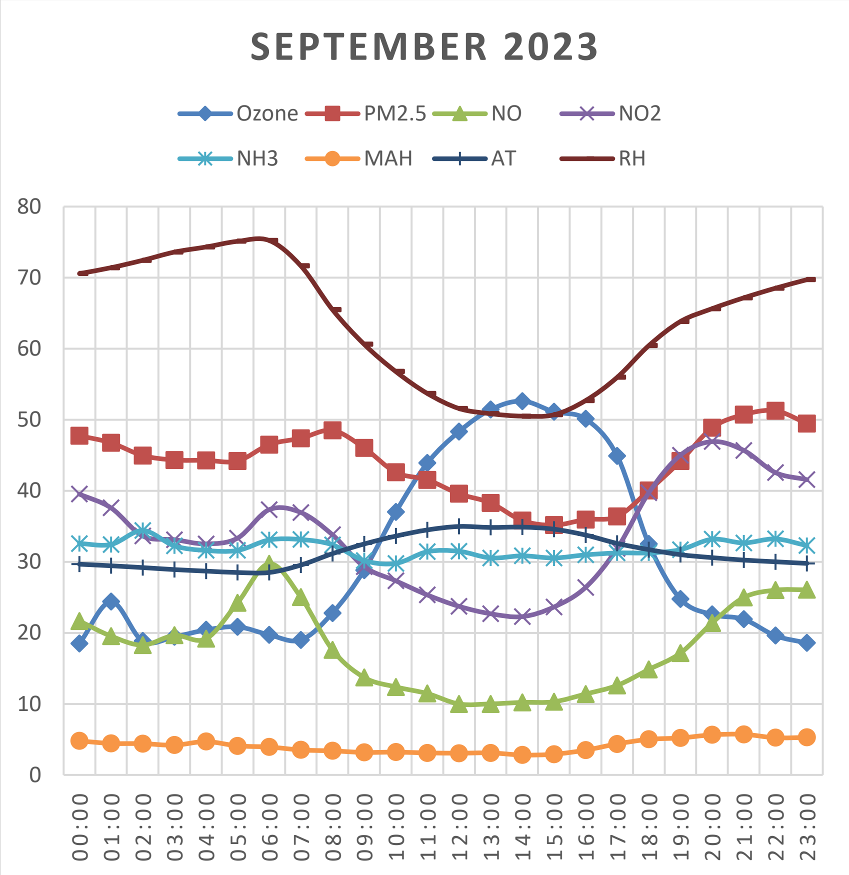
SEPTEMBER 2023
Ozone
PM2.5
NO
NO2
NH3
MAH
AT
RH
0
10
20
30
40
50
60
70
80
00:00
01:00
02:00
03:00
04:00
05:00
06:00
07:00
08:00
09:00
10:00
11:00
12:00
13:00
14:00
15:00
16:00
17:00
18:00
19:00
20:00
21:00
22:00
23:00

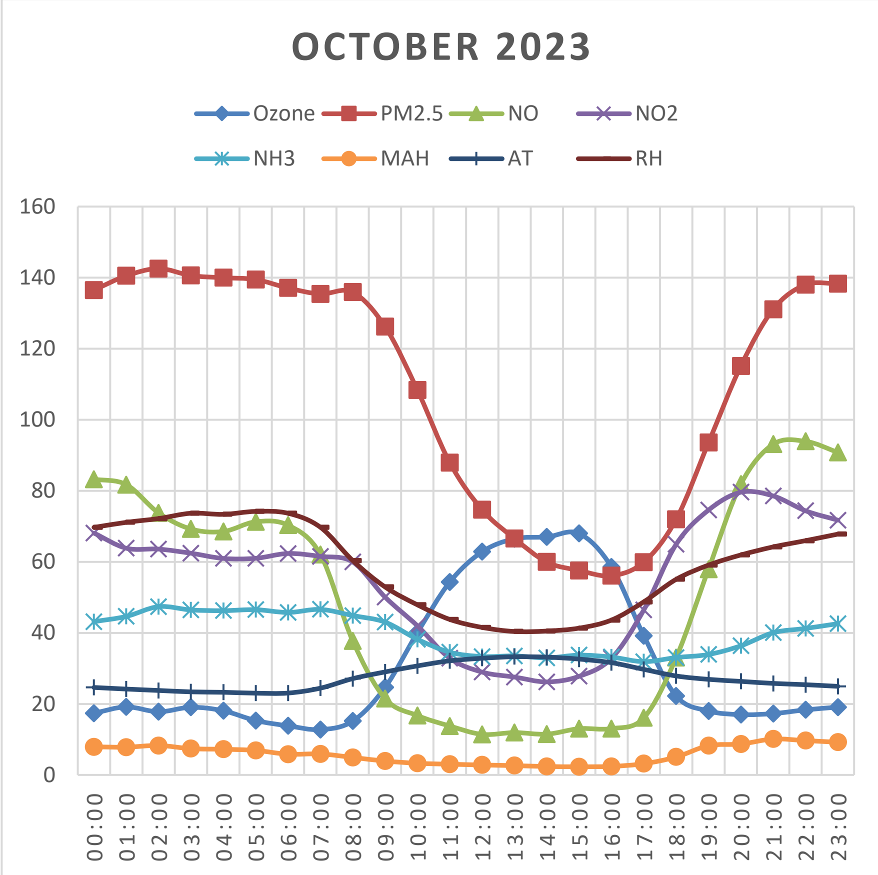
OCTOBER 2023
Ozone
PM2.5
NO
NO2
NH3
MAH
AT
RH
0
20
40
60
80
100
120
140
160
00:00
01:00
02:00
03:00
04:00
05:00
06:00
07:00
08:00
09:00
10:00
11:00
12:00
13:00
14:00
15:00
16:00
17:00
18:00
19:00
20:00
21:00
22:00
23:00

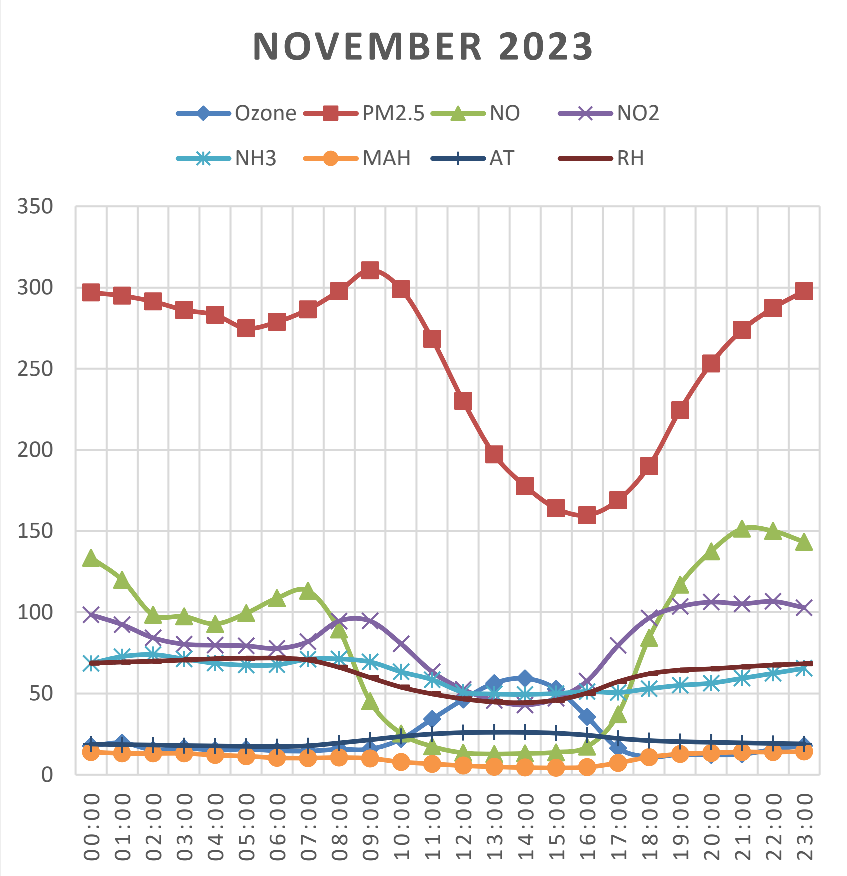
NOVEMBER 2023
Ozone
PM2.5
NO
NO2
NH3
MAH
AT
RH
350
300
250
200
150
100
50
0
00:00 01:00 02:00 03:00 04:00 05:00 06:00 07:00 08:00 09:00 10:00 11:00 12:00 13:00 14:00 15:00 16:00 17:00 18:00 19:00 20:00 21:00 22:00 23:00

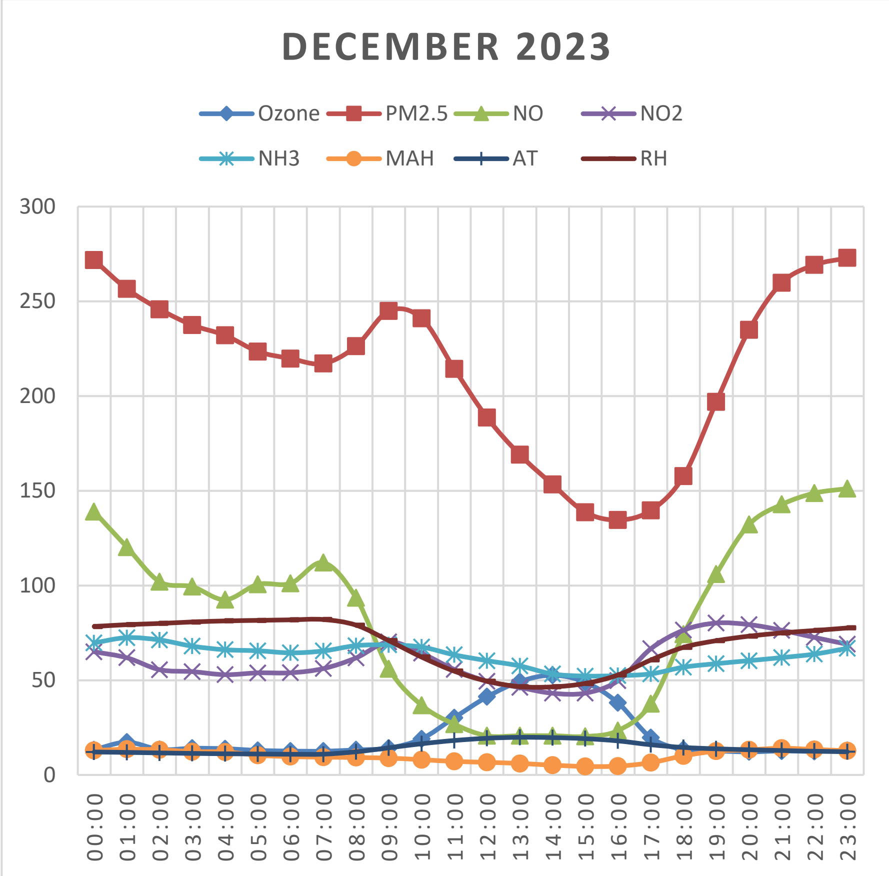
DECEMBER 2023
Ozone
PM2.5
NO
NO2
NH3
MAH
AT
RH
300
250
200
150
100
50
0
00:00 01:00 02:00 03:00 04:00 05:00 06:00 07:00 08:00 09:00 10:00 11:00 12:00 13:00 14:00 15:00 16:00 17:00 18:00 19:00 20:00 21:00 22:00 23:00

Diurnal variations in ozone and parameters that influence it in the year 2020:

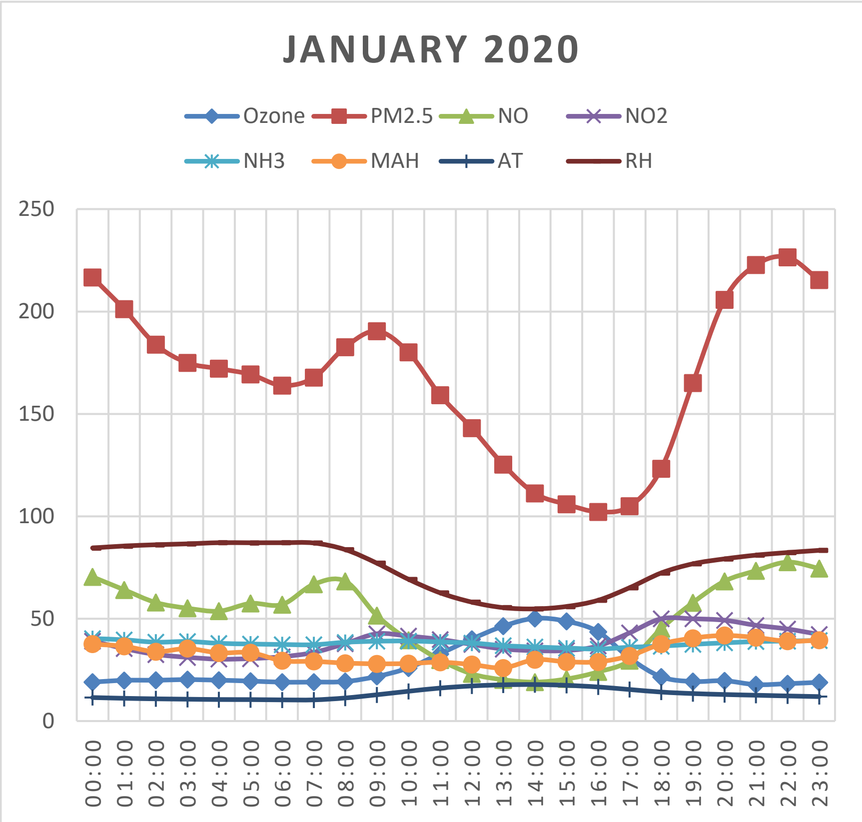

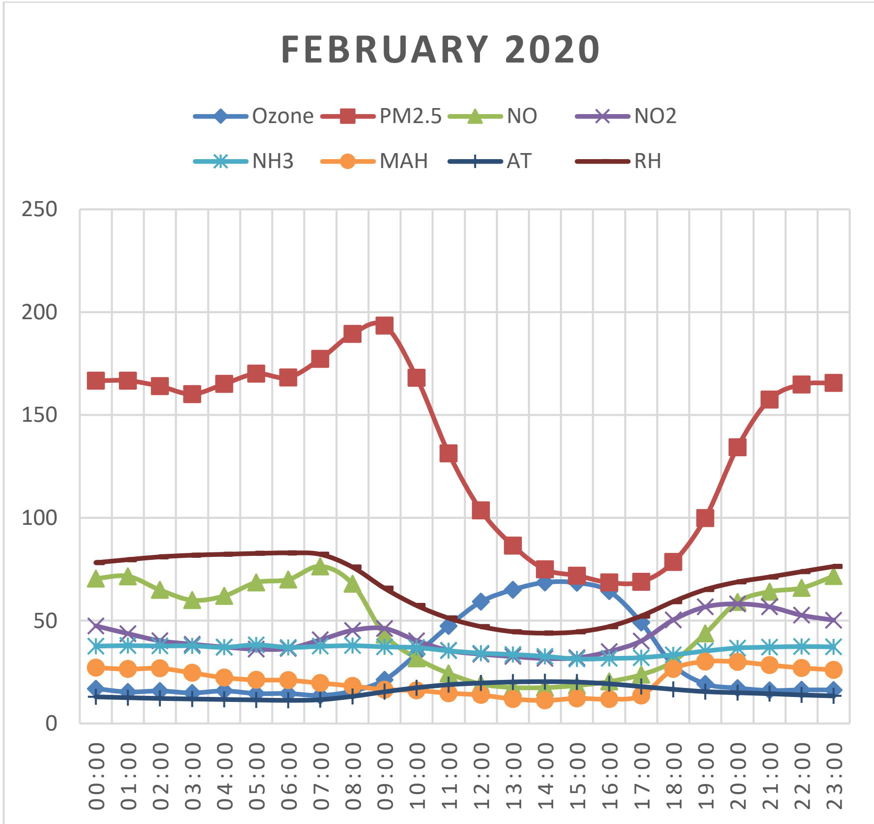

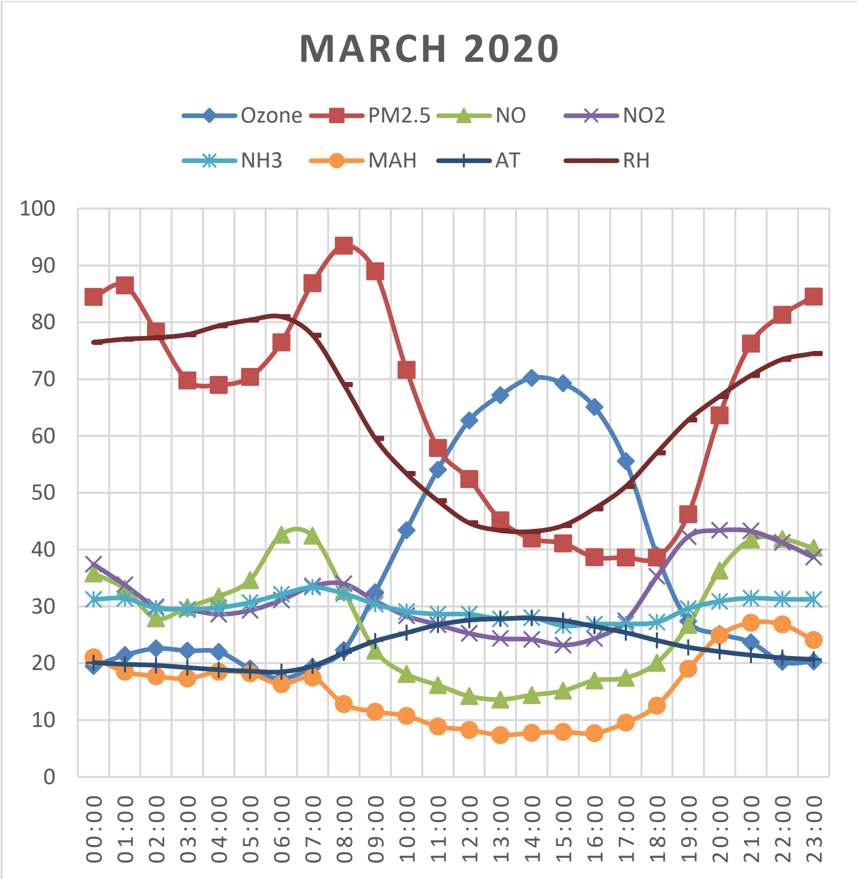
MARCH 2020
Ozone
PM2.5
NO
NO2
NH3
MAH
AT
RH
100
90
80
70
60
50
40
30
20
10
0
00:00
01:00
02:00
03:00
04:00
05:00
06:00
07:00
08:00
09:00
10:00
11:00
12:00
13:00
14:00
15:00
16:00
17:00
18:00
19:00
20:00
21:00
22:00
23:00

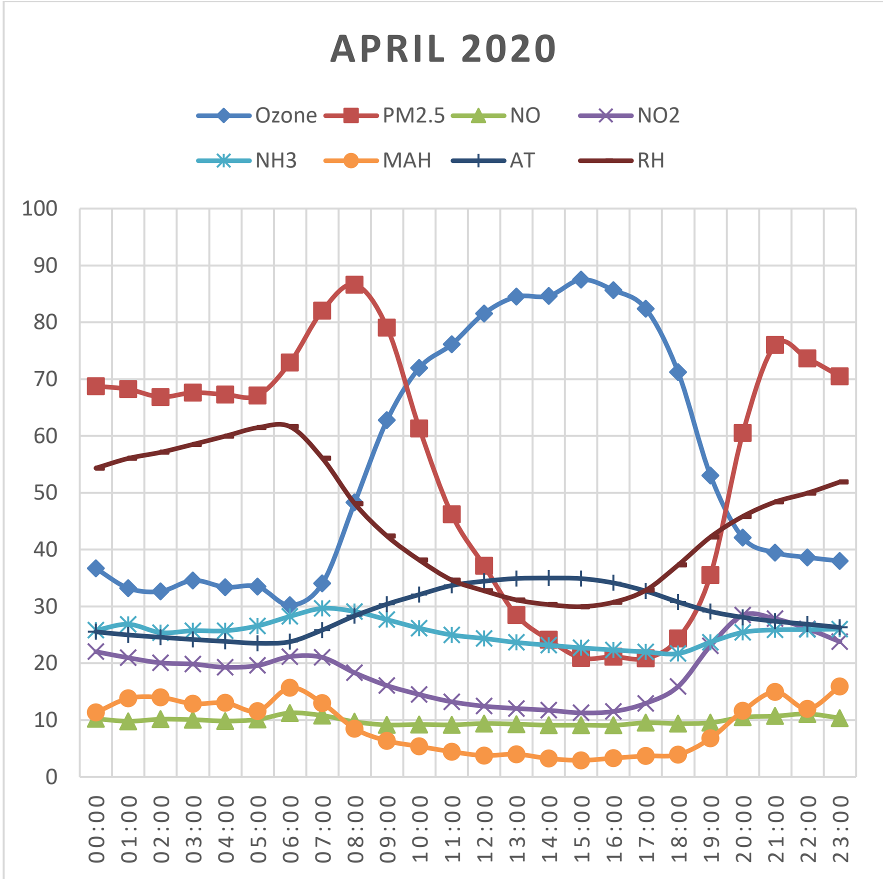
APRIL 2020
Ozone
PM2.5
NO
NO2
NH3
MAH
AT
RH
100
90
80
70
60
50
40
30
20
10
0
00:00
01:00
02:00
03:00
04:00
05:00
06:00
07:00
08:00
09:00
10:00
11:00
12:00
13:00
14:00
15:00
16:00
17:00
18:00
19:00
20:00
21:00
22:00
23:00

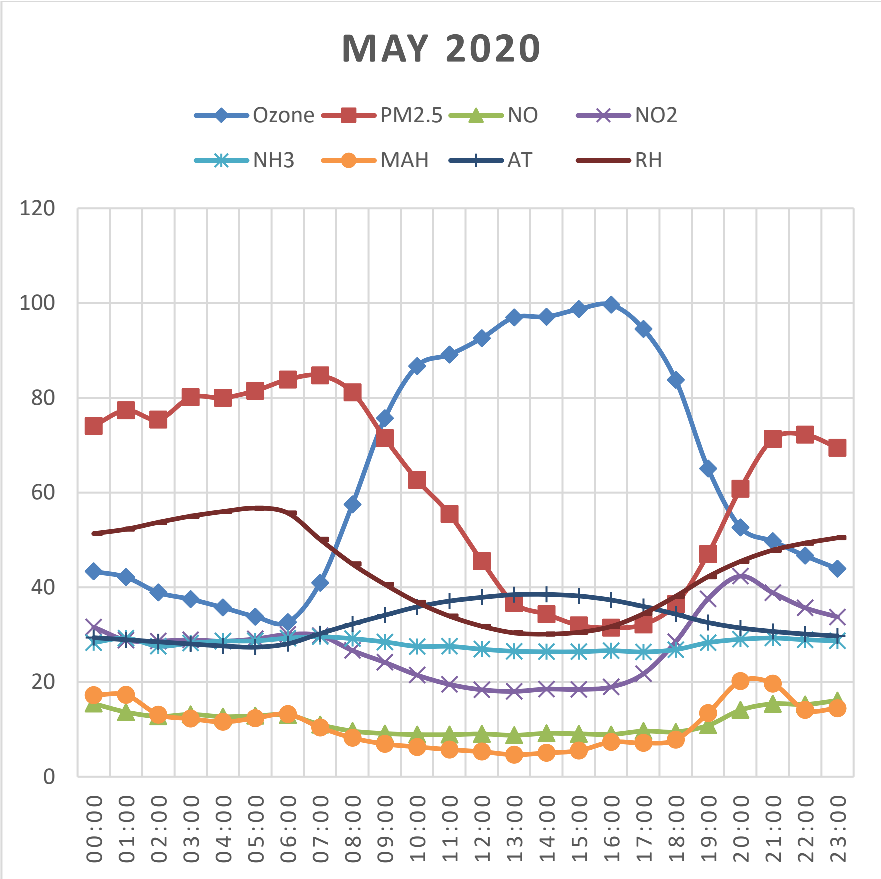
MAY 2020
Ozone
PM2.5
NO
NO2
NH3
MAH
AT
RH
120
100
80
60
40
20
0
00:00
01:00
02:00
03:00
04:00
05:00
06:00
07:00
08:00
09:00
10:00
11:00
12:00
13:00
14:00
15:00
16:00
17:00
18:00
19:00
20:00
21:00
22:00
23:00

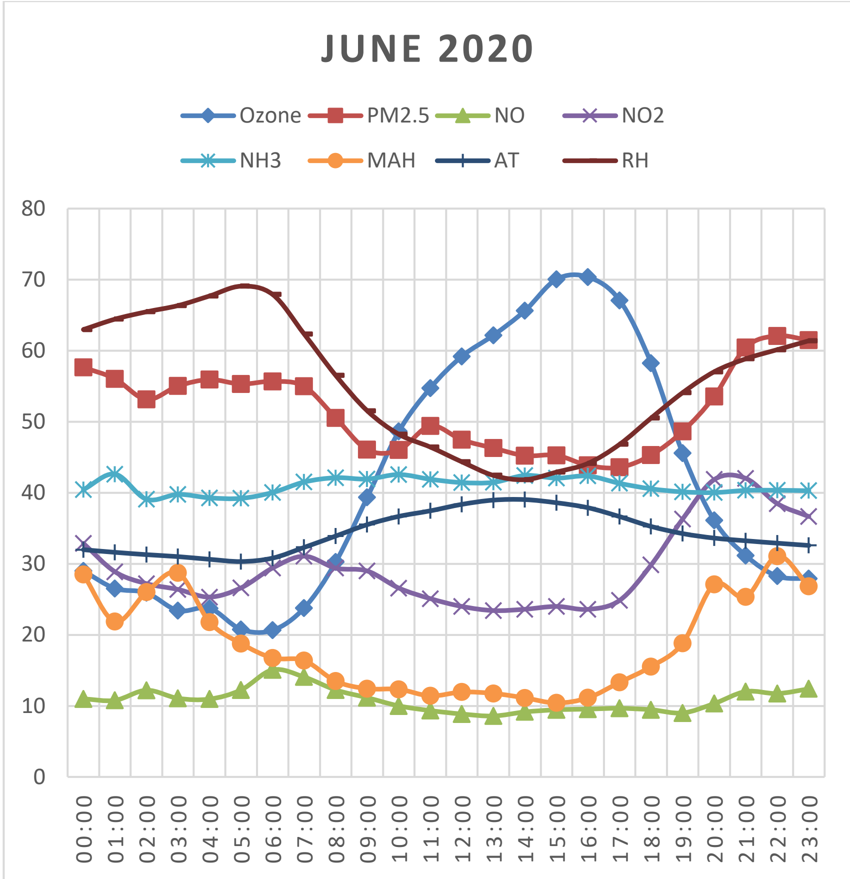
JUNE 2020
Ozone
PM2.5
NO
NO2
NH3
MAH
AT
RH
80
70
60
50
40
30
20
10
0
00:00
01:00
02:00
03:00
04:00
05:00
06:00
07:00
08:00
09:00
10:00
11:00
12:00
13:00
14:00
15:00
16:00
17:00
18:00
19:00
20:00
21:00
22:00
23:00

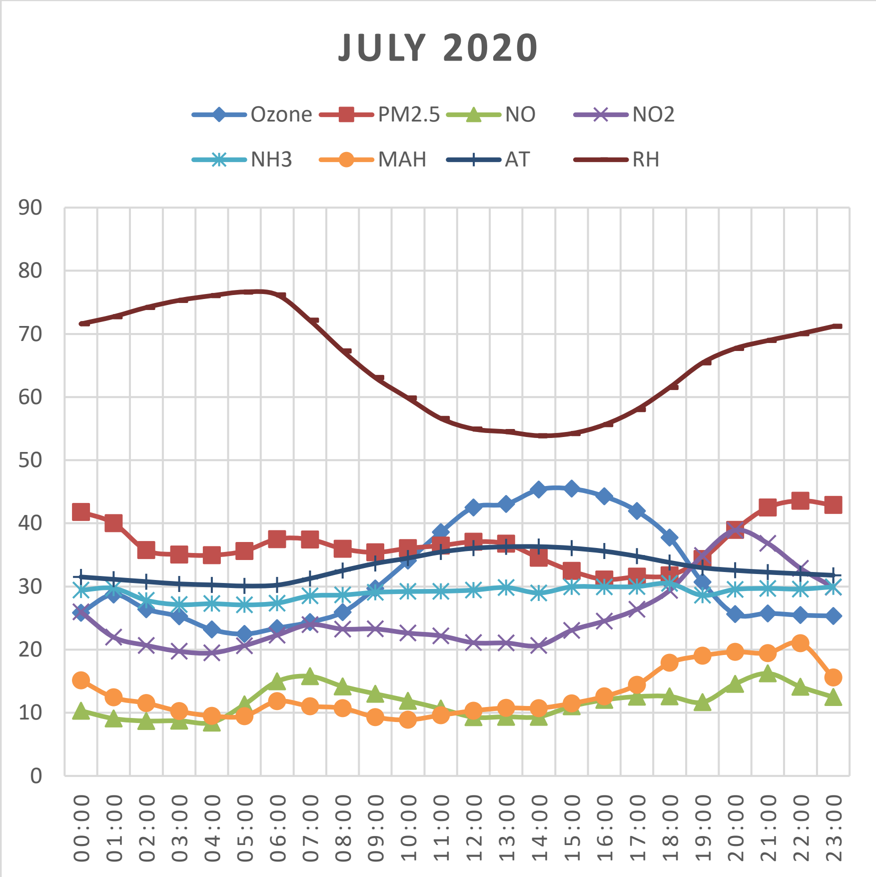
JULY 2020
Ozone
PM2.5
NO
NO2
NH3
MAH
AT
RH
0
10
20
30
40
50
60
70
80
90
00:00
01:00
02:00
03:00
04:00
05:00
06:00
07:00
08:00
09:00
10:00
11:00
12:00
13:00
14:00
15:00
16:00
17:00
18:00
19:00
20:00
21:00
22:00
23:00

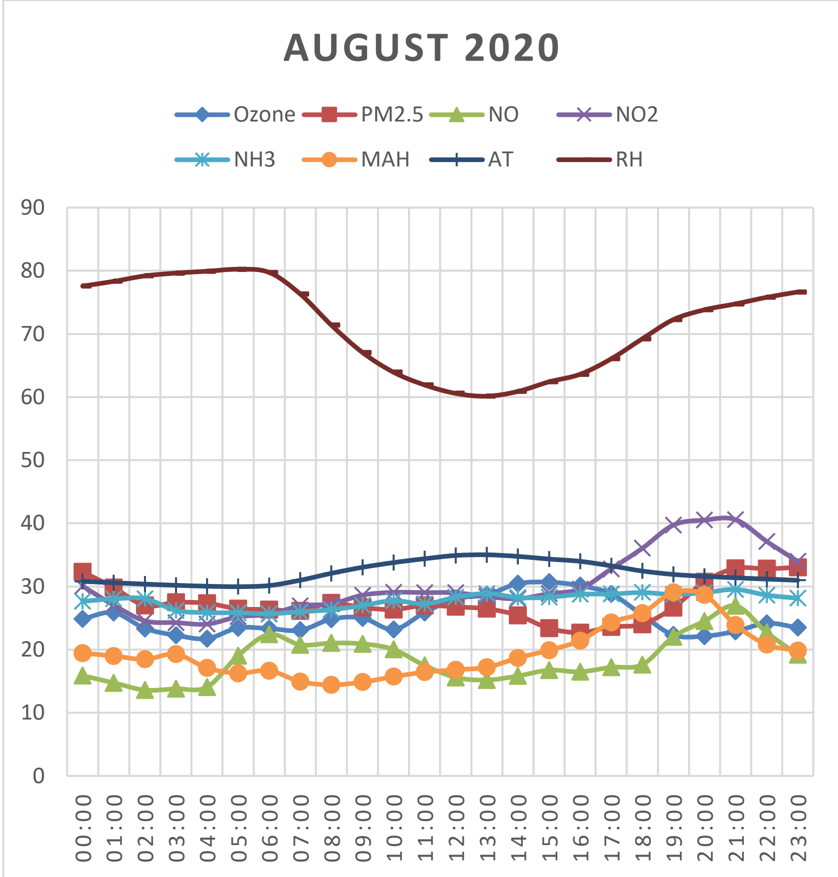
AUGUST 2020
Ozone
PM2.5
NO
NO2
NH3
MAH
AT
RH
0
10
20
30
40
50
60
70
80
90
00:00
01:00
02:00
03:00
04:00
05:00
06:00
07:00
08:00
09:00
10:00
11:00
12:00
13:00
14:00
15:00
16:00
17:00
18:00
19:00
20:00
21:00
22:00
23:00

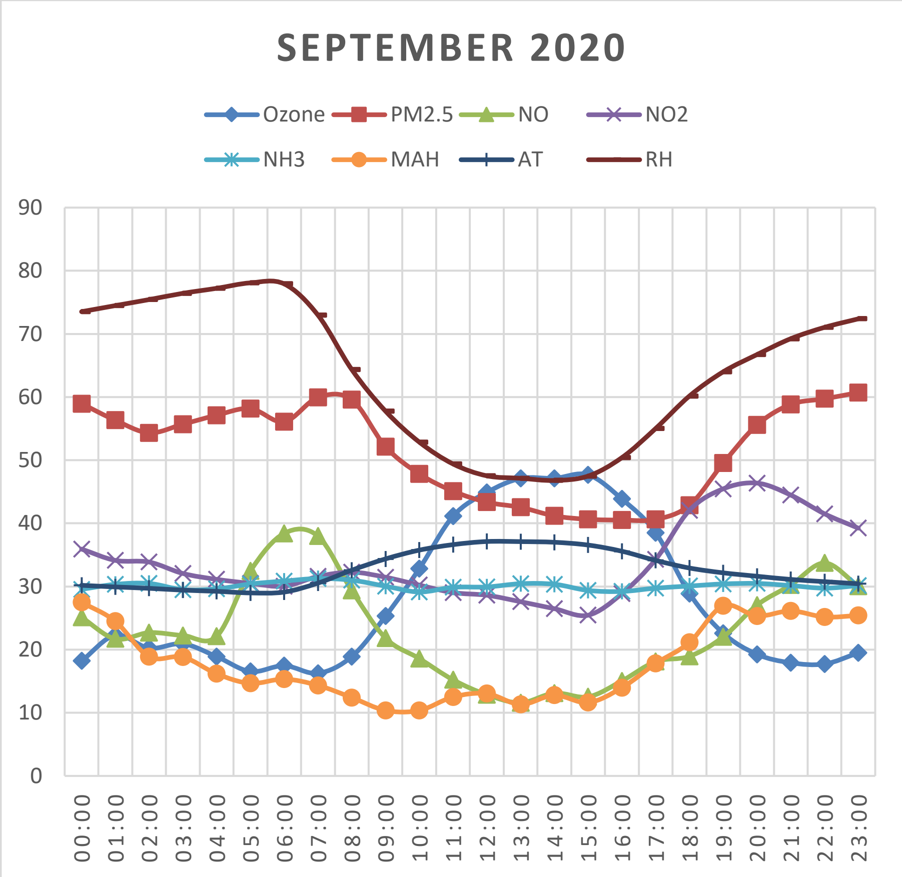
SEPTEMBER 2020
Ozone
PM2.5
NO
NO2
NH3
MAH
AT
RH
90
80
70
60
50
40
30
20
10
0
00:00 01:00 02:00 03:00 04:00 05:00 06:00 07:00 08:00 09:00 10:00 11:00 12:00 13:00 14:00 15:00 16:00 17:00 18:00 19:00 20:00 21:00 22:00 23:00

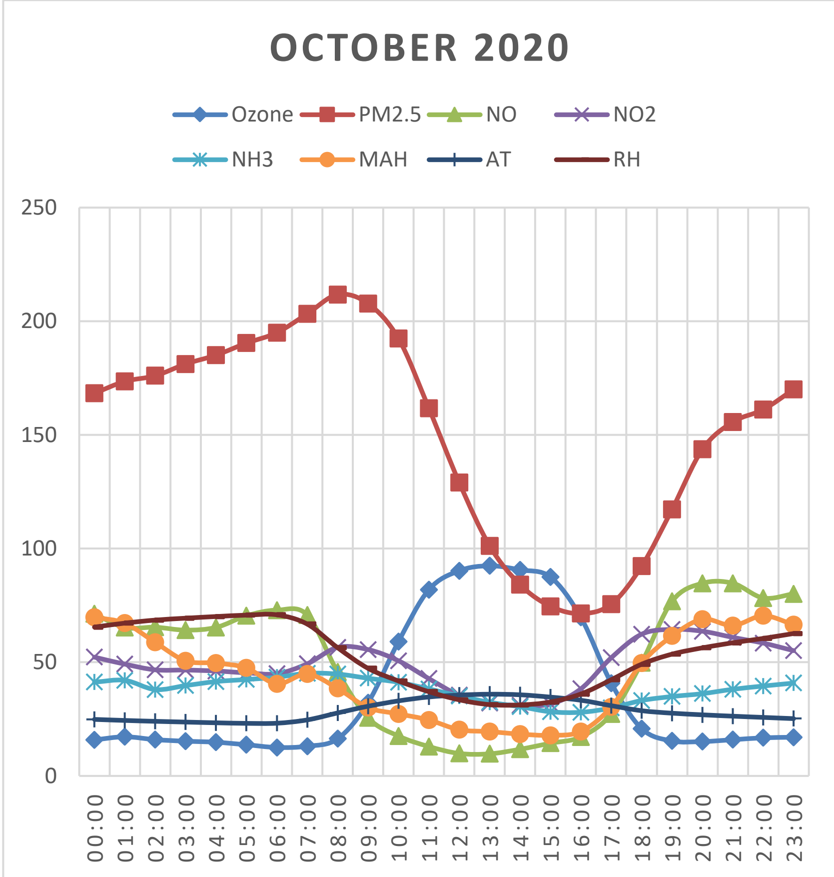
OCTOBER 2020
Ozone
PM2.5
NO
NO2
NH3
MAH
AT
RH
250
200
150
100
50
0
00:00 01:00 02:00 03:00 04:00 05:00 06:00 07:00 08:00 09:00 10:00 11:00 12:00 13:00 14:00 15:00 16:00 17:00 18:00 19:00 20:00 21:00 22:00 23:00

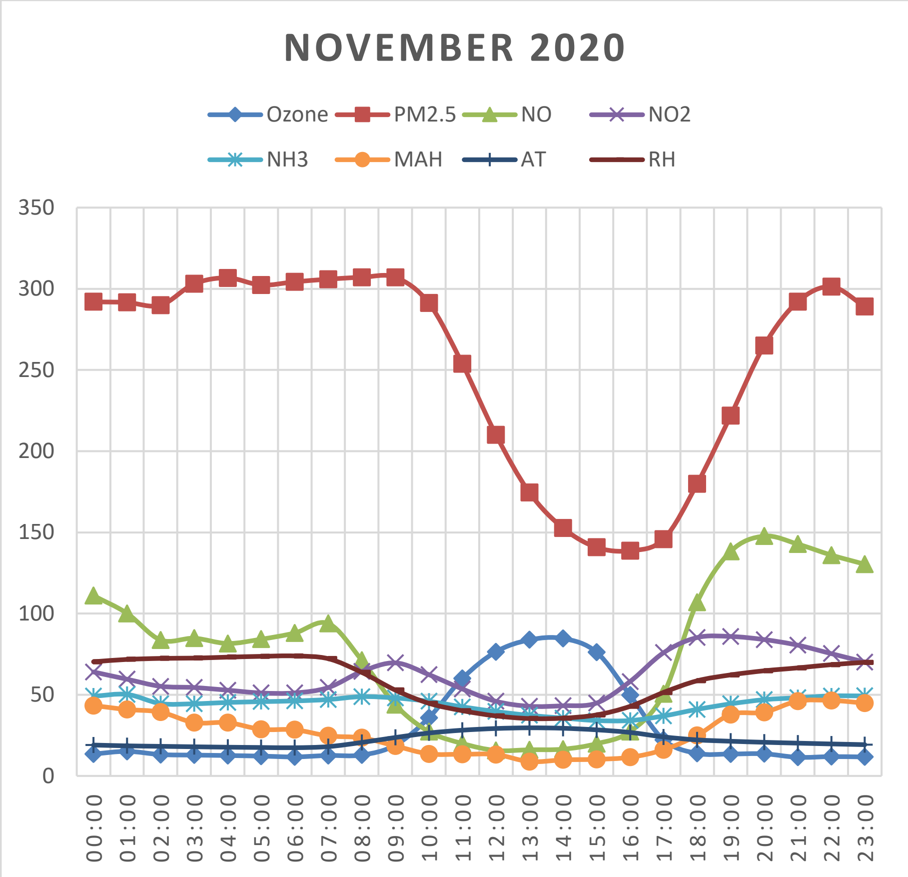
NOVEMBER 2020
Ozone
PM2.5
NO
NO2
NH3
MAH
AT
RH
350
300
250
200
150
100
50
0
00:00
01:00
02:00
03:00
04:00
05:00
06:00
07:00
08:00
09:00
10:00
11:00
12:00
13:00
14:00
15:00
16:00
17:00
18:00
19:00
20:00
21:00
22:00
23:00

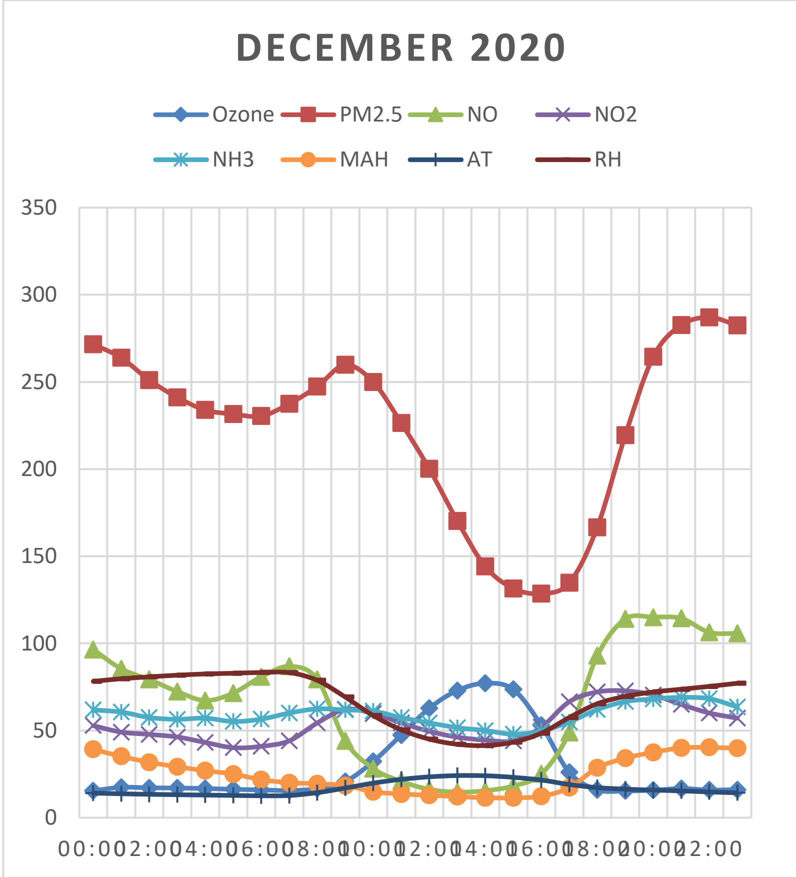
DECEMBER 2020
Ozone
PM2.5
NO
NO2
NH3
MAH
AT
RH
350
300
250
200
150
100
50
0
00:00
02:00
04:00
06:00
08:00
10:00
12:00
14:00
16:00
18:00
20:00
22:00

APPENDIX-III

Season-wise: Statistical Descriptive Tables

Spring 2018	Ozone	PM25	NO	NO2	CO	NH3	AT	RH	WS	SR
Median	32.365	87.595	30.11	56.74	1.065	41.595	23.59	48.32	0.97	21.58
Mean	45.527	100.58	47.717	61.245	1.377	43.32	24.277	48.224	1.122	149.061
95% CI Mean Upper	48.333	104.5	50.754	63.034	1.454	44.145	24.674	49.624	1.17	161.531
95% CI Mean Lower	42.722	96.657	44.68	59.456	1.301	42.494	23.88	46.823	1.075	136.592
Std. Deviation	38.451	54.512	42.196	24.857	1.043	11.472	5.442	19.461	0.662	173.249
Coefficient of variation	0.845	0.542	0.884	0.406	0.757	0.265	0.224	0.404	0.59	1.162
Skewness	0.905	0.9	1.632	1.046	1.911	0.778	0.304	-0.033	0.886	0.709
Std. Error of Skewness	0.091	0.09	0.09	0.09	0.091	0.09	0.091	0.09	0.09	0.09
Kurtosis	-0.203	0.268	2.077	1.282	4.429	0.878	-0.879	-1.115	-0.04	-1.115
Std. Error of Kurtosis	0.181	0.179	0.179	0.179	0.181	0.179	0.182	0.179	0.179	0.179
Minimum	4.38	16	5.06	19.78	0.19	18.22	14.67	8.12	0.15	3.33
Maximum	171.75	291.44	237.02	169.42	7.32	99.72	38.44	86.48	3.15	541.2
25th percentile	12.013	57.573	20.012	43.498	0.65	34.775	19.665	31.623	0.58	6.81
50th percentile	32.365	87.595	30.11	56.74	1.065	41.595	23.59	48.32	0.97	21.58
75th percentile	75.76	135.23	60.538	73.127	1.68	50.242	28.62	65.083	1.53	309.843
95th percentile	117.93	207.19	142.27	107.1	3.616	63.886	33.347	77.619	2.46	459.772
Summer 2018	**Ozone**	**PM25**	**NO**	**NO2**	**CO**	**NH3**	**AT**	**RH**	**WS**	**SR**
Median	29.4	80.06	26.05	53.63	1.49	47.45	32.07	40.095	1.54	135.63
Mean	37.611	94.429	40.212	64.622	2.167	52.477	32.085	40.032	1.867	205.084

95% CI Mean Upper	38.727	96.768	41.835	66.223	2.25	53.416	32.307	40.676	1.935	212.866
95% CI Mean Lower	36.494	92.091	38.589	63.021	2.084	51.537	31.863	39.389	1.799	197.302
Std. Deviation	26.609	55.669	38.673	38.145	1.979	22.395	5.258	15.326	1.614	185.45
Coefficient of variation	0.707	0.59	0.962	0.59	0.913	0.427	0.164	0.383	0.864	0.904
Skewness	1.295	2.532	2.155	2.203	2.456	1.262	0.025	0.126	8.648	0.583
Std. Error of Skewness	0.052	0.052	0.052	0.052	0.052	0.052	0.053	0.052	0.052	0.052
Kurtosis	1.486	14.528	5.138	7.715	7.945	1.987	-0.66	-0.313	160.8	-0.96
Std. Error of Kurtosis	0.105	0.105	0.105	0.105	0.105	0.105	0.105	0.105	0.105	0.105
Minimum	4.3	6.63	1.45	6.97	0.25	12.6	18.5	5.63	0.19	3.75
Maximum	165.08	658.67	262.46	369.14	14.87	166.63	44.55	88.09	37.92	781.61
25th percentile	17.68	57.14	16.645	40.08	0.88	36.63	28.29	29.4	0.88	56.008
50th percentile	29.4	80.06	26.05	53.63	1.49	47.45	32.07	40.095	1.54	135.63

75th percentile	50.72	116.65	46.833	77.93	2.685	63.25	35.962	50.528	2.56	373.905
95th percentile	90.282	199.9	125.51	141.14	6.287	97.446	40.74	65.641	3.95	520.826
Monsoon 2018	**Ozone**	**PM25**	**NO**	**NO2**	**CO**	**NH3**	**AT**	**RH**	**WS**	**SR**
Median	14.36	40.26	13.03	26.885	0.82	35.195	28.96	77.42	1.08	66.695
Mean	19.57	45.05	19.817	29.441	0.926	38.682	29.466	73.613	1.219	142.848
95% CI Mean Upper	20.172	45.955	20.904	29.976	0.945	39.293	29.614	74.26	1.244	149.776
95% CI Mean Lower	18.967	44.146	18.73	28.906	0.908	38.07	29.319	72.966	1.195	135.919
Std. Deviation	14.435	21.676	26.044	12.818	0.445	14.656	3.54	15.509	0.584	166.013
Coefficient of variation	0.738	0.481	1.314	0.435	0.481	0.379	0.12	0.211	0.479	1.162
Skewness	2.114	1.289	4.914	1.345	2.419	1.375	0.384	-0.638	0.835	1.023
Std. Error of Skewness	0.052	0.052	0.052	0.052	0.052	0.052	0.052	0.052	0.052	0.052
Kurtosis	5.505	2.421	30.455	2.617	9.81	2.506	-0.322	-0.609	0.142	-0.239
Std. Error of Kurtosis	0.104	0.104	0.104	0.104	0.104	0.104	0.104	0.104	0.104	0.104
Minimum	4.33	5.5	1.63	5.38	0.3	16.48	19.87	26.72	0.27	2.04
Maximum	116.05	152.5	257.14	96.88	4.56	117.53	40.92	94.41	3.8	665.14
25th percentile	10.205	29.692	7.18	20.25	0.65	27.718	26.75	61.987	0.76	6.12
50th percentile	14.36	40.26	13.03	26.885	0.82	35.195	28.96	77.42	1.08	66.695
75th percentile	23.582	56	22.553	35.323	1.06	45.962	32.03	87.135	1.58	255.787
95th percentile	51.455	85.947	53.622	54.096	1.813	67.668	35.617	92.16	2.367	482.775

Postmonsoon 2018	**Ozone**	**PM25**	**NO**	**NO2**	**CO**	**NH3**	**AT**	**RH**	**WS**	**SR**
Median	23.175	173.92	69.88	74.835	1.74	50.105	22.83	55.825	0.72	12.515
Mean	35.291	192.54	96.411	79.957	2.153	50.834	23.139	54.953	0.864	117.244
95% CI Mean Upper	36.722	198.03	100.68	81.42	2.217	51.568	23.43	55.908	0.888	124.648
95% CI Mean Lower	33.86	187.04	92.147	78.495	2.088	50.101	22.847	53.999	0.841	109.841
Std. Deviation	27.91	107.15	83.173	28.524	1.261	14.316	5.686	18.619	0.457	144.413
Coefficient of variation	0.791	0.557	0.863	0.357	0.586	0.282	0.246	0.339	0.529	1.232
Skewness	1.331	1.091	0.88	0.689	1.105	0.339	0.266	-0.105	1.696	0.895
Std. Error of Skewness	0.064	0.064	0.064	0.064	0.064	0.064	0.064	0.064	0.064	0.064
Kurtosis	0.973	2.144	-0.313	0.351	0.592	0.023	-0.764	-1.167	3.626	-0.763
Std. Error of Kurtosis	0.128	0.128	0.128	0.128	0.128	0.128	0.128	0.128	0.128	0.128
Minimum	6.23	32.38	4.71	18.29	0.42	17.79	12.3	15.53	0.18	3.91
Maximum	146.08	793.25	378.68	210.9	6.93	103.57	36.32	93.27	3.38	501.55
25th percentile	16.008	107.98	24.367	57.773	1.22	40.905	18.63	38.925	0.55	6.13
50th percentile	23.175	173.92	69.88	74.835	1.74	50.105	22.83	55.825	0.72	12.515
75th percentile	49.413	262.78	151.21	99	2.89	59.91	27.182	71.195	1.06	241.618
95th percentile	94.404	377.42	263.7	131.15	4.757	76.127	33.218	82.185	1.765	392.443
Winter 2018-19	**Ozone**	**PM25**	**NO**	**NO2**	**CO**	**NH3**	**AT**	**RH**	**WS**	**SR**
Median	23.11	182.33	47.055	60.3	1.59	42.935	13.825	60.13	0.83	6.7
Mean	28.907	210.77	83.235	66.222	2.122	46.138	14.387	58.698	1.014	101.484
95% CI Mean Upper	29.74	216.08	86.735	67.295	2.184	46.806	14.588	59.375	1.039	107.016
95% CI Mean Lower	28.074	205.46	79.736	65.149	2.06	45.47	14.187	58.022	0.989	95.952

Std. Deviation	19.742	125.87	82.936	25.428	1.479	15.83	4.737	16.038	0.598	131.105
Skewness	1.218	0.857	1.316	1.293	1.355	0.813	0.334	-0.312	1.69	1.045
Std. Error of Skewness	0.053	0.053	0.053	0.053	0.053	0.053	0.053	0.053	0.053	0.053
Kurtosis	1.152	0.139	0.787	2.591	1.222	0.368	-0.659	-0.949	3.479	-0.339
Std. Error of Kurtosis	0.105	0.105	0.105	0.105	0.105	0.105	0.105	0.105	0.105	0.105
Minimum	4.84	23.1	4.38	26.48	0.21	17.82	5.16	21.77	0.17	3.52
Maximum	120.98	706.25	378.92	231.23	8.15	107.42	27.99	87.11	4.15	503.82
25th percentile	14.565	111.76	21.053	48.047	1.09	34.053	10.65	46.182	0.6	6.01
50th percentile	23.11	182.33	47.055	60.3	1.59	42.935	13.825	60.13	0.83	6.7
75th percentile	39.282	285.78	119.45	78.22	2.683	55.442	17.973	72.66	1.25	197.23
95th percentile	68.766	466.9	262.72	117.04	5.32	76.619	22.564	81.352	2.28	356.631
Spring 2019	**Ozone**	**PM25**	**NO**	**NO2**	**CO**	**NH3**	**AT**	**RH**	**WS**	**SR**
Median	21.6	84.435	25.02	49.665	1.11	29.595	20.92	49.725	1.045	19.88
Mean	30.181	95.868	38.717	52.248	1.257	31.393	21.517	46.668	1.243	151.951
95% CI Mean Upper	31.86	99.513	41.307	53.373	1.299	31.963	21.952	47.849	1.291	165.077
95% CI Mean Lower	28.502	92.223	36.126	51.122	1.215	30.824	21.081	45.487	1.194	138.824
Std. Deviation	23.323	50.645	35.991	15.636	0.583	7.916	6.053	16.409	0.671	182.383
Coefficient of variation	0.773	0.528	0.93	0.299	0.464	0.252	0.281	0.352	0.54	1.2
Skewness	0.853	0.917	1.91	0.62	1.214	0.775	0.458	-0.146	1.175	0.8
Std. Error of Skewness	0.09	0.09	0.09	0.09	0.09	0.09	0.09	0.09	0.09	0.09
Kurtosis	-0.316	0.552	3.682	-0.402	1.992	0.083	-0.35	-0.851	0.974	-0.974

Std. Error of Kurtosis	0.179	0.179	0.179	0.179	0.179	0.179	0.179	0.179	0.179	0.179
Minimum	4.51	18.64	3.33	18.99	0.38	18.15	8.84	9.99	0.29	5.27
Maximum	106.31	296.36	208.96	95.93	4.28	62.76	39.78	85.71	3.65	564.97
25th percentile	9.938	56.093	15.19	39.642	0.827	25.435	16.785	32.24	0.73	5.89
50th percentile	21.6	84.435	25.02	49.665	1.11	29.595	20.92	49.725	1.045	19.88
75th percentile	46.998	125.86	50.153	62.715	1.59	36.115	25.69	59.523	1.59	315.667
95th percentile	74.494	192.5	125.64	82.561	2.33	46.83	32.118	70.994	2.59	489.368
Summer 2019	**Ozone**	**PM25**	**NO**	**NO2**	**CO**	**NH3**	**AT**	**RH**	**WS**	**SR**
Median	34.115	72.9	22.985	49.11	1.38	35.82	32.46	33.615	1.17	74.385
Mean	44.914	87.703	39.365	53.418	1.568	38.123	32.723	34.964	1.382	172.838
95% CI Mean Upper	46.337	90.069	41.19	54.334	1.599	38.629	32.971	35.602	1.415	180.856
95% CI Mean Lower	43.491	85.336	37.541	52.501	1.536	37.617	32.475	34.326	1.35	164.82
Std. Deviation	33.91	56.404	43.473	21.838	0.749	12.053	5.88	15.21	0.784	191.084
Coefficient of variation	0.755	0.643	1.104	0.409	0.478	0.316	0.18	0.435	0.567	1.106
Skewness	0.824	1.896	2.41	0.869	1.95	1.929	-0.003	0.397	1.329	0.653
Std. Error of Skewness	0.052	0.052	0.052	0.052	0.052	0.052	0.053	0.052	0.052	0.052
Kurtosis	-0.442	4.964	6.938	0.373	5.179	7.234	-0.674	-0.341	2.489	-1.164
Std. Error of Kurtosis	0.105	0.105	0.105	0.105	0.105	0.105	0.105	0.105	0.105	0.105
Minimum	5.22	9.6	1.96	15.43	0.36	15.35	17.12	5.94	0.2	3.9
Maximum	157.24	430.57	303.45	141.23	5.74	142.34	46.44	87.17	5.9	592.24
25th percentile	15.957	49.492	12.145	37.288	1.09	30.123	28.39	23.235	0.78	6.04
50th percentile	34.115	72.9	22.985	49.11	1.38	35.82	32.46	33.615	1.17	74.385

75th percentile	69.302	108.73	48.805	65.403	1.8	43.12	37.3	45.33	1.82	355.153
95th percentile	109.93	201.23	133.03	96.576	3.05	59.368	42.298	61.533	2.808	511.43
Monsoon 2019	**Ozone**	**PM25**	**NO**	**NO2**	**CO**	**NH3**	**AT**	**RH**	**WS**	**SR**
Median	22.45	40.93	13.4	31.21	1.18	31.565	30.075	66.975	1.05	48.335
Mean	25.374	44.529	18.924	33.273	1.264	32.745	30.621	65.321	1.201	131.494
95% CI Mean Upper	25.96	45.459	19.617	33.724	1.282	33.079	30.762	65.854	1.225	137.775
95% CI Mean Lower	24.789	43.6	18.23	32.821	1.247	32.411	30.479	64.789	1.177	125.212
Std. Deviation	14.031	22.26	16.612	10.816	0.425	8.008	3.392	12.762	0.566	150.512
Coefficient of variation	0.553	0.5	0.878	0.325	0.336	0.245	0.111	0.195	0.471	1.145
Skewness	1.753	0.773	3.005	1.43	1.839	0.912	0.553	-0.431	1.189	0.822
Std. Error of Skewness	0.052	0.052	0.052	0.052	0.052	0.052	0.052	0.052	0.052	0.052
Kurtosis	4.839	0.358	13.864	3.517	5.72	1.225	-0.207	-0.633	1.445	-0.741
Std. Error of Kurtosis	0.104	0.104	0.104	0.104	0.104	0.104	0.104	0.104	0.104	0.104
Minimum	5.9	5.17	3.75	14.87	0.4	13.11	22.6	23.86	0.35	4
Maximum	105.95	142.69	164.5	97.56	3.81	70.61	42.11	88.46	4.06	553.18
25th percentile	15.178	27.65	8.58	26.057	0.99	26.807	28.098	55.51	0.76	5.87
50th percentile	22.45	40.93	13.4	31.21	1.18	31.565	30.075	66.975	1.05	48.335
75th percentile	31.488	57.965	23.46	38.132	1.44	37.392	32.912	76.245	1.52	254.382
95th percentile	51.316	89.009	48.329	53.4	2.037	47.809	36.83	82.452	2.31	415.801
Postmonsoon 2019	**Ozone**	**PM25**	**NO**	**NO2**	**CO**	**NH3**	**AT**	**RH**	**WS**	**SR**
Median	19.455	141.63	32.78	42.505	1.32	32.965	24.165	68.2	0.79	6.935
Mean	31.278	178.31	50.078	45.194	1.59	34.783	24.674	65.065	0.898	100.907

95% CI Mean Upper	32.514	185.38	52.32	45.967	1.637	35.277	24.907	65.787	0.919	107.715
95% CI Mean Lower	30.042	171.24	47.836	44.422	1.542	34.288	24.44	64.344	0.877	94.1
Std. Deviation	24.113	137.92	43.729	15.072	0.927	9.641	4.559	14.069	0.416	132.779
Coefficient of variation	0.771	0.773	0.873	0.333	0.583	0.277	0.185	0.216	0.463	1.316
Skewness	1.289	1.66	1.414	0.868	1.462	0.957	0.223	-0.37	1.59	1.068
Std. Error of Skewness	0.064	0.064	0.064	0.064	0.064	0.064	0.064	0.064	0.064	0.064
Kurtosis	0.639	3.434	1.689	0.772	2.396	0.808	-0.667	-1.058	3.556	-0.328
Std. Error of Kurtosis	0.128	0.128	0.128	0.128	0.128	0.128	0.128	0.128	0.128	0.128
Minimum	8.94	17.27	3.03	17.03	0.21	14.65	14.26	33.73	0.17	3.14
Maximum	120.75	924	247.7	110.77	5.72	68.48	35.23	91.88	2.96	499.04
25th percentile	13.39	76.66	17.527	34.015	0.93	28.247	21.288	52.998	0.61	5.008
50th percentile	19.455	141.63	32.78	42.505	1.32	32.965	24.165	68.2	0.79	6.935
75th percentile	43.727	234.86	71.925	54.233	2.01	39.438	27.883	76.782	1.07	188.083
95th percentile	81.883	462.28	140.49	74.123	3.518	55.368	32.696	83.598	1.71	368.458
Winter 2019-20	**Ozone**	**PM25**	**NO**	**NO2**	**CO**	**NH3**	**AT**	**RH**	**WS**	**SR**
Median	22.375	150.87	33.975	43.065	1.29	39.27	14.09	77.455	0.94	5.88
Mean	27.749	176.74	53.358	47.508	1.66	43.213	14.585	72.968	1.082	96.108
95% CI Mean Upper	28.511	180.87	55.378	48.311	1.707	43.861	14.749	73.609	1.107	101.514
95% CI Mean Lower	26.987	172.6	51.338	46.704	1.614	42.564	14.42	72.327	1.057	90.702
Std. Deviation	18.168	98.486	48.134	19.14	1.117	15.456	3.92	15.276	0.591	128.828
Coefficient of variation	0.655	0.557	0.902	0.403	0.673	0.358	0.269	0.209	0.547	1.34
Skewness	1.461	1.083	1.972	1.086	1.929	2.637	0.448	-0.756	1.719	1.141

Std. Error of Skewness	0.052	0.052	0.052	0.052	0.052	0.052	0.052	0.052	0.052	0.052
Kurtosis	1.724	1.267	4.075	1.119	3.915	11.423	-0.111	-0.626	3.989	-0.126
Std. Error of Kurtosis	0.105	0.105	0.105	0.105	0.105	0.105	0.105	0.105	0.105	0.105
Minimum	6.65	21.15	8.8	15.47	0.38	20.64	5.69	32.43	0.27	3.48
Maximum	113.25	688.88	309.25	136.21	6.78	156.71	26.58	93.18	4.49	466.17
25th percentile	14.848	99.227	21.44	33.487	0.93	33.69	11.772	61.645	0.66	5.18
50th percentile	22.375	150.87	33.975	43.065	1.29	39.27	14.09	77.455	0.94	5.88
75th percentile	33.838	234.11	66.313	57.3	1.95	48.96	17.163	85.75	1.32	176.722
95th percentile	68.915	370.09	157.79	85.598	4.187	69.206	21.727	90.118	2.28	370.929
Spring 2020	**Ozone**	**PM25**	**NO**	**NO2**	**CO**	**NH3**	**AT**	**RH**	**WS**	**SR**
Median	28.02	56.025	18.325	31.14	0.71	29.11	22.41	66.565	1.09	14.855
Mean	35.888	65.913	27.756	31.921	0.905	29.782	22.785	64.033	1.29	145.04
95% CI Mean Upper	37.523	68.784	29.538	33.052	0.946	30.308	23.087	65.188	1.342	157.833
95% CI Mean Lower	34.254	63.043	25.973	30.79	0.864	29.256	22.484	62.878	1.238	132.247
Std. Deviation	22.709	39.883	24.766	15.715	0.572	7.305	4.183	16.048	0.72	177.746
Coefficient of variation	0.633	0.605	0.892	0.492	0.632	0.245	0.184	0.251	0.558	1.225
Skewness	0.967	1.143	2.022	0.869	2.082	0.662	0.279	-0.279	1.367	0.853
Std. Error of Skewness	0.09	0.09	0.09	0.09	0.09	0.09	0.09	0.09	0.09	0.09
Kurtosis	0.04	1.779	3.739	0.749	4.892	0.863	-0.655	-1.067	1.887	-0.833
Std. Error of Kurtosis	0.179	0.179	0.179	0.179	0.179	0.179	0.179	0.179	0.179	0.179
Minimum	6.05	9.69	8.18	8.3	0.18	14.71	14.15	27.91	0.3	3.84

Maximum	109.01	263.61	133.15	98.58	3.81	55.58	32.95	98.68	4.44	579.45
25th percentile	17.925	35.737	12.005	19.01	0.55	25.085	19.75	50.098	0.78	5.33
50th percentile	28.02	56.025	18.325	31.14	0.71	29.11	22.41	66.565	1.09	14.855
75th percentile	49.575	88.15	31.005	40.892	1.022	33.593	25.87	77.412	1.63	293.39
95th percentile	81.514	135.78	86.924	62.207	2.089	43.578	30.257	86.365	2.75	477.112
Summer 2020	**Ozone**	**PM25**	**NO**	**NO2**	**CO**	**NH3**	**AT**	**RH**	**WS**	**SR**
Median	48.18	47.66	9.38	22.25	0.99	30.135	31.925	48.195	1.08	34.425
Mean	53.441	56.212	10.749	25.126	1.06	31.408	31.983	48.204	1.244	152.06
95% CI Mean Upper	54.645	57.674	10.984	25.682	1.076	31.808	32.199	48.802	1.271	159.718
95% CI Mean Lower	52.237	54.75	10.514	24.57	1.043	31.008	31.767	47.606	1.216	144.402
Std. Deviation	28.7	34.833	5.6	13.256	0.399	9.529	5.142	14.253	0.648	182.499
Coefficient of variation	0.537	0.62	0.521	0.528	0.377	0.303	0.161	0.296	0.521	1.2
Skewness	0.528	1.743	4.384	1.977	1.385	0.701	0.091	0.003	1.033	0.883
Std. Error of Skewness	0.052	0.052	0.052	0.052	0.052	0.052	0.052	0.052	0.052	0.052
Kurtosis	-0.659	4.356	25.428	6.585	4.203	0.269	-0.414	-0.834	0.81	-0.671
Std. Error of Kurtosis	0.105	0.105	0.105	0.105	0.105	0.105	0.105	0.105	0.105	0.105
Minimum	11.05	4.55	1.45	8.98	0.28	13.33	18.65	16.53	0.28	3.05
Maximum	135.58	259.43	59.43	129.29	3.84	65.05	45.96	84.88	4.29	686.38
25th percentile	29	32.438	8.26	15.38	0.79	24.352	28.268	36.915	0.74	4.58
50th percentile	48.18	47.66	9.38	22.25	0.99	30.135	31.925	48.195	1.08	34.425
75th percentile	75.825	69.985	11.08	29.89	1.26	37.278	35.66	59.543	1.632	303.395
95th percentile	105.59	125.28	19.528	51.551	1.778	49.346	40.617	70.269	2.478	508.033

Monsoon 2020	**Ozone**	**PM25**	**NO**	**NO2**	**CO**	**NH3**	**AT**	**RH**	**WS**	**SR**
Median	24.76	34.87	13.195	27.75	0.97	28.14	32.205	68.77	1.02	53.035
Mean	28.189	38.409	17.708	29.739	1.046	28.938	32.601	66.942	1.161	136.039
95% CI Mean Upper	28.733	39.245	18.279	30.181	1.062	29.189	32.729	67.433	1.185	142.414
95% CI Mean Lower	27.645	37.574	17.138	29.297	1.03	28.688	32.474	66.451	1.138	129.664
Std. Deviation	13.033	20.016	13.67	10.587	0.376	6.005	3.057	11.76	0.572	152.761
Coefficient of variation	0.462	0.521	0.772	0.356	0.36	0.207	0.094	0.176	0.492	1.123
Skewness	1.12	0.848	3.012	1.288	1.539	0.598	0.309	-0.341	1.571	0.768
Std. Error of Skewness	0.052	0.052	0.052	0.052	0.052	0.052	0.052	0.052	0.052	0.052
Kurtosis	1.06	0.51	13.326	2.621	4.148	0.41	-0.552	-0.767	3.514	-0.871
Std. Error of Kurtosis	0.104	0.104	0.104	0.104	0.104	0.104	0.104	0.104	0.104	0.104
Minimum	6	4.8	3.59	9.67	0.32	14.73	24.5	36.57	0.33	4.4
Maximum	82.37	120.34	125.22	84.24	3.64	54.84	42.23	89.51	4.33	529.22
25th percentile	18.42	23.328	9.395	22.523	0.8	24.65	30.288	57.855	0.75	6.14
50th percentile	24.76	34.87	13.195	27.75	0.97	28.14	32.205	68.77	1.02	53.035
75th percentile	35.192	50.16	21.1	34.87	1.22	32.612	34.88	76.303	1.412	267.05
95th percentile	53.293	74.841	43.246	49.395	1.73	39.677	37.9	84.01	2.22	420.766
Postmonsoon 2020	**Ozone**	**PM25**	**NO**	**NO2**	**CO**	**NH3**	**AT**	**RH**	**WS**	**SR**
Median	17.6	161.96	40.475	50.66	1.74	38.495	25.075	58.78	0.73	7.16
Mean	32.994	200.77	62.89	55.224	2.212	40.829	25.422	56.017	0.825	100.614
95% CI Mean Upper	34.56	207.96	65.862	56.306	2.277	41.407	25.716	56.81	0.844	107.158
95% CI Mean Lower	31.429	193.58	59.918	54.142	2.146	40.25	25.128	55.224	0.806	94.07
Std. Deviation	30.538	140.03	57.976	21.109	1.283	11.289	5.733	15.469	0.371	127.638

Coefficient of variation	0.926	0.697	0.922	0.382	0.58	0.277	0.225	0.276	0.449	1.269
Skewness	1.161	1.707	1.364	0.993	1.212	0.733	0.271	-0.258	1.505	0.989
Std. Error of Skewness	0.064	0.064	0.064	0.064	0.064	0.064	0.064	0.064	0.064	0.064
Kurtosis	0.015	3.766	1.24	1.074	0.717	0.136	-0.794	-1.163	2.927	-0.504
Std. Error of Kurtosis	0.128	0.128	0.128	0.128	0.128	0.128	0.128	0.128	0.128	0.128
Minimum	5.36	29.1	2.48	17.33	0.53	18.76	14.28	21.82	0.24	5.18
Maximum	133.71	998.62	308.98	159.62	6.4	86.81	37.88	84.9	2.74	471.5
25th percentile	10.94	101.21	19.117	39.953	1.27	32.06	20.683	41.58	0.56	5.97
50th percentile	17.6	161.96	40.475	50.66	1.74	38.495	25.075	58.78	0.73	7.16
75th percentile	51.213	252.7	88.418	66.793	2.82	48.872	29.45	69.15	0.99	200.813
95th percentile	95.412	478.24	185.8	94.549	5	60.922	35.92	77.623	1.55	346.69
Winter 2020-21	**Ozone**	**PM25**	**NO**	**NO2**	**CO**	**NH3**	**AT**	**RH**	**WS**	**SR**
Median	22.375	150.87	33.975	43.065	1.29	39.27	14.09	77.455	0.94	5.88
Mean	27.749	176.74	53.358	47.508	1.66	43.213	14.585	72.968	1.082	96.108
95% CI Mean Upper	28.511	180.87	55.378	48.311	1.707	43.861	14.749	73.609	1.107	101.514
95% CI Mean Lower	26.987	172.6	51.338	46.704	1.614	42.564	14.42	72.327	1.057	90.702
Std. Deviation	18.168	98.486	48.134	19.14	1.117	15.456	3.92	15.276	0.591	128.828
Coefficient of variation	0.655	0.557	0.902	0.403	0.673	0.358	0.269	0.209	0.547	1.34
Skewness	1.461	1.083	1.972	1.086	1.929	2.637	0.448	-0.756	1.719	1.141
Std. Error of Skewness	0.052	0.052	0.052	0.052	0.052	0.052	0.052	0.052	0.052	0.052
Kurtosis	1.724	1.267	4.075	1.119	3.915	11.423	-0.111	-0.626	3.989	-0.126

Std. Error of Kurtosis	0.105	0.105	0.105	0.105	0.105	0.105	0.105	0.105	0.105	0.105
Minimum	6.65	21.15	8.8	15.47	0.38	20.64	5.69	32.43	0.27	3.48
Maximum	113.25	688.88	309.25	136.21	6.78	156.71	26.58	93.18	4.49	466.17
25th percentile	14.848	99.227	21.44	33.487	0.93	33.69	11.772	61.645	0.66	5.18
50th percentile	22.375	150.87	33.975	43.065	1.29	39.27	14.09	77.455	0.94	5.88
75th percentile	33.838	234.11	66.313	57.3	1.95	48.96	17.163	85.75	1.32	176.722
95th percentile	68.915	370.09	157.79	85.598	4.187	69.206	21.727	90.118	2.28	370.929
Spring 2021	**Ozone**	**PM25**	**NO**	**NO2**	**CO**	**NH3**	**AT**	**RH**	**WS**	**SR**
Median	25.015	104.1	27.195	42.84	1.145	75.5	23.35	49.495	1.1	13.055
Mean	33.836	114.92	44.076	45.27	1.444	78.606	24.164	49.203	1.322	125.824
95% CI Mean Upper	35.656	119.41	47.436	46.406	1.507	80.379	24.512	50.275	1.372	137.018
95% CI Mean Lower	32.016	110.43	40.716	44.135	1.381	76.833	23.817	48.132	1.272	114.629
Std. Deviation	25.287	62.354	46.688	15.778	0.878	24.636	4.764	14.89	0.695	155.532
Coefficient of variation	0.747	0.543	1.059	0.349	0.608	0.313	0.197	0.303	0.526	1.236
Skewness	0.851	0.953	2.45	1.606	2.099	1.596	0.36	-0.01	1.381	0.89
Std. Error of Skewness	0.09	0.09	0.09	0.09	0.09	0.09	0.091	0.09	0.09	0.09
Kurtosis	-0.475	1.177	6.74	5.844	5.116	6.236	-0.727	-0.991	1.641	-0.761
Std. Error of Kurtosis	0.179	0.179	0.179	0.179	0.179	0.179	0.181	0.179	0.179	0.179
Minimum	6.7	12	5.46	12.74	0.43	38.36	14.96	16.53	0.22	4.83
Maximum	107.38	417	298.91	159.85	6.11	250.63	39.15	82.22	4.31	536.13
25th percentile	11.678	65.855	16.408	34.657	0.87	62.277	20.29	36.365	0.82	5.97
50th percentile	25.015	104.1	27.195	42.84	1.145	75.5	23.35	49.495	1.1	13.055

75th percentile	51.417	153.48	48.765	52.038	1.702	90.755	27.985	61.13	1.61	266.447
95th percentile	81.808	225.03	140.59	72.478	3.26	123.17	32.459	72.367	2.86	404.937
Summer 2021	**Ozone**	**PM25**	**NO**	**NO2**	**CO**	**NH3**	**AT**	**RH**	**WS**	**SR**
Median	28.725	58.55	10.85	29.005	1.28	58.105	30.49	43.375	1.11	46.45
Mean	37.738	72.527	19.279	35.014	1.419	59.542	30.673	45.218	1.343	148.453
95% CI Mean Upper	38.862	74.843	20.196	35.785	1.441	60.06	30.886	45.887	1.375	155.558
95% CI Mean Lower	36.615	70.211	18.362	34.243	1.398	59.025	30.46	44.549	1.312	141.348
Std. Deviation	26.774	55.184	21.846	18.373	0.51	12.328	5.065	15.94	0.746	169.317
Coefficient of variation	0.709	0.761	1.133	0.525	0.36	0.207	0.165	0.353	0.556	1.141
Skewness	1.185	2.791	3.102	1.553	1.998	1.08	0.006	0.484	1.781	0.744
Std. Error of Skewness	0.052	0.052	0.052	0.052	0.052	0.052	0.052	0.052	0.052	0.052
Kurtosis	0.776	11.772	11.878	2.758	5.204	2.282	-0.644	-0.262	4.934	-0.999
Std. Error of Kurtosis	0.105	0.105	0.105	0.105	0.105	0.105	0.105	0.105	0.105	0.105
Minimum	6.02	4	2.83	9.2	0.53	35.95	16.05	17.45	0.38	4.66
Maximum	143.68	503.88	187.28	132.09	4.53	129.05	43.85	93.04	7.58	539.66
25th percentile	17.32	37.415	7.81	22.35	1.09	50.61	26.907	33.15	0.82	5.92
50th percentile	28.725	58.55	10.85	29.005	1.28	58.105	30.49	43.375	1.11	46.45
75th percentile	51.46	89.78	20.747	43.35	1.57	65.857	34.552	56.21	1.67	305.998
95th percentile	92.199	166.02	62.798	71.769	2.5	81.754	38.93	73.411	2.88	458.677
Monsoon 2021	**Ozone**	**PM25**	**NO**	**NO2**	**CO**	**NH3**	**AT**	**RH**	**WS**	**SR**
Median	25	40.155	12.37	23.45	0.94	36.215	31.58	70.44	1.015	23.465
Mean	27.443	43.423	15.919	25.189	1.013	38.044	32.08	68.934	1.168	118.817

95% CI Mean Upper	27.876	44.218	16.399	25.531	1.029	38.517	32.215	69.497	1.189	125.015
95% CI Mean Lower	27.01	42.629	15.439	24.847	0.996	37.571	31.945	68.37	1.146	112.619
Std. Deviation	10.381	19.043	11.504	8.187	0.399	11.343	3.226	13.498	0.521	148.513
Coefficient of variation	0.378	0.439	0.723	0.325	0.394	0.298	0.101	0.196	0.446	1.25
Skewness	1.24	0.801	2.027	1.469	1.186	0.528	0.671	-0.447	1.462	1.048
Std. Error of Skewness	0.052	0.052	0.052	0.052	0.052	0.052	0.052	0.052	0.052	0.052
Kurtosis	1.942	0.826	5.192	3.331	1.917	-0.723	0.045	-0.655	2.966	-0.307
Std. Error of Kurtosis	0.104	0.104	0.104	0.104	0.104	0.104	0.104	0.104	0.104	0.104
Minimum	8.3	4	3.6	11.15	0.29	21.82	25.4	29.66	0.31	5.21
Maximum	82.85	142.67	87.94	73.06	3.11	77.6	43.28	89.85	4.39	531.75
25th percentile	19.928	29.433	8.003	19.46	0.73	27.688	29.56	59.098	0.79	6.3
50th percentile	25	40.155	12.37	23.45	0.94	36.215	31.58	70.44	1.015	23.465
75th percentile	32.83	55.345	19.86	28.91	1.21	47.355	34.185	80.37	1.42	230.075
95th percentile	48.537	79.053	41.037	40.77	1.77	57.496	38.017	87.537	2.177	421.197
Postmonsoon 2021	**Ozone**	**PM25**	**NO**	**NO2**	**CO**	**NH3**	**AT**	**RH**	**WS**	**SR**
Median	20.38	135.78	42.35	51.365	1.62	39.77	24.48	67.24	0.8	7.405
Mean	30.829	164.93	66.475	54.721	1.963	42.03	24.686	63.706	0.879	109.271
95% CI Mean Upper	32.051	171.11	69.561	55.892	2.029	42.562	24.973	64.514	0.896	116.502
95% CI Mean Lower	29.607	158.75	63.388	53.55	1.897	41.498	24.399	62.899	0.862	102.04
Std. Deviation	23.827	120.55	60.204	22.838	1.289	10.384	5.59	15.748	0.334	141.04
Coefficient of variation	0.773	0.731	0.906	0.417	0.657	0.247	0.226	0.247	0.38	1.291
Skewness	1.479	1.048	1.206	0.786	1.269	1.782	0.347	-0.38	1.695	1.037

Std. Error of Skewness	0.064	0.064	0.064	0.064	0.064	0.064	0.064	0.064	0.064	0.064
Kurtosis	1.306	1.273	0.783	0.387	1.507	5.086	-0.714	-1.035	5.076	-0.421
Std. Error of Kurtosis	0.128	0.128	0.128	0.128	0.128	0.128	0.128	0.128	0.128	0.128
Minimum	7.92	4	5.56	14.85	0.28	23.78	14.72	29.02	0.29	4.77
Maximum	133.73	832	318.1	141.34	7.39	102.99	38.5	90.05	3.42	462.06
25th percentile	13.94	66.14	18.805	37.035	0.98	35.08	19.907	50.195	0.65	6.17
50th percentile	20.38	135.78	42.35	51.365	1.62	39.77	24.48	67.24	0.8	7.405
75th percentile	39.177	245.19	101.26	68.247	2.57	46.343	28.71	76.627	1.04	215.02
95th percentile	85.31	369.62	187.31	97.198	4.637	61.057	35.319	85.306	1.51	395.554
Winter 2021-22	**Ozone**	**PM25**	**NO**	**NO2**	**CO**	**NH3**	**AT**	**RH**	**WS**	**SR**
Median	21.015	163.65	37.565	40.885	1.44	39.685	14.22	77.5	0.81	6.73
Mean	28.469	182.65	69.63	44.214	1.775	41.106	14.881	71.898	0.958	97.673
95% CI Mean Upper	29.283	187.32	72.703	44.995	1.824	41.581	15.063	72.605	0.979	103.408
95% CI Mean Lower	27.655	177.98	66.558	43.433	1.726	40.631	14.699	71.192	0.937	91.937
Std. Deviation	19.292	110.69	72.814	18.512	1.161	11.255	4.3	16.728	0.496	135.77
Coefficient of variation	0.678	0.606	1.046	0.419	0.654	0.274	0.289	0.233	0.518	1.39
Skewness	1.295	1.107	1.472	0.966	1.732	0.862	0.548	-0.813	2.324	1.376
Std. Error of Skewness	0.053	0.053	0.053	0.053	0.053	0.053	0.053	0.053	0.053	0.053
Kurtosis	0.704	1.338	1.562	0.902	3.636	1.197	-0.432	-0.512	7.154	0.772
Std. Error of Kurtosis	0.105	0.105	0.105	0.105	0.105	0.105	0.105	0.105	0.105	0.105
Minimum	7.69	11.25	3.62	12.24	0.28	14.19	7.23	26.4	0.29	4.52

Maximum	95.06	634.74	426.13	128.44	7.96	88.5	27.8	92.87	3.77	560.52
25th percentile	14.768	98.33	16.285	30.025	0.97	33.487	11.51	60.74	0.64	6
50th percentile	21.015	163.65	37.565	40.885	1.44	39.685	14.22	77.5	0.81	6.73
75th percentile	36.21	239.78	105.23	53.995	2.18	46.76	17.65	85.68	1.11	172.365
95th percentile	71.564	393.38	233.53	81.001	4.16	61.932	23.249	90.71	1.93	404.048
Spring 2022	**Ozone**	**PM25**	**NO**	**NO2**	**CO**	**NH3**	**AT**	**RH**	**WS**	**SR**
Median	22.81	106.15	19.93	39.465	1.01	34.735	24.885	54.815	0.89	16.4
Mean	34.289	114.03	42.452	42.304	1.232	36.583	25.444	55.05	0.994	156.623
95% CI Mean Upper	36.202	117.97	46.188	43.598	1.288	37.316	25.865	56.342	1.027	170.42
95% CI Mean Lower	32.376	110.1	38.716	41.01	1.175	35.85	25.023	53.758	0.961	142.827
Std. Deviation	26.583	54.716	51.91	17.977	0.782	10.183	5.847	17.955	0.456	191.69
Coefficient of variation	0.775	0.48	1.223	0.425	0.635	0.278	0.23	0.326	0.458	1.224
Skewness	1.099	0.714	2.15	1.206	2.462	1.97	0.256	-0.037	1.097	0.841
Std. Error of Skewness	0.09	0.09	0.09	0.09	0.09	0.09	0.09	0.09	0.09	0.09
Kurtosis	0.468	-0.018	4.588	2.125	9.336	7.858	-0.34	-1.105	0.984	-0.911
Std. Error of Kurtosis	0.179	0.179	0.179	0.179	0.179	0.179	0.179	0.179	0.179	0.179
Minimum	5.5	25.87	3.79	14.07	0.28	17.93	11.66	19.52	0.18	4.82
Maximum	129.29	282.22	292.72	131.81	6.62	110	40.56	88.18	2.8	648.18
25th percentile	13.22	71.263	10.315	29.15	0.72	30.158	21.26	40.042	0.64	6.01
50th percentile	22.81	106.15	19.93	39.465	1.01	34.735	24.885	54.815	0.89	16.4
75th percentile	55.083	146.88	48.383	50.93	1.48	41.167	29.35	70.48	1.24	296.663
95th percentile	82.937	222.73	158.05	75.791	2.804	52.097	35.607	82.944	1.87	507.707

Summer 2022	Ozone	PM25	NO	NO2	CO	NH3	AT	RH	WS	SR
Median	35.35	80.105	18.09	40.325	1.03	40.7	32.825	41.935	0.96	65.875
Mean	46.37	94.892	35.832	45.7	1.234	41.026	33.267	43.919	1.101	165.633
95% CI Mean Upper	47.846	97.19	37.507	46.502	1.262	41.374	33.474	44.535	1.124	173.51
95% CI Mean Lower	44.894	92.594	34.156	44.898	1.205	40.678	33.059	43.303	1.079	157.755
Std. Deviation	35.165	54.767	39.93	19.108	0.679	8.293	4.949	14.679	0.528	187.733
Coefficient of variation	0.758	0.577	1.114	0.418	0.55	0.202	0.149	0.334	0.48	1.133
Skewness	0.931	1.569	1.942	0.986	1.79	0.986	0.182	0.771	1.231	0.742
Std. Error of Skewness	0.052	0.052	0.052	0.052	0.052	0.052	0.052	0.052	0.052	0.052
Kurtosis	-0.074	3.389	3.724	0.637	3.742	4.543	-0.767	0.298	2.477	-1.001
Std. Error of Kurtosis	0.105	0.105	0.105	0.105	0.105	0.105	0.105	0.105	0.105	0.105
Minimum	4.66	9.5	3.61	12.85	0.33	20.1	22.21	18.89	0.3	3.7
Maximum	159.08	420.66	266.17	122.65	5.16	102.71	46.46	92.52	4.7	610.61
25th percentile	16.78	57.345	9.79	30.74	0.79	35.88	29.55	32.73	0.7	5.98
50th percentile	35.35	80.105	18.09	40.325	1.03	40.7	32.825	41.935	0.96	65.875
75th percentile	67.095	119.37	43.462	57.765	1.45	45.34	37.103	52.555	1.42	319.993
95th percentile	117.91	197.58	127.29	82.254	2.718	54.538	41.48	71.9	2.068	505.381
Monsoon 2022	**Ozone**	**PM25**	**NO**	**NO2**	**CO**	**NH3**	**AT**	**RH**	**WS**	**SR**
Median	33.89	34.495	12.375	24.82	0.92	35.245	28.635	69.12	0.92	44.65
Mean	37.001	39.02	17.612	26.996	1.005	35.963	29.016	68.033	1.06	138.844
95% CI Mean Upper	37.609	39.861	18.21	27.376	1.021	36.21	29.138	68.564	1.082	145.702
95% CI Mean Lower	36.393	38.179	17.015	26.617	0.989	35.716	28.894	67.503	1.039	131.987
Std. Deviation	14.576	20.146	14.322	9.094	0.382	5.917	2.924	12.71	0.511	164.315

Coefficient of variation	0.394	0.516	0.813	0.337	0.38	0.165	0.101	0.187	0.482	1.183
Skewness	1.218	0.978	2.571	1.195	1.827	0.833	0.335	-0.184	1.322	0.919
Std. Error of Skewness	0.052	0.052	0.052	0.052	0.052	0.052	0.052	0.052	0.052	0.052
Kurtosis	2.183	0.69	9.073	1.659	4.808	1.932	-0.595	-0.957	1.939	-0.556
Std. Error of Kurtosis	0.104	0.104	0.104	0.104	0.104	0.104	0.104	0.104	0.104	0.104
Minimum	5.67	5.63	2.93	10.13	0.39	20.3	23.07	39.62	0.28	3.82
Maximum	108.73	115.85	118.63	73.34	3.28	72.1	37.08	92.53	3.48	585.78
25th percentile	27.87	24.215	8.428	20.53	0.75	32.04	26.86	57.752	0.68	6.08
50th percentile	33.89	34.495	12.375	24.82	0.92	35.245	28.635	69.12	0.92	44.65
75th percentile	43.98	50.922	22.108	31.57	1.14	39.34	31.152	78.615	1.32	255.132
95th percentile	65.876	80.826	45.332	45.087	1.77	46.392	34.3	87.177	2.06	462.435
Postmonsoon 2022	**Ozone**	**PM25**	**NO**	**NO2**	**CO**	**NH3**	**AT**	**RH**	**WS**	**SR**
Median	18.565	132.02	39.445	63.265	1.3	44.26	22.495	57.17	0.73	6.75
Mean	29.538	146.12	70.747	67.883	1.735	50.237	22.811	56.325	0.823	100.312
95% CI Mean Upper	30.766	150.83	74.357	69.636	1.798	51.304	23.055	57.069	0.84	107.189
95% CI Mean Lower	28.31	141.41	67.137	66.13	1.673	49.169	22.567	55.581	0.806	93.434
Std. Deviation	23.962	91.917	70.412	34.193	1.227	20.823	4.766	14.51	0.336	134.158
Coefficient of variation	0.811	0.629	0.995	0.504	0.707	0.414	0.209	0.258	0.409	1.337
Skewness	1.332	0.87	1.292	0.611	1.56	0.836	0.124	0.218	1.371	1.234
Std. Error of Skewness	0.064	0.064	0.064	0.064	0.064	0.064	0.064	0.064	0.064	0.064
Kurtosis	0.762	1.155	0.877	-0.083	2.453	0.11	-0.509	-0.4	2.037	0.29

Std. Error of Kurtosis	0.128	0.128	0.128	0.128	0.128	0.128	0.128	0.128	0.128	0.128
Minimum	3.85	4.5	1.96	8.81	0.18	17.65	12.59	28.53	0.29	4.65
Maximum	110.39	588.43	343.09	208.46	7.54	132.59	34.24	93.56	2.56	516.33
25th percentile	13.32	74.645	17.495	40.18	0.86	33.107	19.46	44.628	0.59	5.9
50th percentile	18.565	132.02	39.445	63.265	1.3	44.26	22.495	57.17	0.73	6.75
75th percentile	40.385	203.38	107.24	90.25	2.262	64.745	26.072	65.985	0.98	184.435
95th percentile	83.146	309.98	213.86	132	4.27	89.542	31.118	83.217	1.528	393.454
Winter 2022-23	**Ozone**	**PM25**	**NO**	**NO2**	**CO**	**NH3**	**AT**	**RH**	**WS**	**SR**
Median	14.58	154.73	49.355	52.385	1.26	56.58	16.035	65.74	0.92	11.8
Mean	23.414	171.28	75.574	58.9	1.508	57.851	16.744	63.344	1.047	76.484
95% CI Mean Upper	24.266	175.12	78.345	60.096	1.545	58.625	16.944	63.954	1.07	80.843
95% CI Mean Lower	22.563	167.45	72.804	57.705	1.471	57.076	16.544	62.735	1.024	72.124
Std. Deviation	20.181	90.87	65.658	28.335	0.882	18.35	4.737	14.444	0.537	103.309
Coefficient of variation	0.862	0.531	0.869	0.481	0.585	0.317	0.283	0.228	0.512	1.351
Skewness	1.55	0.934	1.511	1.055	1.613	0.71	0.541	-0.35	2.392	1.554
Std. Error of Skewness	0.053	0.053	0.053	0.053	0.053	0.053	0.053	0.053	0.053	0.053
Kurtosis	1.767	1.103	1.642	0.989	2.652	1.59	-0.307	-0.833	9.462	1.62
Std. Error of Kurtosis	0.105	0.105	0.105	0.105	0.105	0.105	0.105	0.105	0.105	0.105
Minimum	4.08	21	4.39	11.82	0.36	18.26	7.81	30.97	0.32	4.25
Maximum	120.93	592.7	335.84	181.78	5.8	171.16	30.83	95.56	4.76	464.88
25th percentile	9.52	101.94	29.88	38.43	0.9	45.825	13.24	52.23	0.69	5.39
50th percentile	14.58	154.73	49.355	52.385	1.26	56.58	16.035	65.74	0.92	11.8

75th percentile	30.72	227.78	100.43	73.593	1.81	67.535	19.86	75.037	1.23	126.49
95th percentile	67.577	333.68	225.8	115.64	3.48	90.337	25.88	81.411	1.94	319.61
Spring 2023	**Ozone**	**PM25**	**NO**	**NO2**	**CO**	**NH3**	**AT**	**RH**	**WS**	**SR**
Median	26.335	71.455	28.46	42.09	1.135	47.99	22.085	56.025	0.94	13.05
Mean	35.584	80.503	45.162	47.225	1.237	49.215	22.965	55.458	1.025	109.611
95% CI Mean Upper	37.399	83.614	48.079	48.865	1.275	49.909	23.239	56.431	1.058	119.483
95% CI Mean Lower	33.769	77.391	42.244	45.586	1.198	48.522	22.692	54.485	0.992	99.739
Std. Deviation	25.22	43.233	40.542	22.784	0.538	9.636	3.8	13.515	0.458	137.16
Coefficient of variation	0.709	0.537	0.898	0.482	0.435	0.196	0.165	0.244	0.447	1.251
Skewness	0.978	0.968	1.951	1.058	0.917	0.783	0.509	0.129	1.417	1.061
Std. Error of Skewness	0.09	0.09	0.09	0.09	0.09	0.09	0.09	0.09	0.09	0.09
Kurtosis	-0.031	0.965	3.666	0.827	0.442	1.091	-0.885	-0.663	3.137	-0.329
Std. Error of Kurtosis	0.179	0.179	0.179	0.179	0.179	0.179	0.179	0.179	0.179	0.179
Minimum	7.83	12.06	4.05	11.78	0.4	28.03	17.1	30.14	0.36	4.58
Maximum	118.65	277.08	220.67	127.92	3.25	90.55	31.73	91.67	3.48	473.1
25th percentile	14.998	46.155	18.902	29.822	0.83	42.435	19.775	43.595	0.68	8.098
50th percentile	26.335	71.455	28.46	42.09	1.135	47.99	22.085	56.025	0.94	13.05
75th percentile	52.235	109.38	55.83	58.947	1.52	54.457	26.072	65.68	1.26	207.718
95th percentile	81.212	159.75	133.9	94.095	2.34	67.458	29.887	77.099	1.87	382.245
Summer 2023	**Ozone**	**PM25**	**NO**	**NO2**	**CO**	**NH3**	**AT**	**RH**	**WS**	**SR**
Median	28.465	51.92	23.285	44.55	1.04	38.095	31.55	49.09	1.03	39.63
Mean	37.186	66.906	38.542	50.574	1.169	39.309	31.506	51.951	1.13	129.804

95% CI Mean Upper	38.324	68.768	40.215	51.627	1.194	39.687	31.725	52.646	1.151	136.233
95% CI Mean Lower	36.048	65.045	36.869	49.521	1.145	38.932	31.287	51.255	1.109	123.376
Std. Deviation	27.126	44.33	39.869	25.096	0.588	8.999	5.219	16.569	0.498	153.165
Coefficient of variation	0.729	0.663	1.034	0.496	0.503	0.229	0.166	0.319	0.441	1.18
Skewness	1.051	1.867	2.232	1.43	2.088	0.698	-0.145	0.52	1.026	0.955
Std. Error of Skewness	0.052	0.052	0.052	0.052	0.052	0.052	0.052	0.052	0.052	0.052
Kurtosis	0.34	4.989	5.284	2.586	7.093	0.574	-0.254	-0.562	1.032	-0.532
Std. Error of Kurtosis	0.105	0.105	0.105	0.105	0.105	0.105	0.105	0.105	0.105	0.105
Minimum	5.07	8.75	2.32	9.09	0.34	17.41	17.51	23.1	0.31	4.54
Maximum	143.57	431.5	250.72	181.65	5.56	76.55	44.21	95.71	3.23	534.78
25th percentile	15.607	37.632	14.027	32.608	0.77	32.95	28.15	39.38	0.75	8.14
50th percentile	28.465	51.92	23.285	44.55	1.04	38.095	31.55	49.09	1.03	39.63
75th percentile	54.078	82.645	45.16	61.455	1.363	44.412	35.105	63.775	1.41	239.16
95th percentile	91.992	157.36	130.64	101.22	2.308	56.562	40.039	83.166	2.09	440.291
Monsoon 2023	**Ozone**	**PM25**	**NO**	**NO2**	**CO**	**NH3**	**AT**	**RH**	**WS**	**SR**
Median	26.69	40.455	15.02	30.6	0.83	37.92	31.34	69.15	0.96	249.355
Mean	29.573	41.97	19.156	32.763	0.884	43.318	31.633	69.149	1.034	237.967
95% CI Mean Upper	30.126	42.655	19.717	33.297	0.897	44.069	31.751	69.681	1.052	245.355
95% CI Mean Lower	29.021	41.286	18.594	32.23	0.871	42.566	31.514	68.618	1.015	230.579
Std. Deviation	13.242	16.401	13.452	12.784	0.317	17.999	2.726	12.641	0.442	170.323
Coefficient of variation	0.448	0.391	0.702	0.39	0.358	0.416	0.086	0.183	0.427	0.716
Skewness	1.502	0.512	2.229	1.134	1.196	1.957	0.257	-0.035	0.738	0.367

Std. Error of Skewness	0.052	0.052	0.052	0.052	0.052	0.052	0.054	0.052	0.052	0.054
Kurtosis	3.172	0.376	7.297	2.009	2.738	4.857	-0.59	-0.511	-0	-0.462
Std. Error of Kurtosis	0.104	0.104	0.104	0.104	0.104	0.104	0.108	0.105	0.104	0.108
Minimum	5.69	6.75	3.34	9.48	0.2	16.88	22.11	32.41	0.06	5.35
Maximum	101.38	111.88	124.82	100.34	2.93	149.99	38.7	99.72	2.74	703.86
25th percentile	20.265	30.53	9.988	23.205	0.66	31.852	29.56	60.245	0.68	72.788
50th percentile	26.69	40.455	15.02	30.6	0.83	37.92	31.34	69.15	0.96	249.355
75th percentile	35.282	52.468	23.76	39.625	1.042	49.16	33.593	78.002	1.3	330.61
95th percentile	55.099	71.491	44.779	56.967	1.447	82.406	36.47	90.076	1.917	560.706
Postmonsoon 2023	**Ozone**	**PM25**	**NO**	**NO2**	**CO**	**NH3**	**AT**	**RH**	**WS**	**SR**
Median	18.585	163.44	36.515	56.475	1.54	46.75	23.765	60.465	0.58	257.11
Mean	27.263	180.62	64.948	68.03	1.922	50.45	24.254	60.171	0.653	298.655
95% CI Mean Upper	28.369	186.29	68.21	70.021	1.985	51.532	24.532	60.845	0.669	305.315
95% CI Mean Lower	26.157	174.96	61.686	66.038	1.859	49.368	23.977	59.497	0.637	291.995
Std. Deviation	21.575	110.41	63.624	38.844	1.23	21.101	5.419	13.148	0.308	129.909
Coefficient of variation	0.791	0.611	0.98	0.571	0.64	0.418	0.223	0.219	0.471	0.435
Skewness	1.315	0.646	1.214	0.877	1.173	0.988	0.067	-0.098	2.103	0.058
Std. Error of Skewness	0.064	0.064	0.064	0.064	0.064	0.064	0.064	0.064	0.064	0.064
Kurtosis	1.133	-0.279	0.484	0.172	0.757	1.023	-0.68	-1.032	9.394	0.751
Std. Error of Kurtosis	0.128	0.128	0.128	0.128	0.128	0.128	0.128	0.128	0.128	0.128
Minimum	4.74	16.4	4.85	10.9	0.46	16.84	13.06	34.33	0.19	7.97

Maximum	127.15	591.63	281.09	216.38	6.39	136.91	36.3	86.35	3.28	639.88
25th percentile	10.995	84.795	15.638	37.258	0.987	35.43	20.76	49.318	0.45	253.207
50th percentile	18.585	163.44	36.515	56.475	1.54	46.75	23.765	60.465	0.58	257.11
75th percentile	38.365	256.59	100.87	94.16	2.56	61.72	28.262	70.747	0.79	348.027
95th percentile	72.139	381.98	201.8	141.42	4.46	93.535	33.627	80.716	1.19	560.282